Government of **Western Australia**
Department of **Mines and Petroleum**

RECORD 2009/19

U-PB AND HF ANALYSIS OF DETRITAL ZIRCONS: IMPLICATIONS FOR PROVENANCE OF THE EARAHEEDY BASIN, CAPRICORN OROGEN

by
KJ Matonia

Geological Survey of
Western Australia

TRaX
Tectonics, Resources and Exploration

Government of Western Australia
Department of Mines and Petroleum

Record 2009/19

U–PB AND HF ANALYSIS OF DETRITAL ZIRCONS: IMPLICATIONS FOR PROVENANCE OF THE EARAHEEDY BASIN, CAPRICORN OROGEN

by Kylie J Matonia[1]

[1] Tectonics, Resources and Exploration (TRaX), School of Earth and Environmental Sciences, The University of Adelaide, Adelaide, SA 5005, Australia

A Manuscript Submitted for the Honours Degree of Bachelor of Science
October 2007
WQRD COUNT: 10,051
Supervisors: Alan Collins and Martin Hand

THE UNIVERSITY OF ADELAIDE AUSTRALIA

TRaX Tectonics, Resources and Exploration

Geological Survey of Western Australia

Notice to the reader
This Record reproduces a BSc Honours thesis arising from research supported by the Geological Survey of Western Australia as part of a collaborative project with the Centre for Tectonics, Resources and Exploration (TRaX), at the University of Adelaide, South Australia. GSWA provided field and laboratory support, but the scientific content of the Record, and the drafting of figures, has been the responsibility of the author. No scientific or stylistic editing has been undertaken by GSWA.

REFERENCE
The recommended reference for this publication is:
Matonia, KJ 2009, U–Pb and Hf analysis of detrital zircons: Implications for provenance of the Earaheedy Basin, Capricorn Orogen: Geological Survey of Western Australia, Record 2009/19, 81p.

National Library of Australia Card Number and ISBN 978-1-74168-271-7

Published 2009 by Geological Survey of Western Australia
This Record is published in digital format (PDF)and is available online at www.dmp.wa.gov.au/GSWApublications. Laser-printed copies can be ordered from the Information Centre for the cost of printing and binding.

Further details of geological publications and maps produced by the Geological Survey of Western Australia are available from:
Information Centre
Department of Mines and Petroleum
100 Plain Street
EAST PERTH, WESTERN AUSTRALIA 6004
Telephone: +61 8 9222 3459 Facsimile: +61 8 9222 3444
www.dmp.wa.gov.au/GSWApublications

Table of Contents

List of Tables

List of Figures

U-Pb and Hf analysis of detrital zircons: Implications for provenance of the Earaheedy Basin, Capricorn Orogen

Kylie J. Matonia*

Continental Evolution Research Group, School of Earth and Environmental Sciences, University of Adelaide, Adelaide, SA 5005, Australia

Abstract

U-Pb dating of 250 detrital zircons from the basal Yelma and middle Chiall Formations of the Earaheedy Basin yields 67 concordant zircons. Detrital populations fall into three groups: 2700 – 2600, 2275 – 2050 and 2000 – 1970 Ma. Zircons within the range of 2700 – 2600 Ma are similar to grains within the Yilgarn Craton whilst clusters at 2000 – 1970 Ma coincide with the Glenburgh Terrane. The origin of 2275 – 2050 Ma zircons is difficult to determine as igneous rocks of that age are scarce in the West Australian Craton.

Hf isotope analysis of zircons confirm provenance from the Yilgarn Craton and the Gascoyne Complex. The majority of 2700 – 2600 Ma analyses plot in ε_{Hf} space between -7.5 to -2, with fewer in the range of 2 to 8.5. Negative and positive Archaean ε_{Hf} values compare well with Hf isotopes measurements in the Narryer Terrane and Murchinson Province, respectively. Palaeoproterozoic Hf isotopes in the range 2000 – 1970 Ma lie in ε_{Hf} space between -6 and -1.5 and are similar to Nd isotopic data from the Glenburgh Terrane in the Gascoyne Complex. Negative ε_{Hf} values within 2275 – 2050 Ma zircons are similar to those in the Narryer Terrane and Yeelirrie Domain of the

Yilgarn Craton. Positive values within the same age range may relate to the Cheela Springs Basalt in the Pilbara Craton.

The age of the youngest concordant detrital zircon in the lower Earaheedy Basin yields 1971±26 Ma and conforms with existing maximum depositional constraints placed on the basal Earaheedy Basin (~1810 Ma, Halilovic et al., 2004). However, ^{40}Ar-^{39}Ar dating of sericite in the deformed northern margin of the Earaheedy Basin yields an age of ~1650 Ma (Pirajno et al., in press). This age fits within the framework of the 1680 – 1620 Ma Mangaroon Orogeny, and contradicts models relating basin deformation to the Yapungku Orogeny.

The combination of U-Pb and Hf isotope analysis of detrital zircon grains reveals the Yilgarn Craton and the Glenburgh Terrane as sources for Archaean and Palaeoproterozoic sediment, respectively. The detrital zircon analyses imply: 1) The maximum depositional age of the basal Earaheedy Basin is 1971±26 Ma; 2) Archaean and Palaeoproterozoic sediment is sourced from the Yilgarn Craton and Glenburgh Terrane, respectively.

Keywords: Earaheedy Basin; Proterozoic; Capricorn Orogen; Provenance; Detrital zircons; Hf isotopes

1. Introduction

The study of sedimentary rocks deposited in basins provides insight into the tectonic evolution of a terrane (e.g. McLennan et al., 1993; Halilovic et al., 2004; Payne et al., 2006). Intraplate and interplate forces produce crustal instabilities that ultimately lead to uplift and subsidence of the landscape; uplifted regions become the source of sediment that feed into basins. Therefore, basin sediments record changes to the ground surface of source regions and preserve subtle features of the orogenic evolution that are often unattainable from within the orogen itself. Fundamental parameters in sedimentary basins include the age of deposition and the location of the sediment source (Hegner et al., 2005). The age of deposition can be linked to regions of tectonism and therefore the forces responsible for initial basin formation. The location of the sediment source can indicate which terranes were proximal and exposed during sediment deposition (Hegner et al., 2005). Such parameters can be resolved by dating basin sediments and comparing ages to that of probable source regions.

The study of heavy minerals is paramount in provenance studies that aim to determine the nature and origin of source regions. Detrital zircons are extensively used in geochronological dating of detrital sediment because they are chemically resistant, able to survive several cycles of erosion and deposition and contain uranium and thorium, which radioactively decay to lead over time (Morton, 1991; Morton and Hallsworth, 1999; Cawood and Nemchin, 2000). If not disturbed, the amount of lead present in a zircon is indicative of the age at which the zircon crystallized (Hawkesworth and Kemp, 2006). U-Pb dating of zircon provides knowledge of not only the age and associated

magmatism and metamorphism of the source rock, but also places constraints on the age of sediment deposition. This premise is based on the assumption that basin magmatism is absent at the time of basin deposition. The youngest detrital zircon deposited in a basin must therefore be older than the age of sediment deposition, whereby constraining the maximum age at which sediment deposited.

U-Pb study of zircons, however, is not the only useful information gained from zircon analysis. The radioactive decay of lutetium (Lu^{176}) to hafnium (Hf^{176}) enables an estimation of the time passed since a rock was extracted from the mantle (Hawkesworth and Kemp, 2006). Compared with lutetium, hafnium is relatively incompatible in the mantle. When the mantle melts, incompatible elements like hafnium are extracted from the mantle and enriched in the crust, leaving the original residual solids depleted in hafnium relative to lutetium (Hawkesworth and Kemp, 2006). The highest concentrations of hafnium are found in zirconium-rich minerals in which hafnium substitutes for zirconium in the zircon structure (Hawkesworth and Kemp, 2006). Hafnium isotope ratios vary depending on the tectonic environment in which they formed; this variation assists in resolving the extent to which the mantle contributed to the generation of a rock (Griffin et al. 2000). For example, basalt generated directly from the depleted mantle would be classified as juvenile or 'young' whilst granite reworked during a period of orogenesis would be categorised as evolved or 'old'. The integration of U-Pb and hafnium isotopic analysis of zircons can therefore potentially clarify the most probable sediment source, and more importantly, distinguish between source terranes that may overlap in zircon age (e.g. Howard et al., 2007).

The Capricorn Orogen (Figure 1) is a Palaeoproterozoic belt of sedimentary and volcanic rocks that were variably deformed during a series of rift and collisional events, including the collision of the Archaean Pilbara and Yilgarn Craton to form the West Australian Craton (Myers et al., 1996). The orogen extends 700km along the northern border of the Yilgarn Craton (Pirajno et al., 2004). Tectonic events within the Capricorn Orogen are thought to coincide with a major phase of continental amalgamation during the construction of Proterozoic Australia (Cawood and Tyler, 2004). The Earaheedy Basin (Figure 2) lies in the southeastern Capricorn Orogen and consists of shallow marine chemical and clastic sediments that were deposited in a trailing passive margin setting (Pirajno et al., 2004). The origin of sequences and the tectonic setting of the Earaheedy Basin is currently uncertain due to a lack of geochronological and structural knowledge (e.g. Halilovic et al., 2004; Pirajno et al., 2004).

Many questions remain unanswered in regards to the development of the Earaheedy Basin and eastern Capricorn Orogen. The sparsity of geological, and particularly geochronological studies, has contributed to the lack of understanding and conflict between competing tectonic models regarding this history of the region. Current models suggest the Earaheedy Basin formed during the 1830 – 1780 Ma Capricorn Orogeny (e.g. Halilovic et al., 2004). These are based upon monazite and zircon dating of the underlying Yerrida Basin and Imbin Inlier, respectively (Rasmussen and Fletcher, 2002; Nelson, 2001; Halilovic et al., 2004). Monazites grow during episodes of thermal activity; monazites associated with sill intrusions in the upper sediment package of the Yerrida Basin yield a growth age of 1843±10 Ma (Rasmussen and Fletcher, 2002). As the basal Earaheedy Basin rests unconformably on the Yerrida Basin, deposition within

the Earaheedy Basin is constrained to be ~1843 Ma. Nelson (2001) dated a rhyodacite in the Imbin Inlier and obtained a U-Pb zircon age of 1990±6 Ma. This zircon age was later interpreted as a maximum depositional age of the Earaheedy Basin based upon the apparent constraint that the Imbin Inlier uncomformably underlies the basin (Pirajno et al., 2002). In agreement with this interpretation, U-Pb dating of zircon grains in sandstones from the Earaheedy Basin yielded maximum depositional ages of 1983±51 and 1808±36 Ma for the oldest and youngest formations in the basin, respectively (Halilovic et al., 2004). This implies that basin development occurred after ~1810 Ma. Minimum depositional ages of the Earaheedy Basin, however, are not as well constrained.

The minimum depositional age of the Earaheedy Basin is suggested to relate to deformation during the 1790 – 1760 Ma Yapungku Orogeny (Bagas, 2004). Although generally restricted to the Rudall Complex (Figure 1), the Yapungku Orogeny may record the collision of the West and North Australian Cratons (Bagas, 2004). Bagas (2004) placed Yapungku-aged deformation in the interval of 1790 – 1760 Ma driven by a south-directed compressional regime. Metamorphism associated with the Yapungku Orogeny has been proposed to record crustal thickening in the Paterson Orogen (Smithies and Bagas, 1997). In the Paterson Orogen, two stages of deformation are seen. In this model, deformation in the Stanley Fold Belt of the northern Earaheedy Basin records the second stage of the Yapungku Orogeny (Bagas, 2004). Hence, the late stages of the Yapungku Orogeny are considered responsible for deformation of the northern Earaheedy Basin (Bagas, 2004) and constrain basin deposition to prior to ~1770 Ma. This assumption, however, is based upon a lack of geochronological data and knowledge of newly defined

tectonic events such as the Mangaroon Orogeny (Sheppard et al., 2005). In addition, Maidment (2007) has queried the very existence of 1790 – 1760 Ma metamorphism in the Paterson Orogen due to metamorphism being poorly constrained.

The recently dated 1680 - 1620 Ma Mangaroon Orogeny caused extensive reworking in the Gascoyne Complex, west of the Earaheedy Basin (Sheppard et al., 2005). Previous work assigned all deformation in the northern Gascoyne Complex to the Capricorn Orogeny (Libby et al., 1986), but recent studies have demonstrated that this deformation is instead related to intracontinental reworking during the newly defined Mangaroon Orogeny (Sheppard et al., 2005). The implications of this event signify that deformation elsewhere in the Capricorn Orogen, such as the Earaheedy Basin, may have to be revised. Sericite from the Stanley Fold Belt has yielded ^{40}Ar-^{39}Ar ages of ~1650 Ma (Pirajno et al., in press) suggesting that at least some, if not all, deformation in the northern Earaheedy Basin is due to the Mangaroon Orogeny. If this is the case, ~1650 Ma would represent the minimum depositional age of the basin. This would extend the relatively tight constraints previously placed on the Earaheedy Basin, which was suggested to have formed between ~1810 Ma (maximum depositional age; Halilovic et al., 2004) and 1790 – 1760 Ma (Halilovic et al., 2004; Bagas, 2004).

The Capricorn Orogen records the collision of the Yilgarn and Pilbara Cratons. The study of the orogen is integral in understanding the development of the West Australian Craton during the construction of Proterozoic Australia. A lack of geochronological constraints associated with the Earaheedy Basin has hindered the development of provenance and tectonic models. This paper integrates the U-Pb dating and Hf analysis of detrital zircons within the Earaheedy Basin to better define and

determine sediment provenance, depositional age and the tectonic regimes that have shaped the eastern Capricorn Orogen.

2. Geological Background

2.1 Regional Geology

The Capricorn Orogen consists of many tectonic units including exotic terranes, sedimentary basins and the reworked margins of adjoining Archaean Cratons (Figure 1) (Cawood and Tyler, 2004). The 2550 – 1620 Ma Gascoyne Complex lies in the western Capricorn Orogen and includes the northern Boora Boora and Mangaroon Zones, the central Limejuice Zone and the southern Glenburgh Terrane (Occhipinti et al., 2004; Sheppard et al., 2005). It is separated from the Narryer Terrane of the Yilgarn Craton by the Errabiddy Shear Zone (Cawood and Tyler, 2004). The Palaeoproterozoic Yerrida, Bryah, Padbury and Earaheedy basins developed along the southern margin of the Capricorn Orogen whilst the Proterozoic Hamersley and Ashburton basins developed along the northern margin of the Capricorn Orogen (Figure 1) (Cawood and Tyler, 2004). The Mesoproterozoic Edmund and Collier Basins unconformably overlie the deformed and reworked tectonic units of the orogen (Martin and Thorne, 2004).

A series of Proterozoic orogenic events contributed to the current geometry of the Capricorn Orogen. Initial studies attributed all deformation within the Capricorn Orogen to the collision of the Pilbara and Yilgarn Cratons during the Capricorn Orogeny (Libby et al., 1986; Myers et al., 1996). Cawood and Tyler (2004) believe the development of the Capricorn Orogen is instead related to one or more 'Wilson Cycles' in which a continual

series of break-up, assembly and reworking of Archaean and Proterozoic cratons and terranes eventually formed the West Australian Craton. Orogenic events that shaped the orogen include the ~2200 Opthalmian, ~2000 Glenburgh, ~1800 Capricorn, ~1770 Yapungku, ~1650 Mangaroon and ~1000 Edmundian Orogenies (Tyler and Thorne, 1990; Occhipinti et al., 2004; Cawood and Tyler, 2004; Bagas, 2004; Sheppard et al., 2005; Sheppard et al., 2007) . A number of basins opened in response to tectonism during the evolution of the Capricorn Orogen. The most prominent and widely recognised of these basins are the Palaeoproterozoic ~2.17 Ga Yerrida, ~2.0 Ga Bryah, ~1.96 Ga Padbury and <1.84 Ga Earaheedy Basins and the poorly constrained unconformably overlying Mesoproterozoic Edmund and Collier Basins (Pirajno et al., 2004; Occhipinti et al., 2004; Martin and Thorne, 2004). Orogenic events and associated basins are presented in detail in Tables 1 and 2.

The Earaheedy Basin (Figure 2) lies southeast of the Yerrida, Bryah and Padbury Basins and unconformably overlies the Yilgarn Craton and Yerrida Basin (Williams et al., 2004; Pirajno et al., 2004). Sedimentary rocks that fill the basin are part of the Earaheedy Group which is subdivided into the lower Tooloo Subgroup which includes, from oldest to youngest, the Yelma, Frere and Windidda Formations and the upper Miningarra Subgroup which consists of the Chiall, Wongawol, Kulele and Mulgarra Formations (Figure 3).

The Yelma Formation forms the base of the Earaheedy Basin and unconformably overlies the Yilgarn Craton and Yerrida Basin (Figure 3). Sedimentary packages in the Yelma Formation include shale and sandstone deposited in a fluvial coastal setting and carbonate deposited in a highly saline coastal lagoon setting; the thickness of the

formation ranges from 3m in the southeast to 500m in the northwest (Pirajno et al., 2004). The Frere Formation indicates a ferric oxide precipitation event and consists of four intervals of granular iron beds separated by shales, siltstones and carbonates (Williams et al., 2004), with an interpreted thickness of 600m (Pirajno et al., 2004). It was formed in a shallow marine environment in which cyclic changes in sea level produced cyclic patterns within the sediment. The Windidda Formation includes shale, siltstone, carbonate and granular iron and reflects an increasingly stable basin environment. The Windidda is equivalent to the upper Frere Formation and was deposited in a carbonate coastal lagoonal environment (Pirajno et al., 2004; Halilovic et al., 2004).

The Chiall Formation records the beginning of deposition of the Miningarra Subgroup (Figure 3). Basal units include thin fine grained shale and siltstone layers intercalated with thick sandstone layers. These units grade up into clastic coarse grained sandstone and breccia layers sourced from uplifted areas to the southwest (Halilovic et al., 2004). The Wongawol Formation includes siltstone, sandstone, carbonate, iron rich shale, some breccia and a thin volcaniclastic layer with a total thickness of 1500m. Mudcracks and ripple marks indicate that the Wongawol Formation was deposited in low energy shallow marine environment (Halilovic et al., 2004) whilst thin volcaniclastic layers are related to far-field ashfall deposits (Pirajno et al., 2004). The 300m thick Kulele Limestone includes cyclic layers of carbonate, shale and siltstone which are attributed to changes in sea level. A sub-tidal to inter-tidal environment is inferred for limestone deposition (Halilovic et al., 2004). The youngest unit in the Earaheedy Basin is the 100m thick Mulgarra Sandstone which is likened to the Wongawol Formation and consists of sandstone, shale and carbonate (Pirajno et al., 2004).

The Earaheedy Basin is constrained by the unconformably underlying Imbin Inlier, Yerrida Basin and Yilgarn Craton and the unconformably overlying Collier Basin (Pirajno et al., 2002, Martin and Throne, 2004). U-Pb dating of the unconformably underlying Imbin Inlier yielded a zircon age of 1990±6 Ma thereby restricting the development of the Earaheedy Basin to post ~1990 Ma (Pirajno et al., 2002). In addition, monazites located in the upper units of the underlying Yerrida Basin yield a growth age of 1843±10 Ma synchronous with sill intrusions (Figure 3) and further constrain basin development and deposition to after ~1843 Ma (Rasmussen and Fletcher, 2002). U-Pb dating of grains in the uppermost Mulgarra Sandstone yielded an age of 1808±36 Ma which is interpreted as the maximum depositional age of the upper Earaheedy Basin (Figure 3) (Halilovic et al., 2004). Minimum depositional ages are difficult to resolve as overlying units of the c. 1395 Ma Collier and c. 1465 Ma Edmund Basins and the events that caused deformation have not been well-dated (Martin and Thorne, 2004).

Deformation within the Earaheedy Basin increases northwards towards the Stanley Fold Belt which is the compressively deformed northern margin of the basin (Pirajno et al., 2004). Structural repetition of the basal Yelma Formation and the unusual thickness of the Wongowol Formation are suggested to relate to faulting and folding during the formation of the Stanley Fold Belt (Halilovic et al., 2004). Bagas (2004) suggests that the Stanley Fold Belt is an expression of latter stages of Yapungku deformation during the collision of the West and North Australian Cratons.

2.2 Local Geology

The region chosen for this study is located in the northern Earaheedy Basin, eastern Capricorn Orogen, Western Australia (Figure 4).

Stratigraphy and sedimentology

Three lithologies are distinguishable within the mapped area (Figure 4). These comprise Palaeoproterozoic sedimentary formations of marine shale/siltstone, ironstone and sandstone. The units correlate with the Frere Formation as recognised by Pirajno et al. (2004), and appear to have been deposited in a cyclical manner (i.e. a series of repeated layers of shale, ironstone and sandstone; Figure 4). The highly weathered outcrops do not preserve contacts between formations or facies, preventing a more detailed study of their conformity.

The shale and siltstone formation forms the oldest stratigraphic unit within repeated sequences and is very fine grained and clay rich. Such units maintain well defined bedding and deformational cleavage planes which are 0.5cm – 3cm and 1mm – 1cm thick, respectively. Outcrops range from homogenous white clay to bimodal laminations of white and purple silt (Figure 5a); highly weathered outcrops are brown to purple in hue and heavily oxidised. Although infrequent, some outcrops show coarsening upwards. It is likely that the shale and siltstone formed predominantly in a low energy deep marine environment that lacked wave and current action (Pirajno et al., 2004).

Banded iron-rich siltstones and sandstones comprise the central unit mapped (Figure 4). Coarse grained quartz rich sandstone and clayey siltstone layers are blocky in

appearance. Layers of highly silicified veins are intercalated parallel to the bedding plane. Iron appears to have been precipitated at a later stage rather than during deposition whilst cuboidal weathering pores suggest the presence of pyrite. Although rare, conglomeratic units with large pebbles (2 – 4cm) crop out, indicating deposition within a high energy environment (Figure 5b). Mudcracks were observed in a small outcrop of silt-rich ironstone, indicating a shallow marine, low energy environment that was possibly exposed due to a decrease in sea level or tidal action (Figure 5c) (Pirajno et al., 2004).

Sandstones comprise the youngest unit mapped and are compositionally mature. Grains are medium (0.2 mm) in size, sub-rounded and well sorted. Small scale, low angle cross-bedding is evident within the major bedding plane which itself can extend from 10cm to 1m in thickness (Figure 5d). Cross-bedding is typical of a shallow marine shelf environment (Pirajno et al., 2004).

Structure

The structural geology of the northern Earaheedy Basin comprises Palaeoproterzoic sedimentary strata folded into of synclines and anticlines that reflect north-south compression during D1 deformation (Figure 4). Small scale local 'z' and 's' folds are located in the limbs of larger folds and characteristic of the overall north-south compressional regime exhibited by large scale structures (Figure 5e). Such structures are clearly defined by a pervasive cleavage that dips to the north at 70° and runs east-west, parallel to the fold axis. Cleavage and bedding are graphically displayed in Figure 4 to show the structural relationships with local folding.

Faults typically form parallel to the pervasive axial planar cleavage. Reverse faulting within the mapped area is interpreted to have downthrown the northern anticlinal region under the southern synclinal region (Figure 4). Faulting is accompanied by east-west trending quartz veining up to 0.5m in width and 3m in length that crops out in the north western region of the study (Figure 5f). The presence of quartz veining indicates possible hydrothermal activity in zones of weakness during late D1 deformation or in a later hydrothermal event. Due to the highly weathered nature of fault planes and presence of extensive quartz veining, the total extent of tectonic movement could not be resolved.

3. Samples and analytical methods

The lithologies and localites of samples are shown in Table 3 and Figure 2, respectively. Petrological images of each sample are presented in Figure 6. All samples ranged from medium to coarse grained and contained monocrystalline and polycrystalline quartz set in a detrital clay matrix (i.e. Figure 6a). Slight variations to the general trend include the replacement of the detrital clay matrix due to quartz overgrowth filling pore spaces (GSWA sample 189743, Figure 6b) and the inclusion of garnet and hematite (GSWA sample 189712, Figure 6c). One sample (GSWA 189712) contained a distinct pervasive cleavage whilst remaining samples were void of a clear structural fabric.

3.1 U-Pb zircon dating

Sample preparation for U-Pb isotopic dating of zircons follow those of Payne et al. (2006). Samples were crushed and sieved manually into three separate fractions; < 400 μm, 400 – 79 μm and > 79 μm. The 400 – 79 μm fraction was retained for isotopic analysis. Gravity separation panning techniques were applied to the fraction of interest in order to separate heavier and lighter minerals. Magnetic minerals were removed from the panned samples using a hand magnet. Samples were further reduced using methylene iodide then hand-picked, mounted in epoxy, polished and carbon coated.

Analytical techniques for U-Pb isotopic dating of zircons follow those of Payne et al. (2006). Zircons were imaged on a Philips XL-20 scanning electron microscope (SEM) at the University of Adelaide using the Gatan cathodoluminescence (CL) instrument. U-Pb dating of singular zircon grains was accomplished using laser ablation inductively coupled plasma mass spectrometry (LA-ICPMS) at the University of Adelaide. The Agilent 7500cs ICP-MS and attached New Wave Nd Yag 213 UV laser with He collision cell was used to measure U and Pb isotope ratios. Following a 60 second gas blank, zircon grains were ablated for 120 seconds with a beam diameter of 30 μm at a rate of 5 Hz. The laser was fired with the shutter closed for 10 seconds prior to ablation to enable beam stability.

The GEMOC GJ-1 zircon standard was used to account for U-Pb fractionation (TIMS normalisation data $^{207}Pb/^{206}Pb$ = 608.3 Ma, $^{206}Pb/^{238}U$= 600.7 Ma and $^{207}Pb/^{235}U$= 602.2 Ma, Jackson et al. 2004). Throughout the course of this study, the reported average normalised ages for GJ-1 were 609.1±5.3, 601.9±1.2 and 603.2±1.2 Ma for the $^{207}Pb/^{206}Pb$, $^{206}Pb/^{238}U$ and $^{207}Pb/^{235}U$ ratios, respectively (n = 129). An in-house Sri

Lankan zircon standard was used to monitor accuracy of standards and unknowns (BJWP-1, $^{207}Pb/^{206}Pb$ = 720.9 Ma, $^{206}Pb/^{238}U$= 720.4 Ma and $^{207}Pb/^{235}U$= 720.5 Ma, Massachusetts Institute of Technology (MIT) TIMS data); the reported average values for BJWP-1 were 730±16, 712.4±3.7 and 717.0±4.7 Ma for the $^{207}Pb/^{206}Pb$, $^{206}Pb/^{238}U$ and $^{207}Pb/^{235}U$ ratios, respectively (n = 22). Data was reduced using GLITTER software (Van Achterbergh et al., 2001) and evaluated using the Excel add-ins Isoplot (Ludwig, 2003) and Age-Display (Sircombe, 2004).

3.2 Hf isotopic analysis

Analytical methods for Hf isotope determination are described in Griffin et al. (2000) and Belousova et al. (2006) and are summarised below. Hafnium analyses were undertaken using the New Wave Research LUV213 laser ablation microprobe and attached Nu Plasma multi-collecter LA-ICPMS at Macquarie University. Zircons were ablated for a period of 120 - 150 seconds after recording 40 seconds of background signal. With the exception of an unusually small zircon grain which was ablated with a beam of 30 μm, all analyses were carried out with a beam of 55 μm at a rate of 5 Hz. As determined by U-Pb analyses, zircons with less than 10% discordance were analysed for hafnium isotopes in order to minimize error.

$^{176}Hf/^{177}Hf$ ratios in zircon must be corrected due to isobaric interference of rare earth elements ^{176}Lu and ^{176}Yb on ^{176}Hf. The interference-free ^{175}Lu isotope is used to correct for ^{176}Lu interference and later calculate $^{176}Lu/^{177}Hf$ (DeBievre and Taylor, 1993). Likewise, the interference-free ^{172}Yb isotope is used to correct for ^{176}Yb and later calculate $^{176}Yb/^{177}Hf$. The international MT-1 zircon standard was employed to evaluate

the precision and accuracy of laser ablation in order to ensure correct measurement of the $^{176}Hf/^{177}Hf$ ratio for unknown zircons (normalisation $^{176}Hf/^{177}Hf$ = 0.282530 Ma). The reported average normalised value for MT-1 during this study was $^{176}Hf/^{177}Hf$ = 0.282519 Ma (n = 9).

For the calculation of ε_{Hf} values, the chondritic values of Blichert-Toft et al. (1997) were used. These values are reported relative to $^{176}Hf/^{177}Hf$ = 0.282163 for the JMC475 standard. There are currently three proposed values for the ^{176}Lu decay constant. ε_{Hf} values and model ages reported here (Table 5) were calculated using the value (1.93 x 10^{-11}year $^{-1}$) proposed by Blichert-Toft et al. (1997), as this number is close to the average value of the other two recently reported values (1.865 x 10^{-11}year $^{-1}$, Scherer et al. (2001); 1.983 x 10^{-11}year $^{-1}$, Bizzarro et al. (2003)).

To calculate model ages (T_{DM}) based on a depleted-mantle source, a model with ($^{176}Hf/^{177}Hf$) = 0.279718 and $^{176}Lu/^{177}Hf$ = 0.0384 has been used (Belousova et al., 2006). This produces a value of $^{176}Hf/^{177}Hf$ (0.28325) similar to that of average mid-ocean ridge basalt (MORB) over 4.65 Ga. T_{DM} ages and ε_{Hf} values are calculated using the measured $^{176}Lu/^{177}Hf$ of the zircon.

3.3 Zircon morphology

Cathodoluminescence zircon images are shown in Figure 7. Images revealed zircons with oscillatory and laminated zoning and were interpreted as being detrital due to their severed morphology. Elongate, sub-rounded, rounded and euhedral zircons were present and ranged in size from 90 to 180µm in length and 30 to 90µm in width. Grains range in colour from pale translucent pink-white to semi-crystalline grey-brown-red.

Metamorphic overgrowth is evident in a small percentage of grains. As metamorphic overgrowth in these zircons was narrower than the beam size chosen for laser ablation (diameter 30 μm), U-Pb metamorphic age was not determined.

4. Results

4.1 U-Pb detrital zircon data

U-Pb ages were acquired from 250 detrital zircon grains from four sandstone samples located in the northern Earaheedy Basin. For future reference, all samples have been entered into the WAROX database at the Geological Survey of Western Australia (GSWA). Samples included two representatives from both the basal Yelma Formation (GSWA 189712, GSWA 189742) and central Chiall Formation (GSWA 189735, GSWA 189743). Eighty zircons were analysed from samples 189712, 189742 and 189743. Due to large amounts of common Pb and time constraints, only ten zircons were analysed from sample 189735. Samples were collected from a variety of locations in order to show spatial and chronological differences in detrital zircon ages.

This study considers data lying within 10% error of the concordia curve as concordant (i.e. 90 – 110 = concordant). Concordancy was calculated using the $^{206}Pb/^{238}U$ and $^{207}Pb/^{235}U$ age estimates and associated sigma 1 errors. LA-ICPMS analyses are represented as U-Pb concordancy plots showing results as sigma 1 error ellipses with *n* number of zircon analyses per diagram (Figure 8). U-Pb zircon ages from all samples are shown in Table 4.

Figure 9 represents $^{207}Pb/^{206}Pb$ ages as a function of both frequency and probability. Frequency bars and probability plots shaded dark grey signify analyses that are less than 10% discordant. Probability plots shaded light grey signify all available data within the given sample. Analogous binary zircon populations are observed in both samples from the Yelma Formation; two major peak intervals in the detrital spectra are observed at 2700 - 2600 and 2200 - 1970 Ma. Two major peak intervals in the detrital spectra of the Chiall Formation are observed at 2850 - 2600 and 2275 - 2050 Ma.

Yelma Formation 189712. Sample 189712 is a medium grained sub-litharenite. Of the 80 analyses, 21 were >90% concordant and 59 were discordant. Archaean $^{207}Pb/^{206}Pb$ zircon ages ranged from 2700 – 2600 Ma, with a major peak at 2628±17 Ma. Two major peaks are evident within the Palaeoproterozoic at 2267±18 and 2025±19 Ma. The youngest detrital zircon grain within 10% discordance was 1980±30 Ma.

Yelma Formation 189742. Sample 189742 is a medium grained sub-litharenite. Of the 80 analyses, 27 were >90% concordant and 53 were discordant. The majority of data lie within an Archaean $^{207}Pb/^{206}Pb$ zircon age range of 2700 – 2600 Ma with a major peak at 2625±18 Ma and a less distinct peak at 2757±22 Ma. Binary clusters appear in the Palaeoproterozoic at 2437±17 and 2030±20 Ma. The youngest zircon within this sample yields an age of 1971±26 Ma, which is the youngest age reported in this study.

Chiall Formation 189743. Sample 189743 is a coarse grained quartz-arenite. Of the 80 analyses, 18 were >90% concordant and 62 were discordant. The >90% concordant analyses are clustered into age groups with $^{206}Pb/^{207}Pb$ ages that range from 2275 - 2050 and 2850 - 2600 Ma. Peaks within these ranges are situated at 2270±24 and 2111±24 Ma and 2760±22 and 2623±21 Ma, respectively. A less distinct peak gives a

$^{206}Pb/^{207}Pb$ zircon age of 3135±17 Ma, which is the oldest zircon age obtained within this study.

Chiall Formation 189735. Sample 189735 is a sub-arkose sandstone. One of the 10 analyses was >90% concordant. Due to enhanced levels of common lead, only 10 zircons from sample 189735 were analysed. A single $^{207}Pb/^{206}Pb$ zircon age of 2681±19 Ma was attained.

4.2 Zircon hafnium isotopic compositions

Hf isotopic results for all samples used in this study are shown in Table 5 and presented comparatively in Figure 10 on a ε_{Hf} vs. time plot. Of the 250 zircons analysed for U-Pb ages, only the 67 concordant zircons were analysed for Hf isotopes.

Yelma Formation 189712. Of the 24 zircons analysed for Hf isotopes within this sample, 21 were considered acceptable based upon <0.0015 Lu^{176}/Hf^{177} ratios. The majority of these analyses plot within age bands of 2700 – 2600 and 2250 – 2000 Ma and lie within negative ε_{Hf} space between -7.5 to -2.5 and -5.5 to -2.5, respectively. Only 5 of 21 analyses lie within positive ε_{Hf} space, all of which plot between Chondritic Uniform Reservoir (CHUR) and the depleted mantle.

Yelma Formation 189742. All 27 Hf isotopic results within this sample were considered acceptable based on standards mentioned earlier. As with sample 189712, the majority of analyses plot in negative ε_{Hf} space within age ranges of 2700 – 2600 and 2250 – 2000 Ma. Compared with sample 189712, an increased number of analyses lie within positive ε_{Hf} space. These data cluster between CHUR and the depleted mantle at +

5 at U-Pb ages of ~2000Ma. A single analysis with an ε_{Hf} of 8.8 plots above the depleted mantle corresponding to the U-Pb age of ~2750 Ma.

Chiall Formation 189743. Sample 189743 is represented by a total of 18 acceptable data points. The majority of analyses plot within age bands of 2850 – 2600 and 2275 – 2050 Ma and lie within negative ε_{Hf} space between -7.5 to -2.0 and -6.5 to -1.5, respectively. Only 6 of 18 analyses lie within positive ε_{Hf} space. Of these, 4 correspond with the 2700 – 2600 Ma age range between CHUR and the depleted mantle. A singular analysis yields an ε_{Hf} value that plots on the depleted mantle at a U-Pb age of ~2830 Ma.

Chiall Formation 189735. One zircon was analysed for Hf isotopes within this sample due to difficulties mentioned previously. A U-Pb age of ~2680 Ma yielded a positive ε_{Hf} value of 2.4, which lies between CHUR and the depleted mantle and corresponds with results from sample 189743 of the Chiall Formation.

5. Discussion

5.1 Timing of deposition in the Earaheedy Basin

Sill-related monazites within the upper Yerrida Basin yield an age of 1843±10 Ma (Rasmussen and Fletcher, 2002). Peperites found proximal to sill intrusions indicate that the magma was injected into relatively wet sediment of the upper Yerrida Basin. As the Earaheedy Basin unconformably overlies the Yerrida Basin, monazite ages constrain deposition within the Earaheedy Basin to post ~1843 Ma (Rasmussen and Fletcher, 2002).

The four samples from the Yelma and Chiall Formations used for U-Pb zircon dating in this study are presented separately on frequency/probability vs. age plots (Figure 9). The maximum age of deposition during the mid stages of basin development is constrained by the youngest concordant (>90%) detrital zircon of 2068±21 Ma within the Chiall Formation (Figure 8). The youngest detrital group within the 67 grain population extends from 2000 – 1970 Ma. Along with the youngest single concordant (>90%) grain of 1971±26 Ma, this population is exclusive to the basal Yelma Formation and constrains the maximum depositional age of the basal Earaheedy Basin to ~1970 Ma. This age is consistent with a study by Halilovic et al. (2004) that found the maximum depositional age of the basal Earaheedy Basin to be 1983±51 Ma. Despite this, Halilovic et al. (2004) constrained maximum deposition of the entire Earaheedy Basin to the youngest detrital zircon found in the upper-most formation (Mulgarra Sandstone), which yielded an age of 1808±36 Ma. This interpretation was based upon the assumption that the basin was deformed by the 1790-1760 Ma Yapungku Orogeny and therefore deposition was tightly constrained to between ~1810 and 1760 Ma. Maximum depositional ages reported here and by Halilovic et al. (2004) are consistent with monazite growth in the unconformably underlying upper Yerrida basin. It is therefore interpreted that deposition within the basal Earaheedy Basin occurred after ~1843 Ma at around ~1810 Ma.

^{40}Ar-^{39}Ar dating of sericite within the Stanley Fold Belt of the Earaheedy Basin yields an age of ~1650 Ma which is interpreted as the approximate time that sericite cooled past its closure temperature (Pirajno et al., in press). The 1680 – 1620 Ma Mangaroon Orogeny has been shown to cause intracontinental reworking in the

Gascoyne Complex, west of the Earaheedy Basin (Sheppard et al., 2005). As the ^{40}Ar-^{39}Ar date sits within this time frame, it is possible that the Mangaroon Orogeny deformed the northern Earaheedy Basin to create the Stanley Fold Belt. This varies from previous suggestions that interpreted the poorly dated ~1770 Ma Yapungku Orogeny as the minimum depositional age of the Earaheedy Basin (Halilovic et al., 2004; Bagas 2004). These new data, combined with previous interpretations and data reported here, constrain deposition of the Earaheedy Basin to between ~1810 Ma and ~1650 Ma (Halilovic et al., 2004; Pirajno et al., in press).

5.2 Provenance of the Yelma and Chiall Formations

5.2.1 U-Pb detrital zircon geochronology

U-Pb zircon ages are displayed in frequency/probability vs. age plots in Figure 9. Archaean to Palaeoproterozoic detrital zircon U-Pb ages are present in all samples from the Earaheedy Basin. Such detrital signatures indicate that sediment was sourced from either a singular province consisting of Archaean and Palaeoproterozoic aged rocks or multiple provinces of distinct ages.

The basal Yelma Formation was deposited during the early stages of basin development. The combination of data from two samples of the Yelma Formation show increased amounts of Archaean detrital zircons compared with Palaeoproterozoic aged zircons. This trend is repeated in the combined data of two samples from the Chiall Formation, which records the mid stages of basin evolution. Trend repetition within conformable sequences suggests that the basin was most likely fed from a constant source

throughout the early to mid stages of development. The provenance of both formations will be discussed coincidently for 2700 – 2600 and 2275 – 2050 Ma time frames. Detrital zircon ages within the 2000 – 1970 Ma time frame are found within the Yelma Formation only. Hence, the discussion of that time frame will focus upon possible sources for the basal Yelma Formation.

The majority of Archaean-aged grains range from 2700 – 2600 and 2850 – 2600 Ma in the Yelma and Chiall Formations, respectively. These ages are widespread through the Yilgarn Craton, including 2750 – 2620 Ma granite and gabbro from the Narryer Terrane (Nutman et al., 1993; Kinny 2004) and 2700 – 2600 Ma granite from the Errabiddy Shear Zone (Occhipinti et al., 2004). The oldest singular Archaean grain (Chiall Formation) records a U-Pb age of 3125±17 Ma which although rare in this sample, is similar to zircons in granites of the Yarlarweelor Complex in the Narryer Terrane which obtain crystallisation ages that extend to 3300 Ma (Nutman et al., 1993). A comparison of U-Pb ages from the Earaheedy Basin and Yilgarn Craton is presented in Figure 11a. These data suggest that basal to mid Archaean detritus was sourced from the Yilgarn Craton and further implies the Yilgarn Craton was uplifted relative to, and southwest of, the Earaheedy Basin (Figure 11c).

Zircons within Archaean data sets show oscillatory and laminated zoning and range from euhedral and elongate to well rounded (Figure 7). Zircons with a well preserved morphology (i.e. euhedral and elongate) are interpreted to have traveled a small distance prior to deposition; the proximal Narryer Terrane is the likely source for these grains. Well rounded zircon morphology reflects lengthened transportation and indicates

the source terrane was distal to the Earaheedy basin, or that zircons had moved through several cycles of erosion and deposition prior to sediment accumulation.

Peaks in the Palaeoproterozoic detrital spectra of the Yelma and Chiall Formations include 2275 – 2050 Ma and 2000 – 1970 Ma. Detritus within the range of 2000 – 1970 Ma is found only within the Yelma Formation and overlaps with the Dalgaringa Supersuite which intruded the Glenburgh Terrane from 2005 to 1970 Ma (Sheppard et al., 2004). Well dated members of this suite include a 1997±8 Ma granitic gneiss and the Carrandibby Inlier (Figure 1), which yields ages from 2003±8 Ma down to ~1985 Ma (Kinny et al., 2004; S.Sheppard, pers. comm., 2007). The youngest Palaeoproterozoic grain reported here is aged 1971±26 Ma and is similar to that of the ca. 1975 Ma Nardoo Granite, which intruded the southern Glenburgh Terrane (Sheppard et al., 2004). A comparison of U-Pb ages from the Yelma Formation and Glenburgh Terrane is presented in Figure 11b. The Glenburgh Terrane of the southern Gascoyne Complex is therefore the most probable source of 2000 – 1970 Ma aged sediment in the basal Earaheedy Basin (Figure 11c). However, as the Yelma Formation does not contain a large number of 2000 – 1970 Ma aged zircons it is likely that the Glenburgh Terrane did not provide much detritus to the basal Earaheedy Basin.

Detrital populations that fall within the 2275 – 2050 Ma age range are difficult to reconcile with known source rocks in Australia. Source regions with such zircon ages, be they xenocrystic or magmatic, are rare in Western Australia. The Darling Fault runs north-south along the border of the Yilgarn Craton and Perth Basin. The Mullingarra Complex (Figure 1), which forms part of the Pinjarra Orogen and is currently positioned west of the Darling Fault, yields zircon ages of about 2.2 Ga (Cobb et al., 2001).

Although early Archaean to Palaeoproterozoic movement on the Darling Fault remains uncertain (Fitzsimons, 2003), it is plausible that the Mullingarra Complex was positioned near, and supplied sediment to, the Earaheedy Basin at some stage during fault evolution. In addition, granitoid zircons in the Narryer Terrane of the Yilgarn Craton exhibit peaks at 2.2 Ga (Figure 11a) and rare rims on zircons in the basement of the Glenburgh Terrane yield ages within the 2.4 – 2.2 Ga range (Griffin et al., 2004; Kinny et al., 2004). These domains are further possible provenances for 2275 – 2050 Ma detrital zircons.

A variety of factors may explain the lack of 2275 – 2050 Ma zircons throughout the Capricorn Orogen, including tectonothermal and erosional removal and lack of exposure. The complex tectonothermal events that shaped the orogen during and after the 2275 – 2050 Ma time frame include the ~2200 Ma Opthalmian, ~2000 Ma Glenburgh, ~1800 Ma Capricorn, ~1650 Ma Mangaroon and ~1050 Ma Edmundian Orogenies (Cawood and Tyler, 2004). It is possible that thermal activity and faulting during these events may have removed certain source terranes. Likewise, the source terrane may currently be overlain by younger sediment and as a consequence, undiscovered. Many of the older tectonic units in the Capricorn Orogen are unconformably overlain by the Mesoproterozoic Edmund and Collier Basins (Martin and Thorne, 2004). With this in mind, comparison with like-aged terranes distal to the Capricorn Orogen is required.

An additional potential source of 2275 – 2050 Ma aged zircons in the Earaheedy Basin includes the South African Continent (SAC). The SAC was proximal to the Pilbara Craton during the Columbia supercontinent (Figure 12a) (Zhao et al., 2002). The lithostratigraphy of the Pilbara Craton is broadly similar to that of the Kaapvaal Craton in southern South Africa (Figure 12b) (Zhao et al., 2002). A three-layer relationship exists

between the two cratons which includes a package of 2.47 – 2.20 Ga volcanic units (Zhao et al., 2002). These stratigraphic relationships are interpreted by Zhao et al. (2002) to indicate that the now detached cratons were once continuous as part of the Vaalbara continent within the supercontinent Columbia (Figure 12b). The growth of the supercontinent Columbia extended from 1.8 – 1.3 Ga (Zhao et al., 2002), thus overlapping with deposition of the Earaheedy basin (i.e. maximum deposition ~1810 Ma; Halilovic et al., 2004) and permitting the Kaapvaal Craton as a reasonable source terrane.

Zircons within the 2275-2050 Ma population are rounded and exhibit some metamorphic overgrowth (Figure 7). These two properties further support South African related provenance; rounded morphology may reflect extended sediment transportation from the Kaapvaal Craton to the Earaheedy Basin. In addition, metamorphic overgrowth may relate to metamorphism associated with long-lived Limpopo orogenesis, reported to extend from 3700 – 2000 Ma (Figure 12b) (Watkeys et al., 1983). Although metamorphic overgrowth is not dated here due to difficulties mentioned earlier, metamorphic rims are assumed to have grown between core ages of 2275 – 2050 Ma and the maximum depositional age of the Earaheedy Basin (~1810 Ma). If metamorphism occured after Earaheedy deposition, overgrowth would be expected on a larger percentage of grains. If these interpretations are accurate, ~2.3 – 2.2 Ga volcanics (Kaapvaal Craton) and Limpopo related source regions of South Africa may have provided the 2275 – 2050 Ma aged detrital zircons to the Earaheedy Basin (Figure 12b). This interpretation, however, is difficult to reconcile with northeasterly palaeocurrent direction (Halilovic et al., 2004) and must be further explored.

Contrary to earlier findings (Halilovic et al., 2004), there is a notable lack of detrital zircons in the age range of 1950 – 1780 Ma. This indicates that the 1830 – 1780 Ma Moorarie Supersuite of the Gascoyne Complex (Occhipinti et al., 1998) did not contribute Palaeoproterozoic sediment to the basal Earaheedy Basin, as suggested by Halilovic et al. (2004). The extent to which an area contributed to sedimentary units within the upper Earaheedy basin (i.e. Mulgarra Sandstone) is beyond the scope of this study. However, continued uplift during the Capricorn Orogeny over the development of the Earaheedy Basin may have exposed Capricorn-related intrusives (i.e. ~1780 Moorarie Supersuite) and provided detritus to the upper basin (Halilovic et al., 2004).

5.2.2 Hf isotopes

ε_{Hf} data from the Yelma and Chiall Formations is displayed in ε_{Hf} vs. age plots in Figure 10. The Hf isotopic signature of three specific time frames are addressed; 2700 – 2600, 2000-1970 and 2275 – 2050 Ma. Aside from the 2000 – 1970 Ma aged zircons in the Yelma Formation, the data from both samples are analogous and will be discussed coincidently.

Samples in both the basal Yelma and middle Chiall Formations are dominated by Archaean detrital zircon ages that sit within the time interval of 2700 – 2600 Ma. This peak is consistent with zircon ages associated with magmatism in the Narryer Terrane and Murchison Province of the Yilgarn Craton (Nutman et al., 1993; Griffin et al., 2004). A comparison of ε_{Hf} values from the Yilgarn Craton with those of the Earaheedy Basin is displayed in Figure 13a. ε_{Hf} values of specific Archaean Yilgarn source terranes are compared with those of the Yelma and Chiall Formations in Figure 14. ε_{Hf} values in the

age range of 2.7 – 2.6 Ga in the Narryer Terrane range from +1 to -10 (Griffin et al., 2004). The majority of detrital data from 2.7 – 2.6 Ga reported here plot between -7.5 and -2 in ε_{Hf} space, across all samples. Such negative ε_{Hf} values reflect remelting of older crust without the addition of juvenile magma. As zircons in the Narryer Terrane have similar ages and Hf isotopic ratios as detrital sediment within the Earaheedy Basin it is likely that the Narryer Terrane was one significant source for 2.7 – 2.6 Ga zircons in the Earaheedy Basin (Figure 14b).

In addition, it is possible that Archaean units of the Gascoyne Complex provided such sediment. A comparison of ε_{Hf} values from the Gascoyne Complex the Earaheedy Basin is presented in Figure 13b. ε_{Nd} values from a variety of samples throughout the Gascoyne Complex were obtained for comparison with detrital zircons from the Earaheedy Basin (S.Sheppard, pers. comm., 2007). ε_{Hf} values were determined by applying a terrestrial Hf-Nd array formulated by Vervoort et al. (1999). For example, an ε_{Hf} value of approximately -6.14 was calculated by applying the Hf-Nd array to an to $\varepsilon_{Nd\ (2700Ma)}$ value of -6.68 in the Warrigal Gneiss (Glenburgh Terrane). Along with samples from the Warrigal Gneiss, the 2630 Ma Beedarry Plug and a 2687 Ma monzogranite of the Gascoyne Complex yielded ε_{Hf} values of -7.37 and -5.23, similar to the predominately negative values obtained within the Earaheedy Basin (Figure 13b).

Sources of positive ε_{Hf} Archaean zircons include the Murchison Province and Marymia Inlier which yield ε_{Hf} values between 0 and 4 and 1 and 8, respectively (Griffin et al., 2004). Such data is indicative of increased interaction between older crust and juvenile components as compared to the dominantly old crustal source discussed earlier. A population of zircons within the Yelma and Chiall Formations (n = 13) also plot within

positive ε_{Hf} space at 2.7 to 2.6 Ga (Figure 14a). The majority of these analyses lie between the depleted mantle and CHUR and range from 2 to 8.5, with a major cluster at ~4. With this in mind, it is suggested that positive ε_{Hf} detrital zircons were sourced predominately from the Murchison Province (Figure 14b), with minor input from the Marymia Inlier.

Palaeoproterozoic detrital zircons from the Yelma Formation are dominated by ε_{Hf} values that lie beneath CHUR in the time frame of 2000 – 1970 Ma (Figure 13b). Unlike Hf isotope values within the Archaean data set, there is no significant cluster of positive ε_{Hf} values, indicating that the magmatic source rock/s were highly evolved. A variety of samples from the Gascoyne Complex exhibit negative ε_{Hf} values similar to that of detrital zircons within the Earaheedy Basin (Figure 13b). In particular, mafic and felsic members of the ca. 1975 Nardoo Granite of the Glenburgh Terrane produce values between -3.86 to -2.55 (Sheppard et al., 2004). These compare well with negative Hf isotope data from 2000– 1970 Ma aged grains in the Yelma Formation, including the youngest detrital grain of 1971±26 Ma. In addition, the small quantity of positive ε_{Hf} 2000 – 1990 Ma grains dated here (i.e. 1993±20 Ma) may correspond with that of ~1900 Ma amphibolite and granulite within the Gascoyne Complex, which yield ε_{Hf} values of 3.64 and 5.92 (GSWA data, unpublished), respectively. This implies that the Gascoyne Complex, and particularly the Glenburgh Terrane, provided 2000 – 1970 Ma zircons to the basal Earaheedy Basin.

Due to a sparsity of 2275 – 2050 Ma aged zircons throughout the Capricorn Orogen, the source of such sediment remains difficult to determine. Five zircons in the Yelma and Chiall Formations yielded ages of ~2271, ~2269, ~2278, ~2250 and ~2215

Ma with ε_{Hf} values from -5.7 to 8.6. These findings do not favour a strictly juvenile or reworked crustal source. Although rare, the Yeelirrie Domain and Narryer Terrane of the Yilgarn Craton contain magmatic zircons within the 2275 – 2050 Ma time frame (Figure 14b) (Griffin et al., 2004). Rare granitoid zircons in the Yeelirrie Domain exhibit a peak at 2.28 Ga. All such zircons have negative ε_{Hf} values that extend to -30 and are indicative of old remelted crust with no juvenile mantle addition (Griffin et al., 2004). Furthermore, Griffin et al. (2004) reports zircons peak ages in silicic granitoids from the Narryer Terrane that cluster at approximately 2.33 Ga. As with the Yeelirrie Domain, the ε_{Hf} signature of such zircons are highly negative (-5 to -18). It is therefore possible that 2275 – 2050 Ma aged zircons with negative ε_{Hf} signatures found in Earaheedy Basin were sourced from the Yeelirrie Domain and the Narryer Terrane (Figure 14b).

Magmatism in the Pilbara at ~2.2 Ga may provide an answer for the source of positive ε_{Hf} zircons in the 2275 – 2050 Ma age range. The Cheela Springs Basalt of the northern Hamersley Province yielded ~2.2 Ga zircons (Martin et al., 1998). Although these zircons have not yet been analysed for hafnium, it is reasonable to assume positive ε_{Hf} values (i.e. juvenile). Therefore, magmatism associated with the Cheela Springs Basalt may have provided some of the 2275 – 2050 Ma aged zircons.

It is important to note that Griffin et al. (2004) obtained Hf isotope analyses from detrital zircons in modern stream sediments within the northern Yilgarn Craton, rather than from rocks. Although it is likely that such streams contain zircons from elsewhere (i.e. the Capricorn Orogen), the reported ages are still considered appropriate indicators of Yilgarn-related provenance of detrital zircons in the Earaheedy Basin. This is based upon two important factors: 1) detrital zircon samples were taken from streams located

solely within distinct domains of the Yilgarn Craton (i.e. Yeelirrie Domain), therefore reflecting bedrock within that domain and 2) samples are dominated by Archaean detrital zircon signatures typical of the Yilgarn Craton. If modern stream sediment was sourced from the Capricorn Orogen itself, zircon ages ranging from 2000 – 1050 Ma, as found within currently exposed regions of the Capricorn Orogen, would be expected.

5.3 Implications for the West Australian Craton and Proterozoic Australia

The Proterozoic marks a period of continental amalgamation in which diverse terranes and crustal fragments formed three distinct Australian cratons (Myers et al., 1996). Early studies suggested that the Proterozoic Australian cratons assembled during a period of orogenesis to form a section of the supercontinent Rodinia at 1330 – 1100 Ma (Myers et al., 1996). In this model the West, North and South Australian Cratons developed separately before assembly. Betts and Giles (2006) proposed an updated model for the 1800 – 1100 Ma evolution of Australia and demonstrated that the Australian cratons are more likely to have amalgamated earlier than suggested by Myers et al. (1996).

The amalgamation of the Australian Cratons is currently associated with the presence of two plate margins that developed along the southern and eastern borders of the North Australian Craton (Betts and Giles, 2006). The first plate margin was situated along the southern border of the North Australian Craton (NAC) and initiated between 1800 – 1600 Ma. The onset of subduction at this plate margin caused surrounding ocean to subduct northwards under the NAC, which itself began to migrate to the south (Figure 14a) (Betts and Giles, 2006). In this model, the 1790 – 1770 Ma Yapungku Orogeny

records the cessation of northwards subduction and the continent-continent collision of the WAC and NAC along the southwestern margin NAC (Figure 14b) (Bagas, 2004). The Capricorn Orogen, Rudall Complex and Arunta Inlier are inferred to record this event (Betts and Giles, 2006; Bagas, 2004). Recent work by Geoscience Australia however, questions the significance, and even instance, of the Yapungku Orogeny (Maidment, 2007). The Gawler Craton later collided with the NAC along the southern margin at 1740 – 1690 Ma (Betts and Giles, 2006).

Maximum depositional ages reported here and by Halilovic (et al., 2004) place sediment deposition within the Earaheedy basin to <1810 Ma. Furthermore, ^{40}Ar-^{39}Ar ages of ~1650 Ma in the deformed northern margin of the Earaheedy Basin constrain basin deformation to 1680 – 1620 Ma during to the Mangaroon Orogeny (Pirajno et al., in press). This contradicts previous tectonic models (i.e. Betts and Giles, 2006; Bagas, 2004), which suggest the formation of the strongly deformed Stanley Fold Belt in the northern Earaheedy Basin occurred during the Yapungku Orogeny. With this in mind, the Yapungku Orogeny cannot have caused cessation of northwards subduction along the southern NAC resulting in the collision of the NA and WA Cratons. Furthermore, the collision of the NAC and WAC may not have occurred until ~1680 – 1620 Ma, coeval with the Mangaroon Orogeny.

Previous studies have suggested that the development of the Earaheedy Basin occurred due to uplift west of the basin during the 1830 – 1780 Ma Capricorn Orogeny (Halilovic et al., 2004). In such models, the uplifted Yilgarn Craton and Glenburgh Terrane were considered the most likely sources for Archaean and Palaeoproterozoic sediment, respectively. The ages presented here are consistent with this notion (Figure

11). Maximum depositional ages and basin deformation place basin development between ~1810 Ma (Halilovic et al., 2004) and the ~1650 Mangaroon Orogeny, which lies within the constraints of the 1830 – 1780 Ma Capricorn Orogeny. However, sediment within the basin dominantly consists of fine grained shales and siltstones and mature quartz sandstones. These sedimentary elements are suggestive of a relatively inactive source terrane rather than an active orogenic belt, which typically sheds thick immature high energy sediment (i.e. Yerrida Foreland Basin; Pirajno et al., 2004). Here, it is suggested that the extensive orogenic activity associated with the Capricorn Orogeny was responsible for the uplift of source terranes. However, the Earaheedy Basin may have formed in a trailing passive margin distal to the orogenic front (Pirajno et al., 2004).

6. Conclusions

1. Depositional Constraints

U-Pb ages of detrital zircons within the Yelma and Chiall Formations of the Earaheedy Basin constrain maximum sediment deposition to 1971±26 and 2068±21 Ma for basal and mid detritus, respectively. These depositional ages are consistent with previously reported constraints, including the ~1843 Ma age of sill intrusion into underlying Yerrida Basin (Rasmussen and Fletcher, 2002) and the ~1810 Ma maximum depositional age of the upper Earaheedy Basin (Halilovic et al., 2004). In addition, ^{40}Ar-^{39}Ar dating of sericite in the Stanley Fold Belt of the northern Earaheedy Basin yields ~1650 Ma (Pirajno et al., in press) Therefore, the 1680 – 1620 Ma Mangaroon Orogeny

provides an upper limit on sediment deposition. These newly defined constraints indicate that deposition occurred over a longer time frame than originally conceived.

2. Provenance

Detrital zircons fall into three distinct populations: 2700 – 2600, 2275 – 2050 and 2000 – 1970 Ma, with the latter only present in the basal Yelma Formation. Archaean aged zircons exhibit similar U-Pb ages and negative hafnium isotopic signatures to the Narryer Terrane in the northwestern Yilgarn Craton. Archaean zircons with positive ε_{Hf} values are similar to the Murchinson Province and Marymia Inlier which lie southwest and northwest of the Earaheedy Basin, respectively. The Yilgarn Craton and adjoining Marymia Inlier are the dominant providers of Archaean aged detrital zircons in the basal to mid Earaheedy Basin.

Palaeoproterozoic detritus within the Yelma Formation lies within the U-Pb range of 2000 – 1970 Ma. The detrital age spectrum and hafnium isotopic composition of this population is consistent with the Nardoo Granite and Dalgaringa Supersuite of the Glenburgh Terrane. 2000 – 1970 Ma zircons in the basal Yelma Formation are likely to be sourced from the Glenburgh Terrarne.

Due to the scarsity of zircon populations within the range of 2275 – 2050 Ma in Western Australia, the source of detritus is difficult to determine. The lack of homogeneity in hafnium isotopic data is also problematic as it does not suggest a strictly juvenile or evolved crustal source. Zircons with negative ε_{Hf} values may be sourced from the Narryer Terrane of the Yilgarn Craton, which exhibits negative ε_{Hf} values. Similar

aged volcanics (2.3 – 2.2 Ga; Kaapvaal Craton) and metamorophism (3700 – 2000; Limpopo Belt) indicate South Africa may have provided Palaeoproterozoic sediment to the Earaheedy Basin during the evolution of the supercontinent Columbia.

Acknowledgements

Firstly I would like to thank my supervisors Alan Collins and Martin Hand for their feedback, discussion and encouragement throughout the year. In particular Alan for putting up with my constant state of stress and putting life into perspective when I got a bit batty and/or deranged.

Special thanks go to Steve Sheppard and Franco Pirajno from the Geological Survey of Western Australia. Steve – I really appreciate everything you have done for me this year, ranging from assisting in the field, answering my endless (and sometimes ridiculous) questions and making me feel at home in Perth. To Franco - the coffee, chocolate and random 'rock tests' during sampling made my last day in the field fun and entertaining.

To Jim Quadrio from Granite Peak Homestead. Thankyou for allowing me to use your property for my project. Further thanks for cooking up rad barbeque and roast dinners which were especially exciting after living off of canned food for two weeks. Keep up the good work and if you ever need help fencing, give me a call.

Hank JP/ Hanky Panky /Mr. Llama Man. Thanks for the skateboarding tips, showing me around Freo in ‘hoes-mans’ pimped out car and giving me a roof over my head during my extended trip to Perth.

To Ms. Horne and Mr. Speed. I thoroughly enjoyed my time with you in Sydney. Your hospitality and kind spirits were refreshing. Diablo forever!

To Angus Netting and Peter Self at Adelaide Microscopy for always lending a helping hand when technology didn’t quite go my way. In particular, thanks to Angas for coming into work on the weekends to fix the CL machine. You’re a champ! I still claim that the CL hates me, even though it’s not actually alive….

Many thanks to Elena Belousova from Macquarie University for assistance during hafnium analyses and Ric Daniel and Saju Menacherry at the Adelaide School of Petroleum for point counting and sandstone mineralogy lessons.

Big shout out to Jessie Davey for showing me how to use ArcMap, bringing in baked goods when our energy levels were low and making us laugh. Watch out for saliva man. He could be hiding under your bed.

Thankyou to CERG for funding, and those who gave me a push in the right direction:

- Katie Howard for everything. Full stop. EVERYTHING! Good luck with your future endeavors sister girlfriend (Marcia Hines style)

- Ben Wade for setting up the laser for me at 8am every morning. Salad fingers represent!
- Justin Payne for lessons on sieving and panning
- Mike Spzunar for helpful tips on how to maintain scientific integrity
- Rod King for calming me during anxiety fits
- Lochie Hallet for being a GIS guru to the max and solving all related problems

To the Matonia posse – Rowena, Rob, Nicole and Bailee – Love to you all. Also to my beautiful cugina Lilo Glazbrook. No-one can make me laugh like you do; thanks for the good times when I've been down to my last two bob.

To my fellow honours compadre Joanna McMahon. Our laughs, cries, crazy behavior and general misadventures have made this year an absolute b-l-a-s-t. 'Kangaroo Club Sensual Kanga' and 'Korl'… I'm laughing thinking about these things. In the words of Peter, Bjorn & John: We don't care about the young folks, talkin' 'bout the young style, and we don't care about the old folks, talkin' 'bout the old style too (if I hear you play that one more time…). Love you to pieces.

Finally, I would like to thank the geo crew who have made the last four years of my life amazing. I wish everyone the best – enjoy your lives and make the most of everyday. I really love you all. It's so cliché, but very true. It's going to be very sad not to see your little faces in my life. "Bless your souls"… You better stay in contact with me or I'll hunt you down.

References

Bagas, L., 2004. Proterozoic evolution of the northwest Paterson Orogen, and assembly of the West and North Australian cratons, Western Australia. Precambrian Research 128, 475 – 496.

Belousova, E.A., Griffin, W.L., O'Reilly, S.Y., 2006. Zircon crystal morphology, trace element signatures and Hf isotope composition as a tool for petrogenic modelling: examples from eastern Australian granitoids. Journal of Petrology 47, 329 – 353.

Betts, P.G., Giles, D., 2006. The 1800 – 1100 Ma tectonic evolution of Australia. Precambrian Research 144, 92 – 125.

Bizzarro, M., Baker, J.A., Haack, H., Ulfbeck, D., Rosing, M., 2003. Early history of Earth's crust-mantle system inferred from hafnium isotopes in chondrites. Nature 421, 931 – 933.

Blichert-Toft, J., Chauvel, C., Albarede, F., 1997. The Lu-Hf geochemistry of chondrites and the evolution of the mantle-crust system. Earth and Planetary Science Letters 148, 243 – 258.

Cawood, P., Tyler, I.M., 2004. Assembling and reactivating the Proterozoic Capricorn Orogen: lithotectonic elements, orogenies and significance. Precambrian Research 128, 201 – 218.

Cawood, P.A., Nemchin, A.A., 2000. Provenance record of a rift basin: U/P ages of detrital zircons from the Perth Basin, Western Australia. Sedimentary Geology 134, 209 – 234.

Cobb, M., Cawood, P.A., Fitzsimons, I., Kinny, P., 2001. SHRIMP U–Pb zircon ages from the Mullingarra Complex, Western Australia: Isotopic evidence for allochthonous blocks in the Pinjarra Orogen and implications for East Gondwana assembly. Geological Society of Australia, Abstracts No. 64, 21–22.

DeBievre, P., Taylor. P., 1993. Table of the isotopic composition of the elements. International Journal of Mass Spectrometry. Ion Processes 123, 149.

Fitzsimons, I.C.W., 2003. Proterozoic basement provinces of southern and south-western Australia, and their correlation with Antarctica. In: Yoshida, M., Windley, B.F., Dasgupta, S. (Eds). Proterozoic East Gondwana —Supercontinent Assembly and Breakup. Geological Society, London 93–129, Special Publication.

Griffin, W.L., Belousova, E.A., Shee, S.R., Pearson, D.J., O'Reilly, S.Y., 2004. Archaean crustal evolution in the northern Yilgarn Craton: U-Pb and Hf-isotope evidence from detrital zircons. Precambrian Research 131, 231 – 282.

Griffin, W.L., Pearson, N.J., Belousova, E., Jackson, S.E., O'Reilly, S.Y., van Achterberg, E., Shee, S.R., 2000. The Hf isotope composition of cratonic mantle: LAM-MC-ICPMS analysis of zircon megacrysts in kimberlites. Geochim. Cosmochim. Acta 64, 133-147.

Halilovic, J., Cawood, P.A., Jones, J.A., Pirajno, F., 2004. Provenance record of the Earaheedy Basin: implications for the assembly of the WA Craton. Precambrian Research 128, 343 – 366.

Hawkesworth, C.J and Kemp, A.I.S., 2006. Using hafnium and oxygen isotopes in zircon to unravel the record of crustal evolution. Chemical Geology 226, 144 – 162.

Hegner, E., Gruler, M., Hann, H.P., Chen, F., Guldenpfenning, M., 2005. Testing tectonic models with geochemical provenance parameters in greywacke. Journal of the Geological Society 162, 87 – 96.

Howard, K.E., Reid, A. J., Hand, M.P., Barovich, K.M., Belousova, E.A., 2007. Does the Kalinjala Shear Zone represent a palaeosuture zone? Implications for distribution of styles of Mesoproterozoic mineralisation in

the Gawler Craton, Minerals and Energy South Australia Journal 43, 16-20.

Jackson, S.E., Pearson, N.J., Griffin, W.L., Belousova, E.A., 2004. The application of laser ablation-inductively coupled plasma-mass spectrometry to in-situ U-Pb zircon geochronology. Chemical Geology 211, 47 – 69.

Kinny, P., Nutman, A.P., Occhipinti, S.A., 2004. Reconnaissance dating of events recorded in the southern part of the Capricorn Orogen. Precambrian Research 128, 279 – 294.

Libby, W.G., de Laeter, J.R., Myers, J.S., 1986. Geochronology of the Gascoyne Province. Western Australia Geological Survey Report 50, p. 31.

Ludwig, K.R., 2003. User's Manual for Isoplot 3.00. Berkeley Geochronological Center, Special Publication No.4, p. 71.

Maidment, D., 2007. New timing constraints on the evolution of the Rudall Complex, Western Australia – Implications for Proterozoic Reconstructions. Structural Geology and Tectonics Specialist Group of the Geological Society of Australia Conference, Alice Springs, 9-13th July 2007, p. 32.

Martin, D.McB., Thorne, A.M., 2004. Tectonic setting and basin evolution of the Bangemall Supergroup in the northwestern Capricorn Orogen. Precambrian Research 128, 385 – 409.

Martin, D.McB., 1998. Lithostratigraphy and structure of the Palaeoproterozoic Padbury Group, Milgun 1:100 000 sheet, Western Australia. Western Australia Geological Survey, Report 62, p. 57.

McLennan, S.M., Hemming, S., McDaniel, D.K., Hanson, G.N., 1993. Geochemical approaches to sedimentation, provenance and tectonics. Geological Society of America, Special Paper 284, 21 – 40.

Morton, A.C., Hallsworth, C.R., 1999. Processes controlling the composition of heavy mineral assemblages in sandstones. Sedimentary Geology 124, 3-29.

Morton, A.C., 1991. Geochemical studies of detrital heavy minerals and their application to provenance studies. In: Morton, A.C., Todd, S.P., and Haughton, P.D.W., (eds.) Developments in Sedimentary Provenance. Volume 57, Geological Society of London, Special Publication, 31-45.

Myers, J.S., Hocking, R.M., 1998. Geological map of Western Australia, 1:250,000, 13th ed. Western Australia Geological Survey.

Myers, J.S., Shaw, R.D., Tyler, I.M., 1996. Tectonic evolution of Proterozoic Australia. Tectonics 15, 1431 – 1446.

Nelson, D.R., 2001. Compilation of SHRIMP U–Pb Zircon Geochronology Data, 2000: GSWA, Record 2001/2, 72–74.

Nutman, A.P., Bennet, V.C., Kinny, P.D. and Price, R., 1993. Large-scale crustal structure of the northwestern Yilgarn Craton, Western Australia: evidence from Nd isotopic data and zircon geochronology. Tectonics 12, 971–981.

Occhipinti, S.A., Sheppard, S., Passchier, C., Tyler, I.M., Nelson, D., 2004. Palaeoproterozoic crustal accretion and collision in the southern Capricorn Orogen. The Glenburgh Orogeny. Precambrian Research 128, 237- 255.

Occhipinti, S.A., Sheppard, S., Nelson, D.R., Myers, J.S., Tyler, I.M., 1998. Syntectonic granite in the southern margin of the Palaeoproterozoic Capricorn Orogen, Western Australia. Aust. J. Earth Sci. 45, 509–512.

Payne, J.L., Barovich, K.M., Hand, M., 2006. Provenance of metasedimentary rocks in the northern Gawler Craton, Australia: Implications for Palaeoproterozoic reconstructions. Precambrian Research 148, 275 – 291.

Pirajno, F., Hocking, R., Reddy, S., Jones, A., (in press). The geology and mineral systems of the Palaeoproterozoic Earaheedy Basin, Western Australia.

Pirajno, F., Jones, J.A., Hocking, R.M., Halilovic, J., 2004. Geology and tectonic evolution of Palaeoproterozoic basins of the eastern Capricorn Orogen, Western Australia. Precambrian Research 128, 315 – 342.

Pirajno, F., Jones, J.A., Hocking, R.M., Halilovic, J., 2002. Geology, tectonic evolution and mineralisation of Palaeoproterozoic basins of the eastern Capricorn Orogen,

Western Australia, in Geoscience 2002: expanding Horizons edited by V.P. Preiss:16th Australian Geological Convention, Adelaide, S.A., July 2002; Geological Society of Australia, Abstracts Volume, no. 67, p. 141.

Rasmussen, B., Fletcher, I.R., Sheppard, S., 2005. Isotopic dating of the migration of low-grade metamorphic front during orogenesis. Geology 33, 773-776

Rasmussen, B. & Fletcher, I.R., 2002. Indirect dating of mafic intrusions by SHRIMP U-Pb analysis of monazite in contact metamorphosed shale: an example from the Palaeoproterozoic Capricorn Orogen, Western Australia. Earth Planet. Sci. Lett. 197, 287 – 299.

Scherer, E., Munker, C., Mezger, K., 2001. Calibration of the lutetium-hafnium clock. Science 293, 683 – 687.

Sheppard, S., Rasmussen, B., Muhling, J.R., Farrell, T.R., Fletcher, I.R., 2007. Grenvillian-aged orogenesis in the Palaeoproterozoic Gascoyne Complex, Western Australia: 1030 – 950 Ma reworking of the Proterozoic Capricorn Orogen. Journal of Metamorphic Geology 25, 477 – 494.

Sheppard, S., Occhipinti, S.A., Nelson, D.R., 2005. Intracontinental reworking in the Capricorn Orogen Western Australia: The 1680 – 1620 Ma Mangaroon Orogeny. Journal of Earth Sciences 52, 443 – 460.

Sheppard, S., Occhipinti, S.A., Tyler, I.M., 2004. A 2005 – 1970 Ma Andean-type batholith in the southern Gascoyne Complex, Western Australia. Precambrian Research 128, 257 – 277.

Sircombe, K.N., 2004. AgeDisplay: an EXCEL workbook to evaluate and display univariate geochronological data using binned frequency histograms and probability density distributions. Computers & Geosciences 30, 21-31.

Smithies, R.H., Bagas, L., 1997. High pressure amphibolite-granulite facies metamorphism in the Palaeoproterozoic Rudall Complex, central Western Australia. Precambrian Research 83, 243 – 265.

Tyler, I.M. and Thorne, A.M., 1990. The northern margin of the Capricorn Orogen, Western Australia—an example of an Early Proterozoic collision zone. J. Struct. Geol. 12, 685–701. Abstract

Van Achterbergh, E., Ryan, C.G., Jackson, S.E., Griffin, W.L., 2001. Data reduction software for LA-ICP-MS. In: Sylvester P (ed) Laser-ablation-ICPMS in the earth sciences: principles and applications. Mineralogical Association of Canada, Short Course 29, pp 239–243

Vervoort, J.D., Patchett, P.J., Blichert-Toft, J., Albarede, F., 1999. Relationship between Lu-Hf and Sm-Nd isotopic systems in the global sedimentary system. Earth and Planetary Science Letters 168, 79 – 99.

Watkeys, M.K., Light, M.P.R., Broderick, T.J., 1983. A retrospective view of the Central Zone of the Limpopo Belt, Zimbabwe. Geol. Soc. S.Afr., Spec. Publ.8: 65 – 80.

Williams, G.E., Schmidt, P.W., Clark, D.A., 2004. Palaeomagnetism of iron-formation from the late Palaeoproterozoic Frere Formation, Earaheedy Basin, Western Australia: palaeogeographic and tectonic implications. Precambrian Research 128, 367 – 383

Zhao, G., Cawood, P.A., Wilde, S.A., Sun, M., 2002. Review of global 2.1 – 1.8 Ga orogens: implications for a pre-Rodinia supercontinent. Earth Sciences Review 59, 125 – 162.

Figure Captions

Figure 1. Map of the Capricorn Orogen showing the location of the main tectonic units in colour. Grey denotes areas that not are classified as part of the orogen but are integral in the understanding of the West Australian Craton. Archaean Cratons are defined by crosses. Areas outlined in black and void of colour define post-Proterozoic cover. Modified after Myers and Hocking (1998).

Figure 2. Simplified map of the Earaheedy Basin. The Yerrida Basin and Marymia Inlier represent adjoining tectonic units of the Capricorn Orogen. The Archaean Yilgarn Craton and the post-Proterozoic Officer and Gunbarrel Basins are also shown. Sample locations are indicated by blue (Yelma Formation) and pink (Chiall Formation) stars. Boundaries adapted from Pirajno et al., (2004).

Figure 3. Stratigraphic column of the Earaheedy Group, Earaheedy Basin, demonstrating known ages and rock types. Detrital zircons from Halilovic et al. (2004) represent maximum depositional ages. Detrital zircons from Matonia (2007) represent maximum depositional ages obtained from this study. Monazites from Rasmussen and Fletcher (2002) represent the age at which sills intruded into wet sediment of the Yerrida Basin, which unconformably underlies the basal Earaheedy Basin. Adapted from Halilovic et al., (2004).

Figure 4. 1:25,000 Geological Map from a section of the northern Earaheedy Basin, Capricorn Orogen. Insets include a map of interpreted bedrock geology, a diagrammatic cross section and stereonet projection of local folding.

Figure 5. Images of local geology including (a) banded purple-white fine grained siltstone (b) quartz clasts in conglomeratic ironstone (c) mud-cracks in banded ironstone (d) cross bedded medium grained sandstone (e) a small-scale fold in the limb of large synclinal structure, showing the hinge and dip/dip direction of folded beds (e) quartz vein cropping out between highly weathered siltstone formation.

Figure 6. Microscopic images of the petrological composition of sandstone samples from the Earaheedy Basin. (a) Medium grained monocrystalline detrital quartz fragments set in a clay rich matrix; interpreted as a sub-arkose sandstone. Sample GSWA 189735. (b) Coarse grained monocrystalline quartz showing replacement of clay matrix by quartz over-growth; interpreted as a quartz arenite sandstone. Sample GSWA 189743. (c) Fine grained sub-litharenite showing hematite inclusions and monocrystalline quartz fragments. Sample GSWA 189712. (d) Medium grained sub-litharenite consisting of mono- and polycrystalline quartz. Sample GSWA 189742.

Figure 7. Cathodoluminescence images of zircon grains from samples within the Yelma and Chiall Formations. The red circle represents the laser ablation position;

adjoining text indicates the age and error obtained from the zircon and the associated spot number. Grains shown are concordant (>90%) and indicative of the population of zircon ages in source terranes.

Figure 8. U-Pb concordia plots of single detrital zircons from sandstones in the (a,b) Yelma Formation and (b,c) Chiall Formation of the Earaheedy Basin. Grains shown are less than 10% discordant, with *n* = number of concordant analyses/total number of analyses. Error ellipses are at the 68.3% confidence interval. Inset U-Pb concordia plots show all data obtained for the corresponding sample, including discordant analyses.

Figure 9. U-Pb zircon frequency and probability histograms of (a,b) Yelma Formation and (c,d) Chiall Formation. Probability plots shaded dark grey represent grains that are less than 10% discordant with arrows indicating peak ages within the data set. Probability plots shaded light grey indicate all data. Red bars indicate the amount of concordant analyses within a particular bin (bin width = 25 Ma).

Figure 10. ε_{Hf} versus time (Ma) diagrams: (a) Combined ε_{Hf} data from the Yelma and Chiall Formations with the green arrow indicating recycling of old crust and (b) ε_{Hf} data from separate samples of the Yelma and Chiall Formations displayed comparatively. A legend is presented to enable differentiation between data obtained from specific samples.

Figure 11. Comparative U-Pb zircon probability histograms of samples from the Earaheedy Basin with possible source terranes. Grains shown are less than 10% discordant. Red dashed lines indicate peak detrital ages to be compared.

(a) Comparison of the Archaean ages in the Yelma and Chiall Formations with various domains in the Yilgarn Craton. U-Pb detrital signatures from the Marymia Inlier, which adjoins the Earaheedy Basin to the northwest, are also presented. U-Pb data from the Yilgarn Craton and Marymia Inlier is adapted from Griffin et al., (2004).

(b) Comparison of Palaeoproterozoic ages in the Yelma Formation with the Glenburgh Terrane of the Gascoyne Complex. Data from the Gascoyne Complex is from S. Sheppard (pers. comm., 2007).

(c) Model inter-relating the detrital signatures from the Yilgarn Craton and Glenburgh Terrane with a possible depositional model.

Figure 12. Diagrams indicating potential source regions of 2275 – 2050 Ma aged detrital zircons within the Earaheedy Basin. Boundaries are derived from Zhao et al. (2002).

(a) A model of the 1.8 – 1.3 Ga supercontinent Columbia as proposed by Zhao et al. (2002), with the red square indicating the position of the West Australian Craton in relation to the South African Craton.

(b) Map of the Pilbara Craton and Capricorn Orogen of West Australia in relation to the Kaapvaal and Zimbabwe Cratons and Limpopo Orogen of South

Africa. The blue star represents the position of the Earaheedy Basin as compared with potential source regions.

Figure 13. Comparative ε_{Hf} versus time (Ma) diagrams of samples from the Yelma and Chiall Formations with the (a) Yilgarn Craton and (b) Gascoyne Complex. ε_{Hf} data from the Yilgarn Craton is from Griffen et al., (2004). ε_{Hf} values from the Gascoyne Complex are derived from ε_{Nd} data from S. Sheppard (pers. comm., 2007). Discordant (>10%) grains are not used. Grey bands indicate the position of dominant ε_{Hf} trends across samples.

Figure 14. ε_{Hf} versus time (Ma) diagrams of (a) samples from the Yelma and Chiall Formations and (b) samples within distinct domains of the Yilgarn Craton, indicating the Narryer Terrane, Murchinson Province and Yeelirrie Domian are probable source terranes for Archaean detrital zircons in the Earaheedy Basin.

Figure 15. Model of the 1.79 – 1.76 construction of Proterozoic Australia, proposed by Betts and Giles (2006). (a) Northwards subduction of ocean under the NAC causing collision of the NAC with the Rudall Complex (b) Halilovic et al. (2004) and Betts and Giles (2006) propose that the amalgamated WAC collided with the Rudall Complex during the 1790 Ma – 1760 Ma Yapungku Orogeny, causing the formation of the Stanley Fold Belt in the northern Earaheedy Basin.

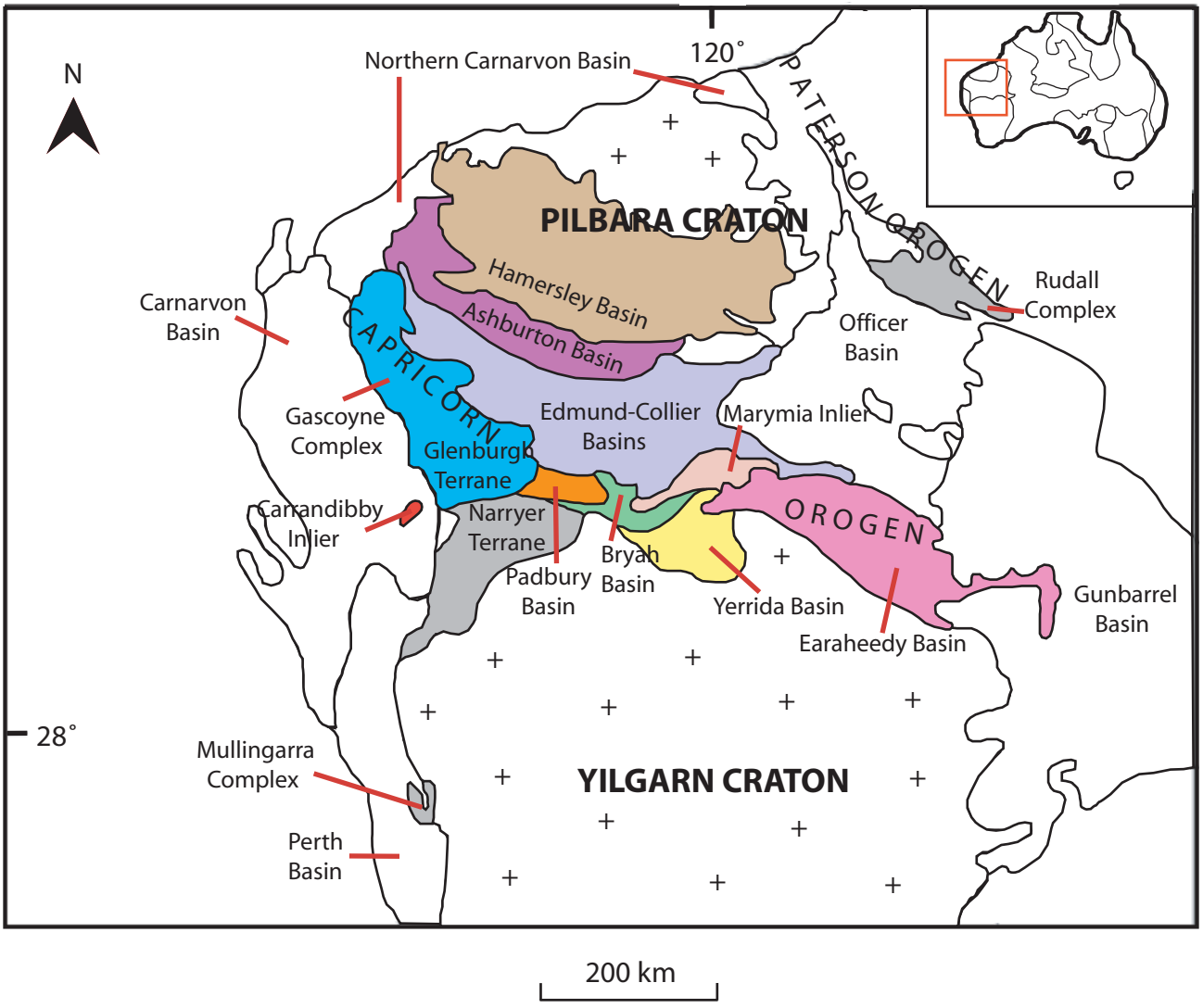
N
120°
28°
Northern Carnarvon Basin
PATERSON OROGEN
PILBARA CRATON
Hamersley Basin
Ashburton Basin
Carnarvon Basin
CAPRICORN
Gascoyne Complex
Glenburgh Terrane
Edmund-Collier Basins
Marymia Inlier
Officer Basin
Rudall Complex
Carrandibby Inlier
Narryer Terrane
Padbury Basin
Bryah Basin
Yerrida Basin
OROGEN
Earaheedy Basin
Gunbarrel Basin
Mullingarra Complex
YILGARN CRATON
Perth Basin
200 km

Figure 1

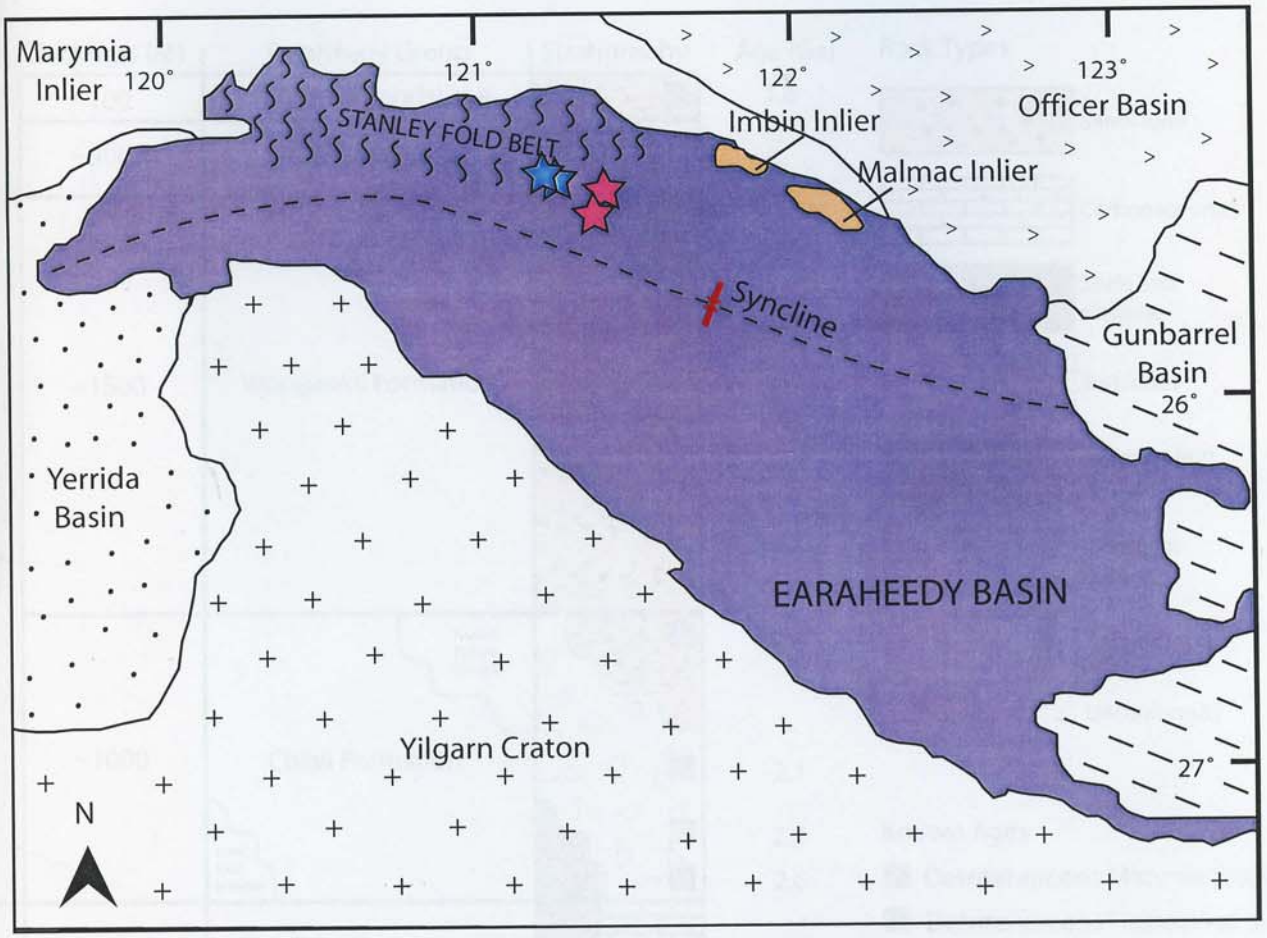
Marymia Inlier
120°
121°
122°
123°
Officer Basin
STANLEY FOLD BELT
Imbin Inlier
Malmac Inlier
Syncline
Gunbarrel Basin
26°
Yerrida Basin
EARAHEEDY BASIN
Yilgarn Craton
27°
N
100 km
Sample: Yelma Formation
Sample: Chiall Formation
Deformation

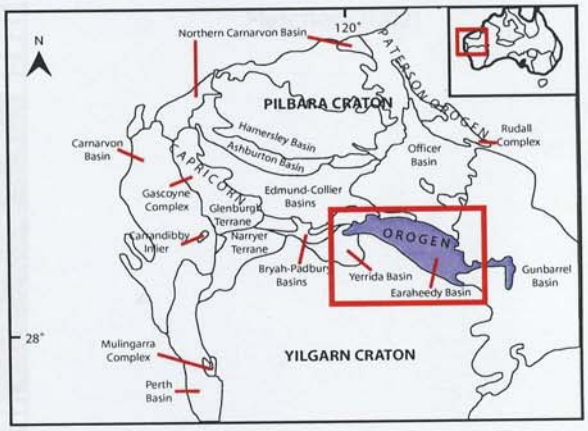
N
Northern Carnarvon Basin
120°
PATERSON OROGEN
PILBARA CRATON
Hamersley Basin
Ashburton Basin
Carnarvon Basin
Officer Basin
Rudall Complex
Gascoyne Complex
Edmund-Collier Basins
Glenburgh Terrane
Narryer Terrane
Yarandibby Inlier
OROGEN
Bryah-Padbury Basins
Yerrida Basin
Earaheedy Basin
Gunbarrel Basin
28°
Mulingarra Complex
YILGARN CRATON
Perth Basin

Figure 2

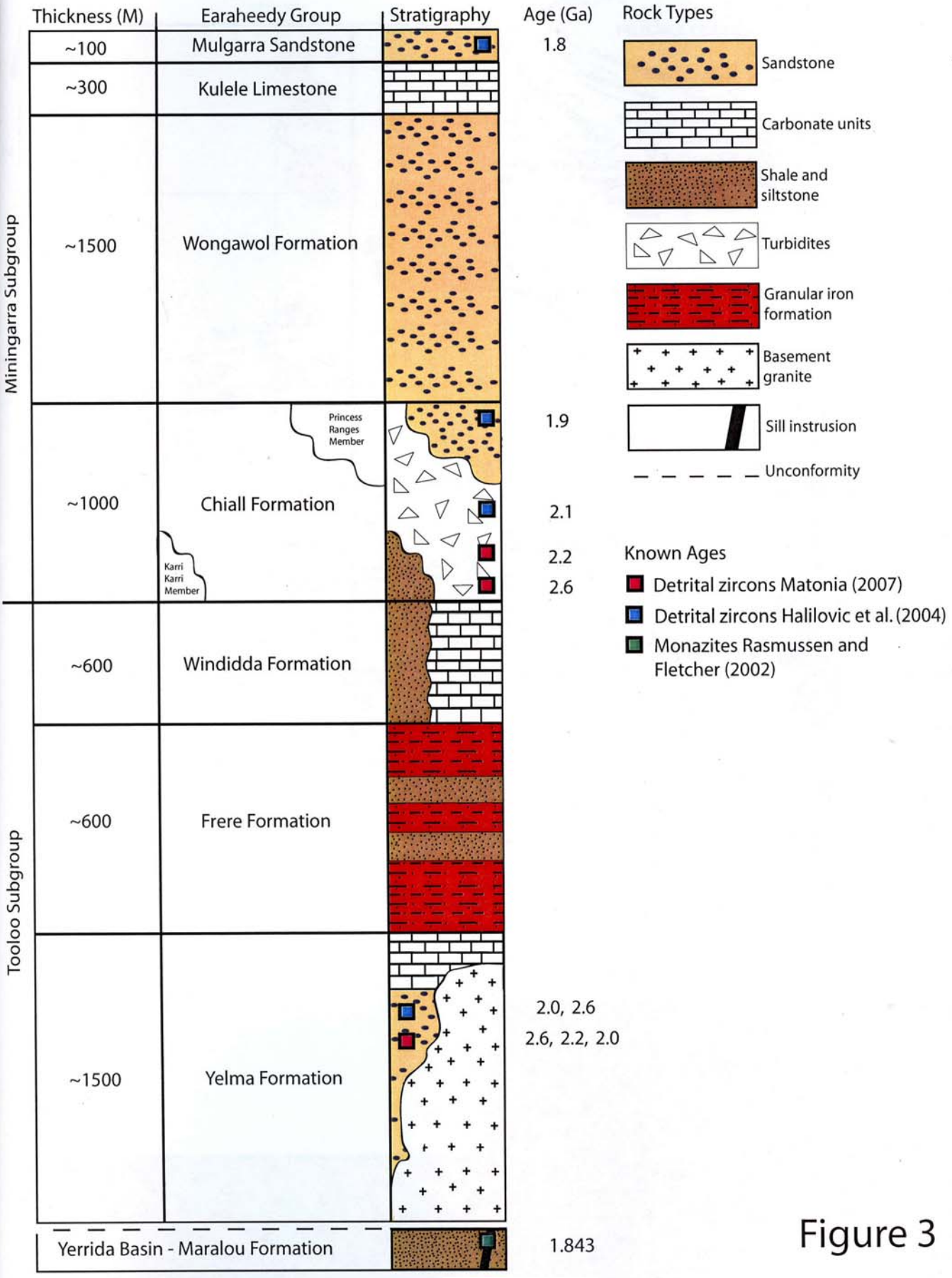
Thickness (M)
Earaheedy Group
Stratigraphy
Age (Ga)
Rock Types
~100
Mulgarra Sandstone
1.8
~300
Kulele Limestone
~1500
Wongawol Formation
Miningarra Subgroup
~1000
Chiall Formation
Princess Ranges Member
Karri Karri Member
1.9
2.1
2.2
2.6
~600
Windidda Formation
~600
Frere Formation
Tooloo Subgroup
~1500
Yelma Formation
2.0, 2.6
2.6, 2.2, 2.0
Yerrida Basin - Maralou Formation
1.843
Sandstone
Carbonate units
Shale and siltstone
Turbidites
Granular iron formation
Basement granite
Sill instrusion
Unconformity
Known Ages
Detrital zircons Matonia (2007)
Detrital zircons Halilovic et al. (2004)
Monazites Rasmussen and Fletcher (2002)

Figure 3

1:25,000 Geological Map of the Northern Earaheedy Basin

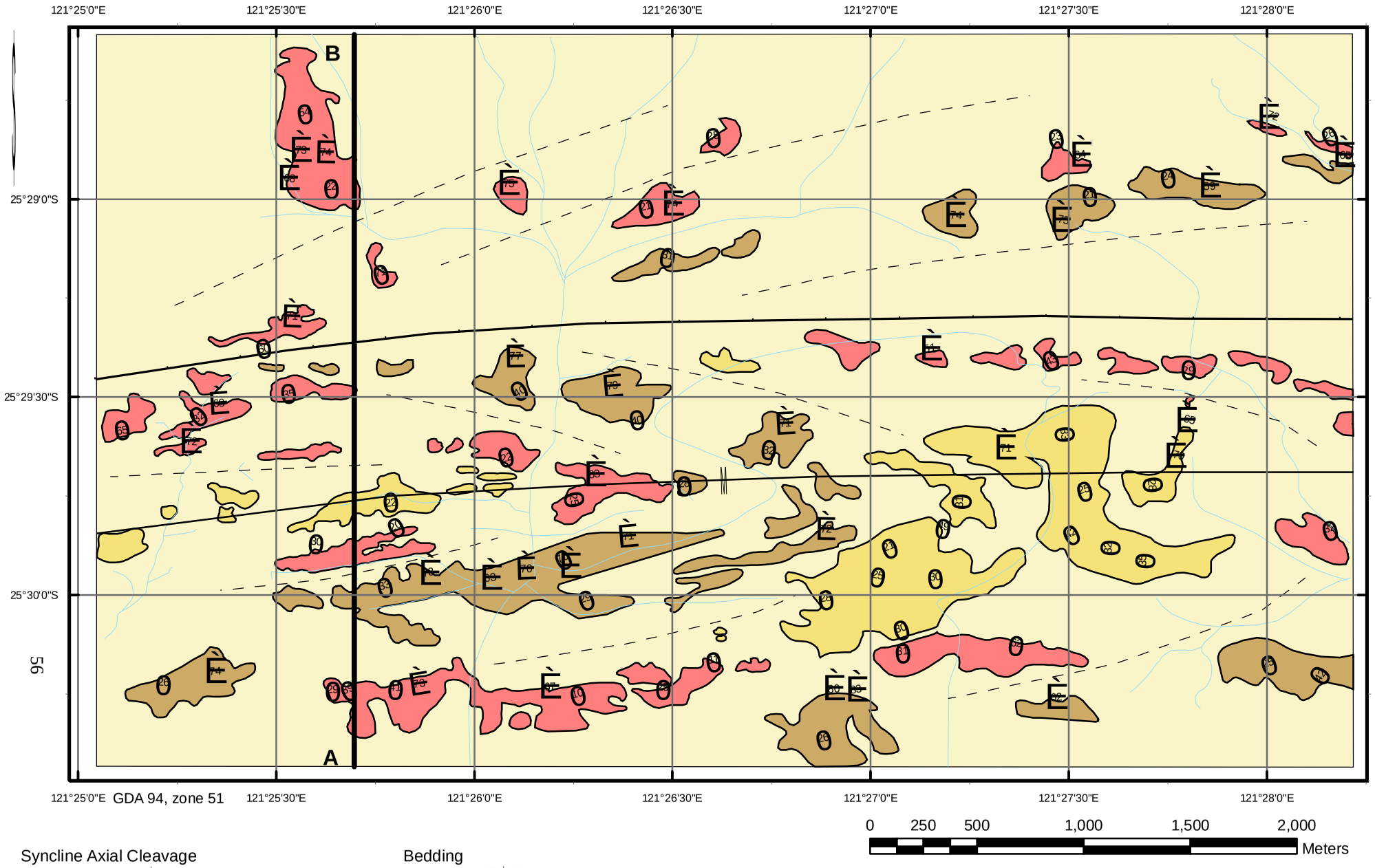

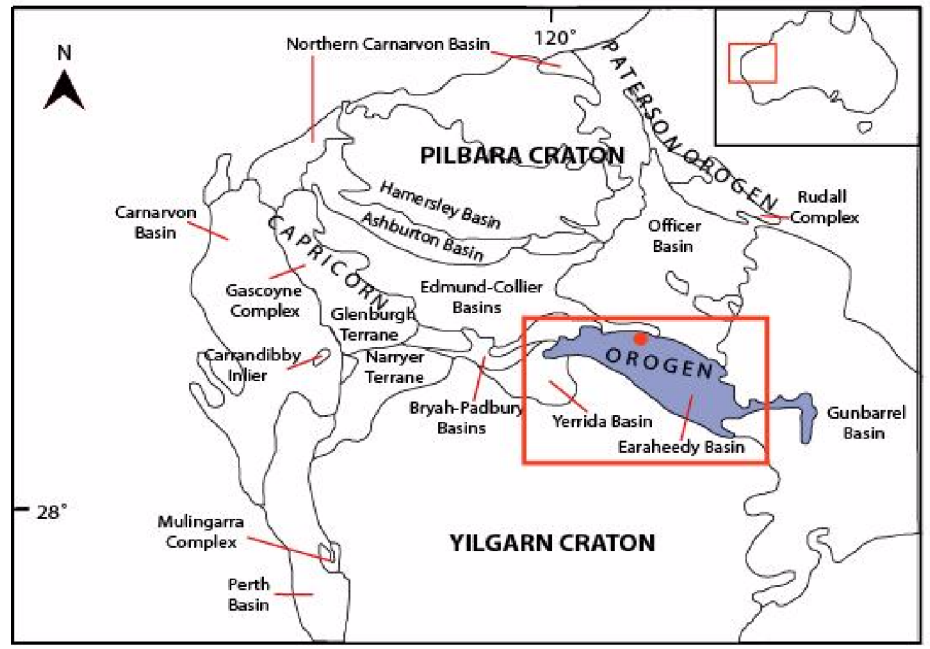

Stratigraphic Column

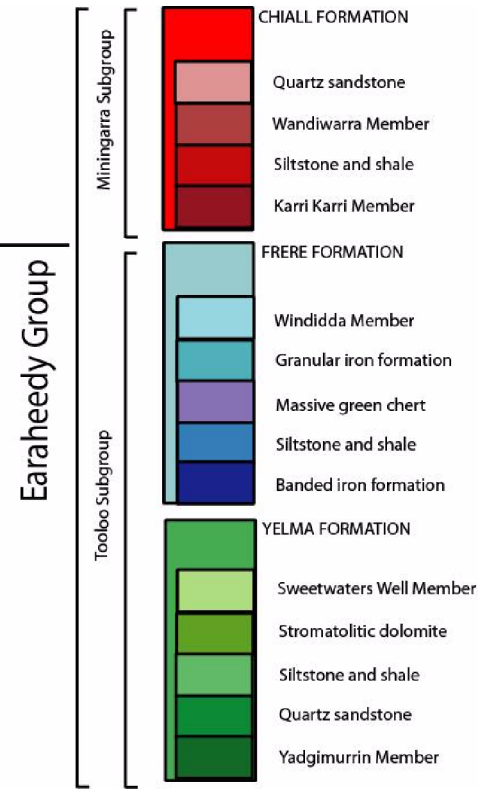

Map Units

- Laminar iron formation with intercalated layers of siliceous sandstone and siltstone
- Medium grained well sorted quartz arenitesandstone; compositional maturity; minor cross bedding
- Siltstone and shale; red to brown; very fine grained with minor bimodal purple-white laminations; deformed; coarsening upwards
- Cover sequences

Structure Key

- Bedding, inclined
- Cleavage, inclined
- Interpreted bedding trends
- Reverse fault
- Syncline
- Drainage

Syncline Axial Cleavage

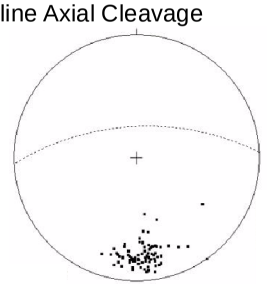

Bedding

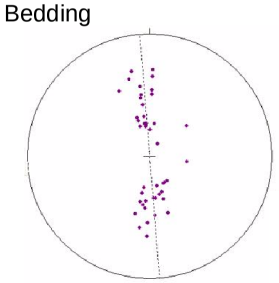

Diagrammatic Cross Section

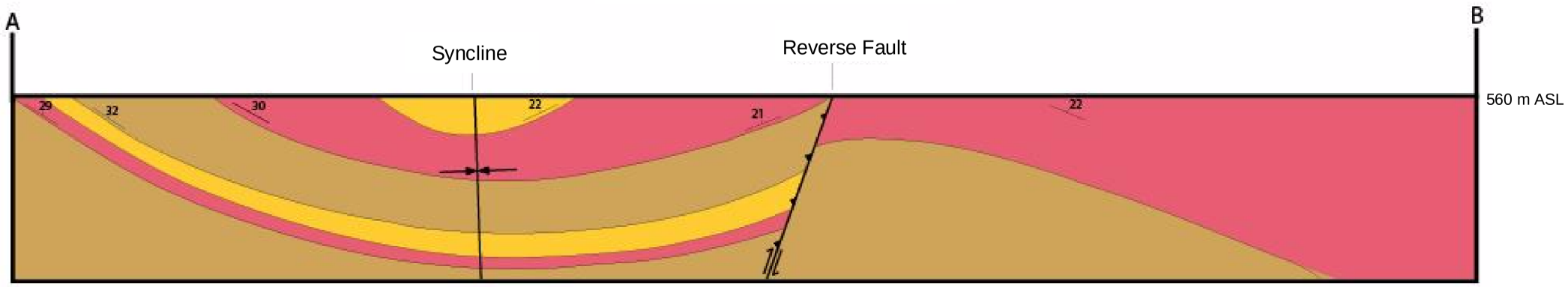

Interpreted Bedrock Geology

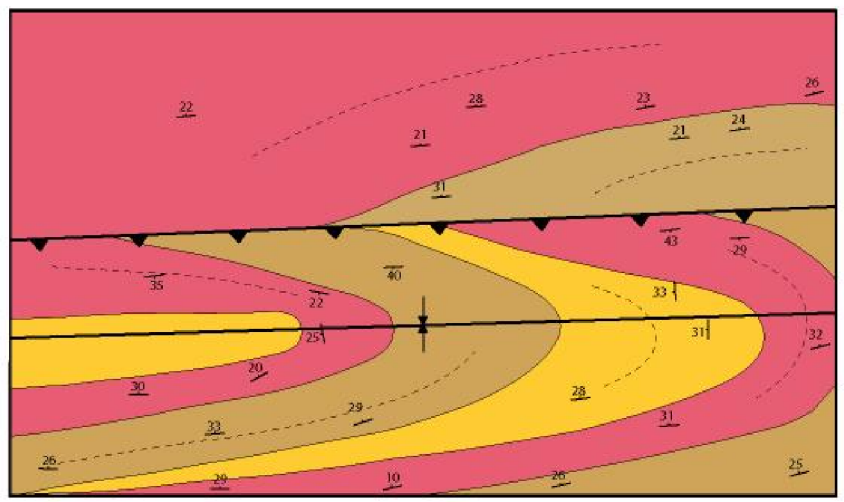

Figure 4

Figure 5

a)

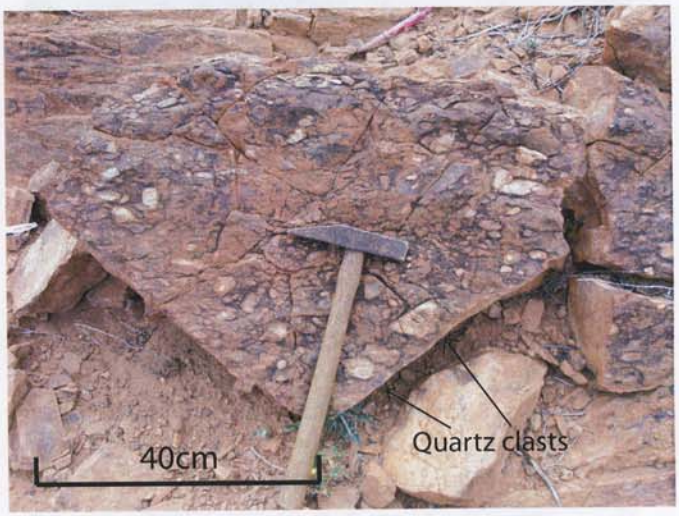

b)

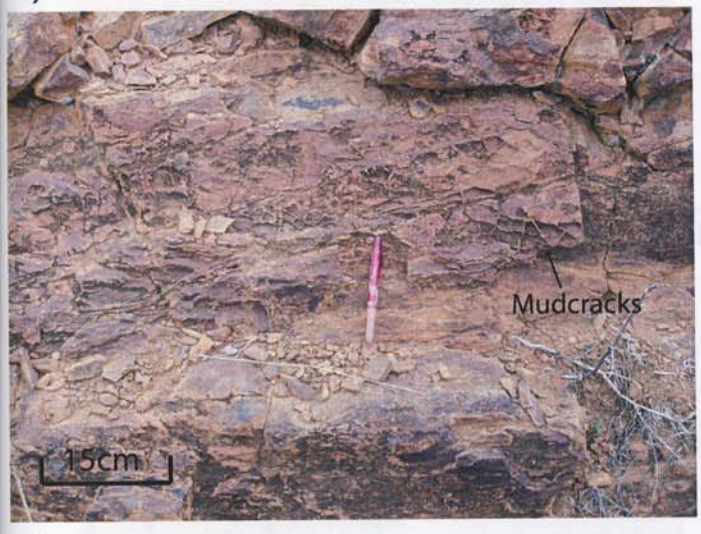

c)

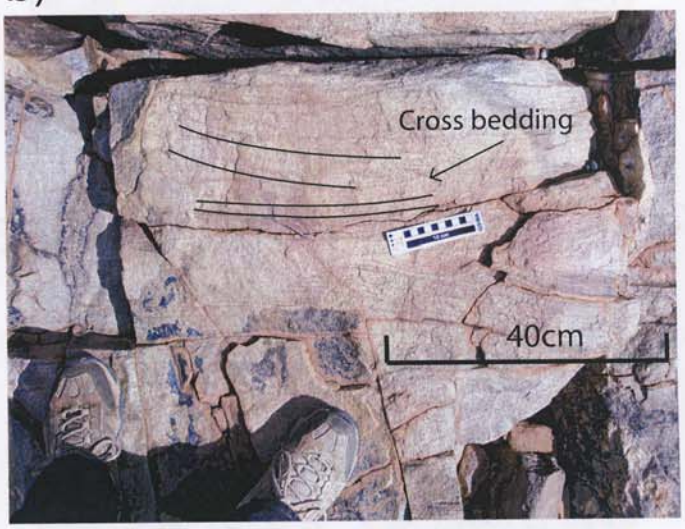

d)

e)

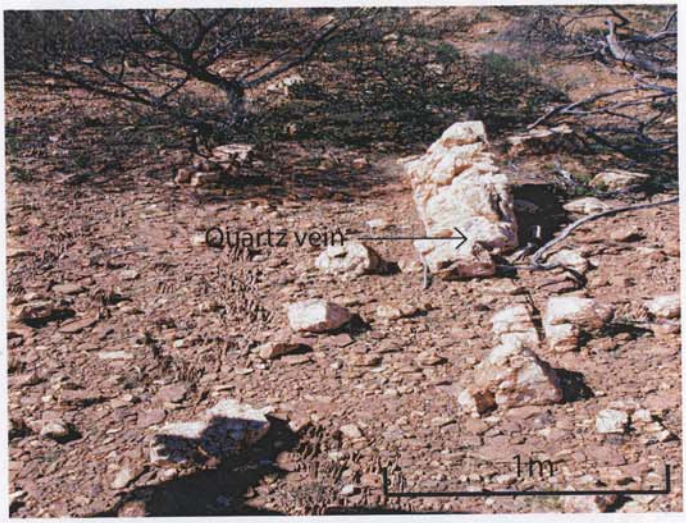

f)

Figure 6

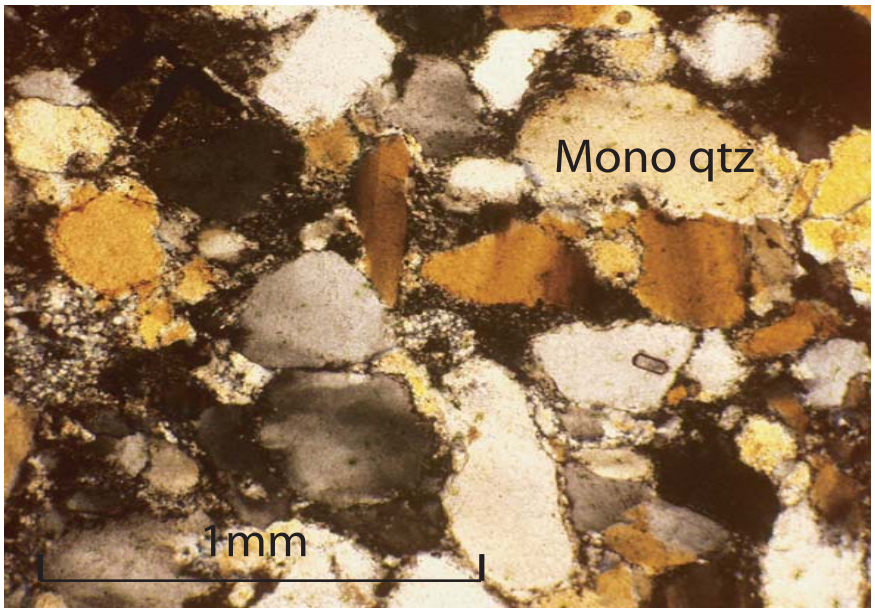

a)

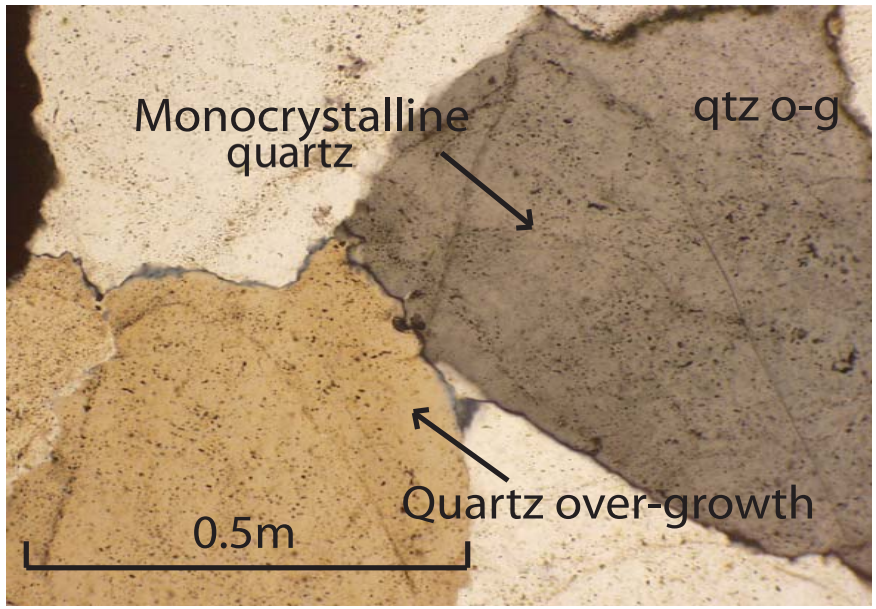

b)

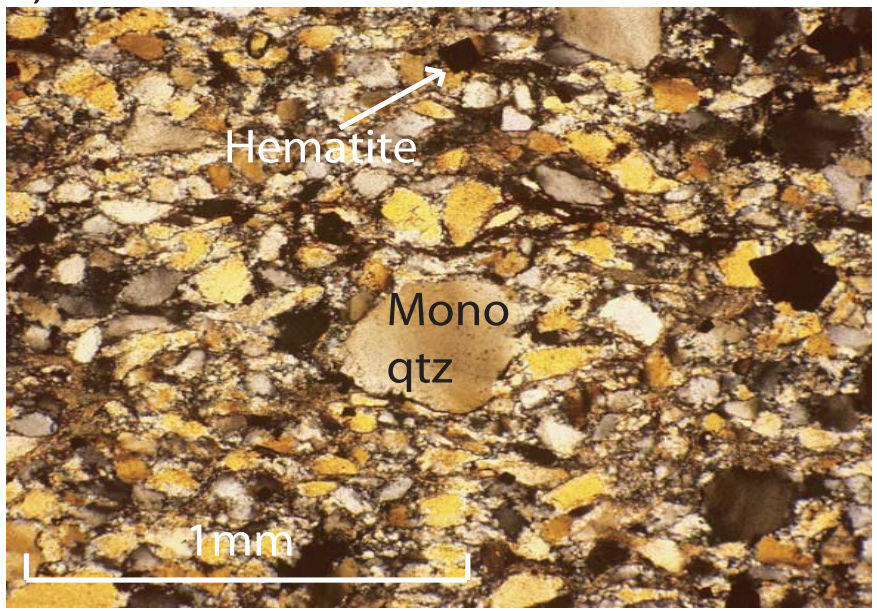

c)

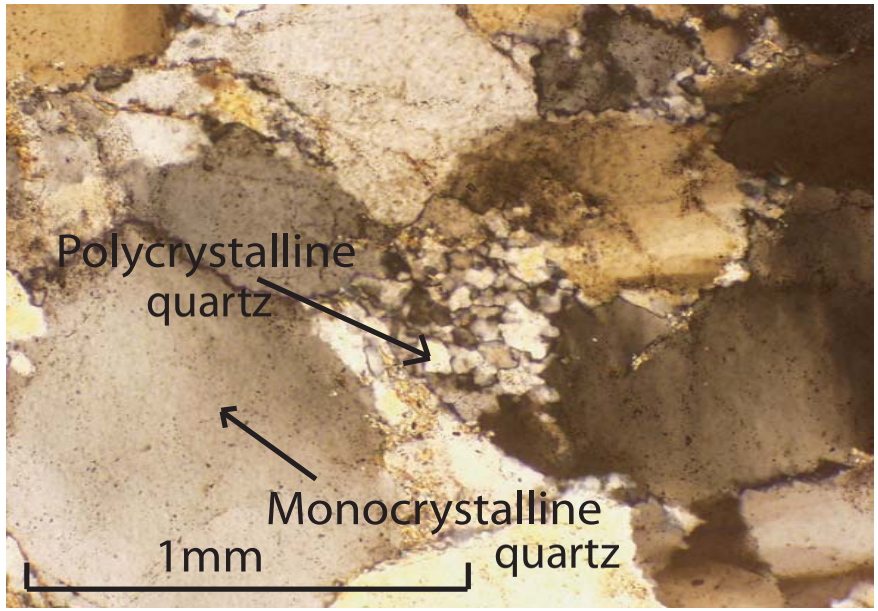

d)

Figure 7

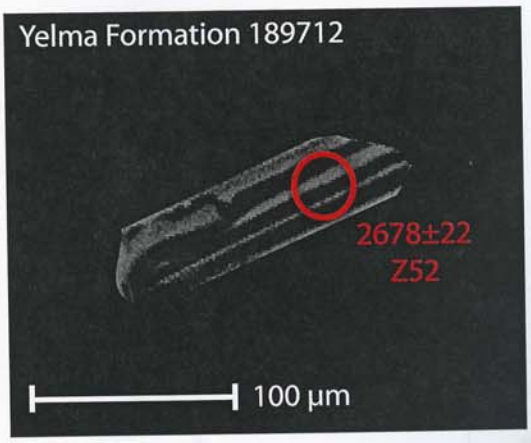
Yelma Formation 189712
2678±22
Z52
100 µm

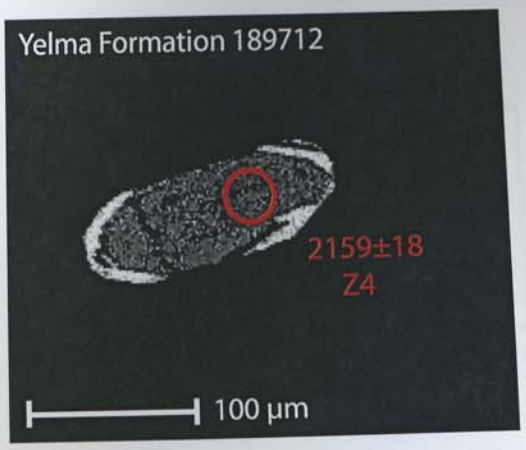
Yelma Formation 189712
2159±18
Z4
100 µm

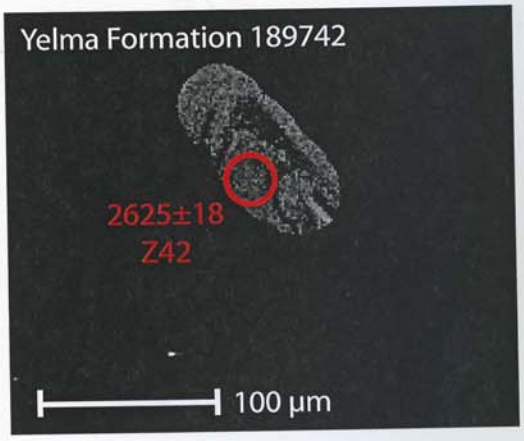
Yelma Formation 189742
2625±18
Z42
100 µm

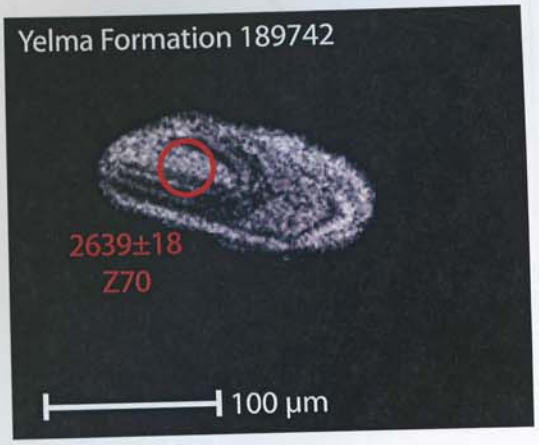
Yelma Formation 189742
2639±18
Z70
100 µm

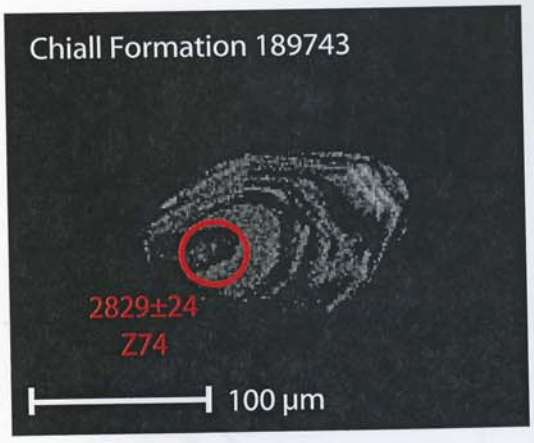
Chiall Formation 189743
2829±24
Z74
100 µm

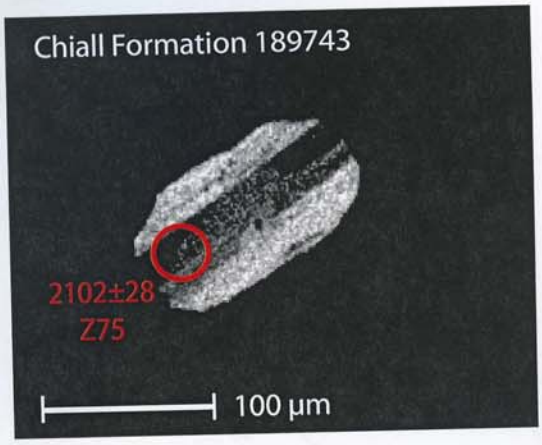
Chiall Formation 189743
2102±28
Z75
100 µm

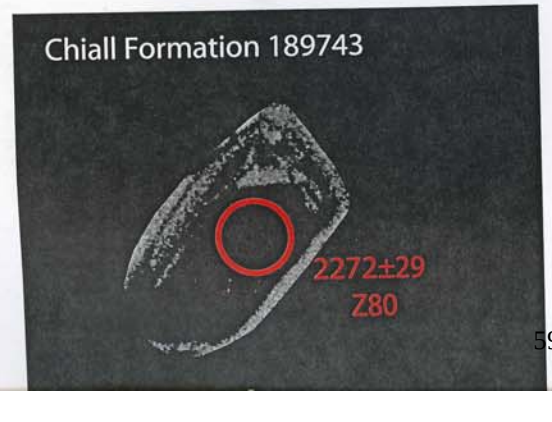
Chiall Formation 189743
2272±29
Z80


Chiall Formation 189735
2681±19
Z4
100 µm

Figure 8

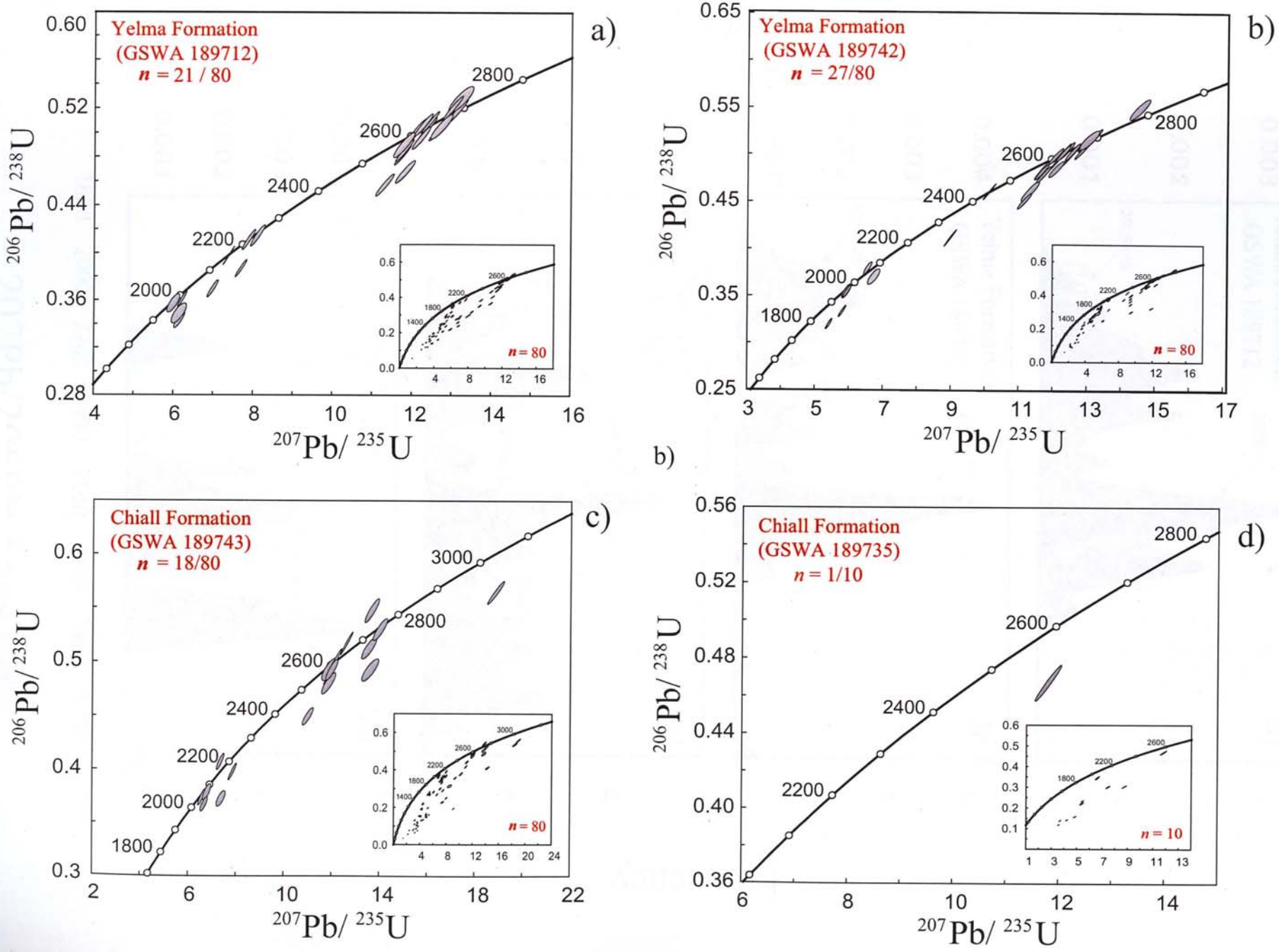
a)
Yelma Formation
(GSWA 189712)
n = 21 / 80
206Pb/ 238U
207Pb/ 235U
n = 80
b)
Yelma Formation
(GSWA 189742)
n = 27/80
206Pb/ 238U
207Pb/ 235U
n = 80
c)
Chiall Formation
(GSWA 189743)
n = 18/80
206Pb/ 238U
207Pb/ 235U
n = 80
d)
Chiall Formation
(GSWA 189735)
n = 1/10
206Pb/ 238U
207Pb/ 235U
n = 10

Figure 9

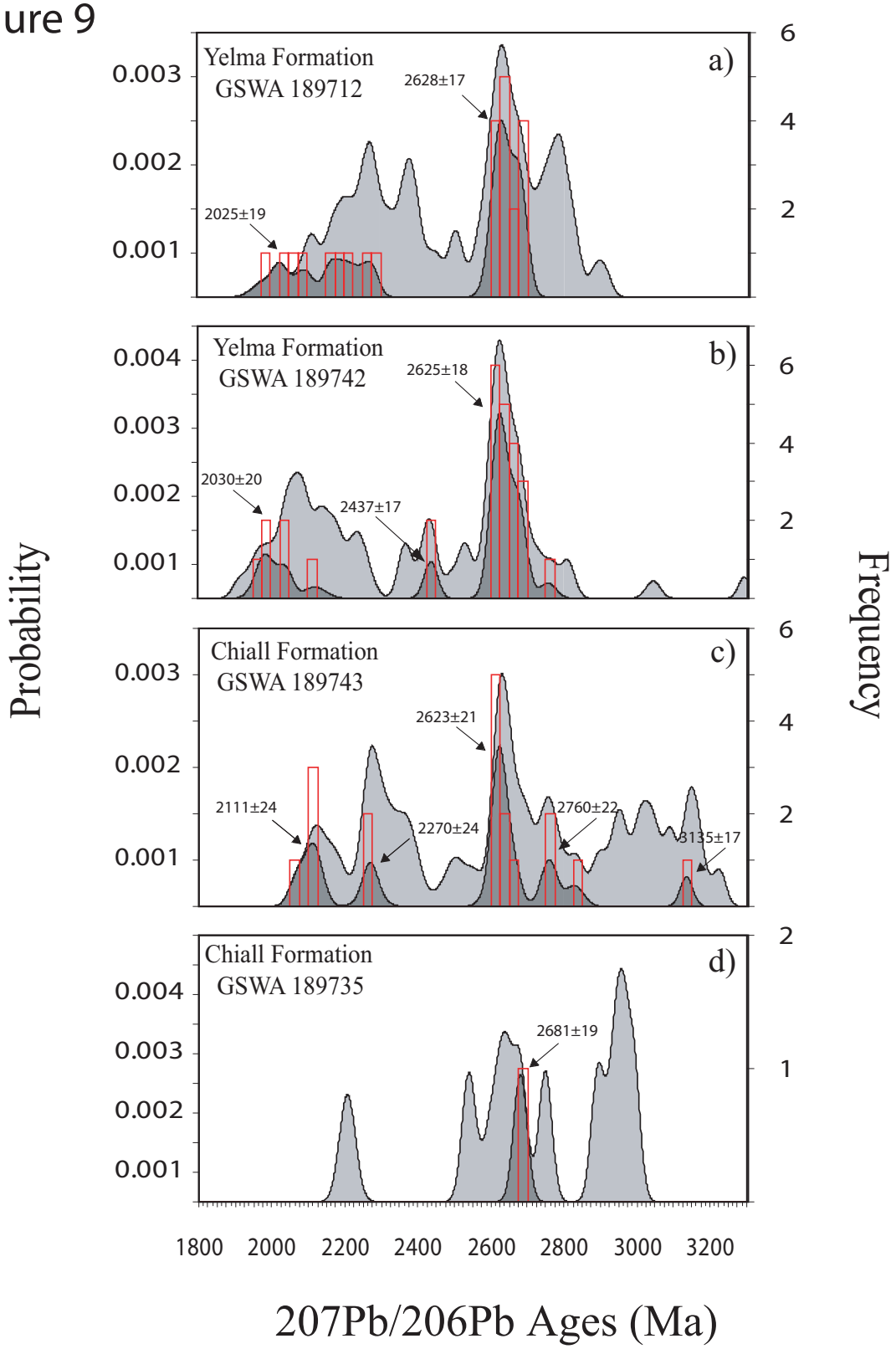
Yelma Formation
GSWA 189712
a)
2628±17
2025±19
Yelma Formation
GSWA 189742
b)
2625±18
2030±20
2437±17
Chiall Formation
GSWA 189743
c)
2623±21
2111±24
2270±24
2760±22
3135±17
Chiall Formation
GSWA 189735
d)
2681±19
Probability
Frequency
0.001
0.002
0.003
0.004
2
4
6
1
1800
2000
2200
2400
2600
2800
3000
3200
207Pb/206Pb Ages (Ma)

Figure 10

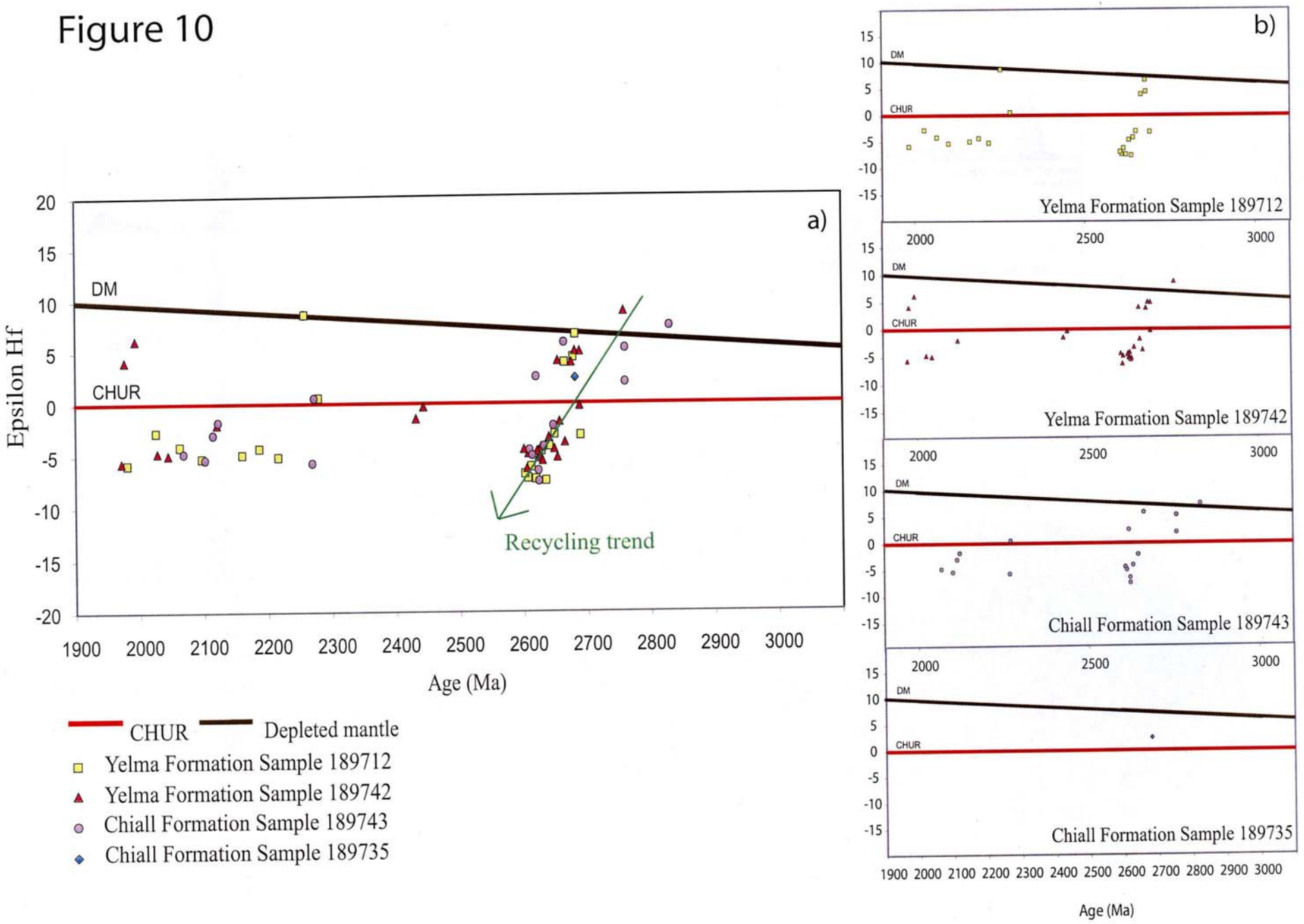
a)
DM
CHUR
Recycling trend
Epsilon Hf
Age (Ma)
CHUR
Depleted mantle
Yelma Formation Sample 189712
Yelma Formation Sample 189742
Chiall Formation Sample 189743
Chiall Formation Sample 189735
b)
Yelma Formation Sample 189712
Yelma Formation Sample 189742
Chiall Formation Sample 189743
Chiall Formation Sample 189735
Age (Ma)

Figure 11

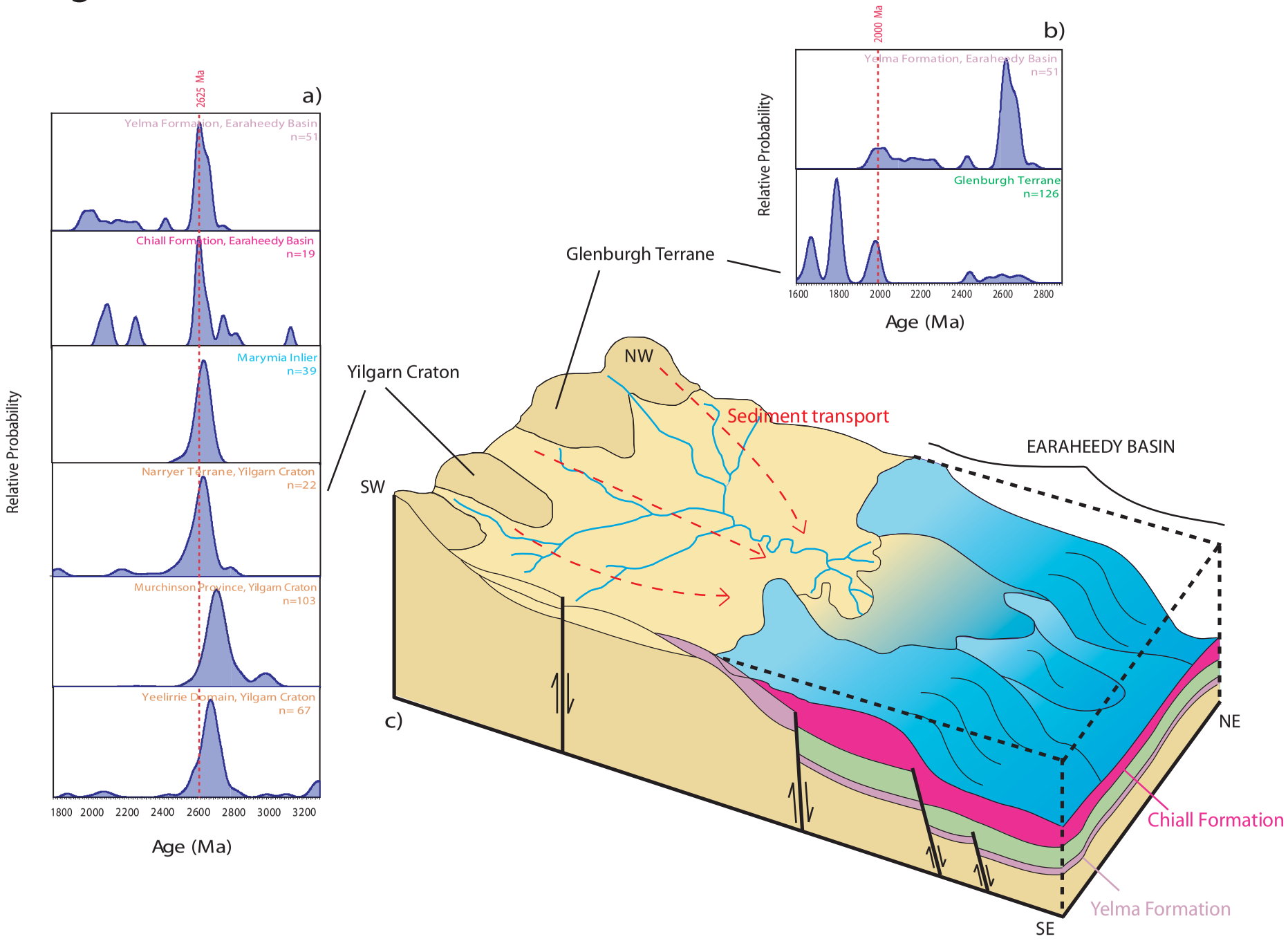
a)
2625 Ma
Yelma Formation, Earaheedy Basin
n=51
Chiall Formation, Earaheedy Basin
n=19
Marymia Inlier
n=39
Narryer Terrane, Yilgarn Craton
n=22
Murchinson Province, Yilgarn Craton
n=103
Yeelirrie Domain, Yilgarn Craton
n= 67
Relative Probability
1800 2000 2200 2400 2600 2800 3000 3200
Age (Ma)
b)
2000 Ma
Yelma Formation, Earaheedy Basin
n=51
Glenburgh Terrane
n=126
Relative Probability
1600 1800 2000 2200 2400 2600 2800
Age (Ma)
Glenburgh Terrane
Yilgarn Craton
NW
SW
Sediment transport
EARAHEEDY BASIN
c)
NE
SE
Chiall Formation
Yelma Formation

Figure 12

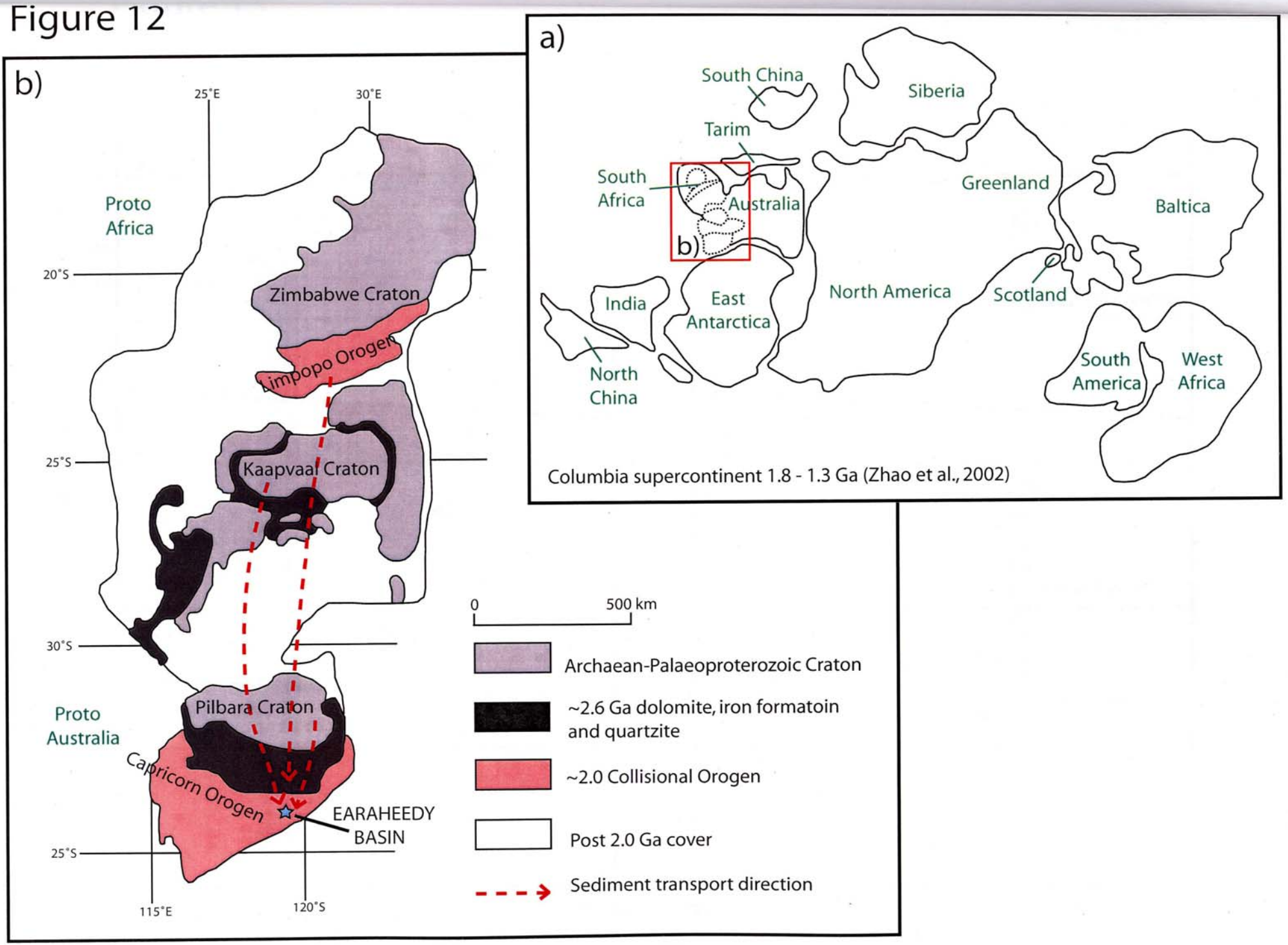
a)
South China
Siberia
Tarim
South Africa
Australia
b)
Greenland
Baltica
India
East Antarctica
North America
Scotland
North China
South America
West Africa
Columbia supercontinent 1.8 - 1.3 Ga (Zhao et al., 2002)
b)
25°E
30°E
Proto Africa
20°S
Zimbabwe Craton
Limpopo Orogen
25°S
Kaapvaal Craton
30°S
Proto Australia
Pilbara Craton
Capricorn Orogen
EARAHEEDY BASIN
25°S
115°E
120°S
0
500 km
Archaean-Palaeoproterozoic Craton
~2.6 Ga dolomite, iron formatoin and quartzite
~2.0 Collisional Orogen
Post 2.0 Ga cover
Sediment transport direction

Figure 13

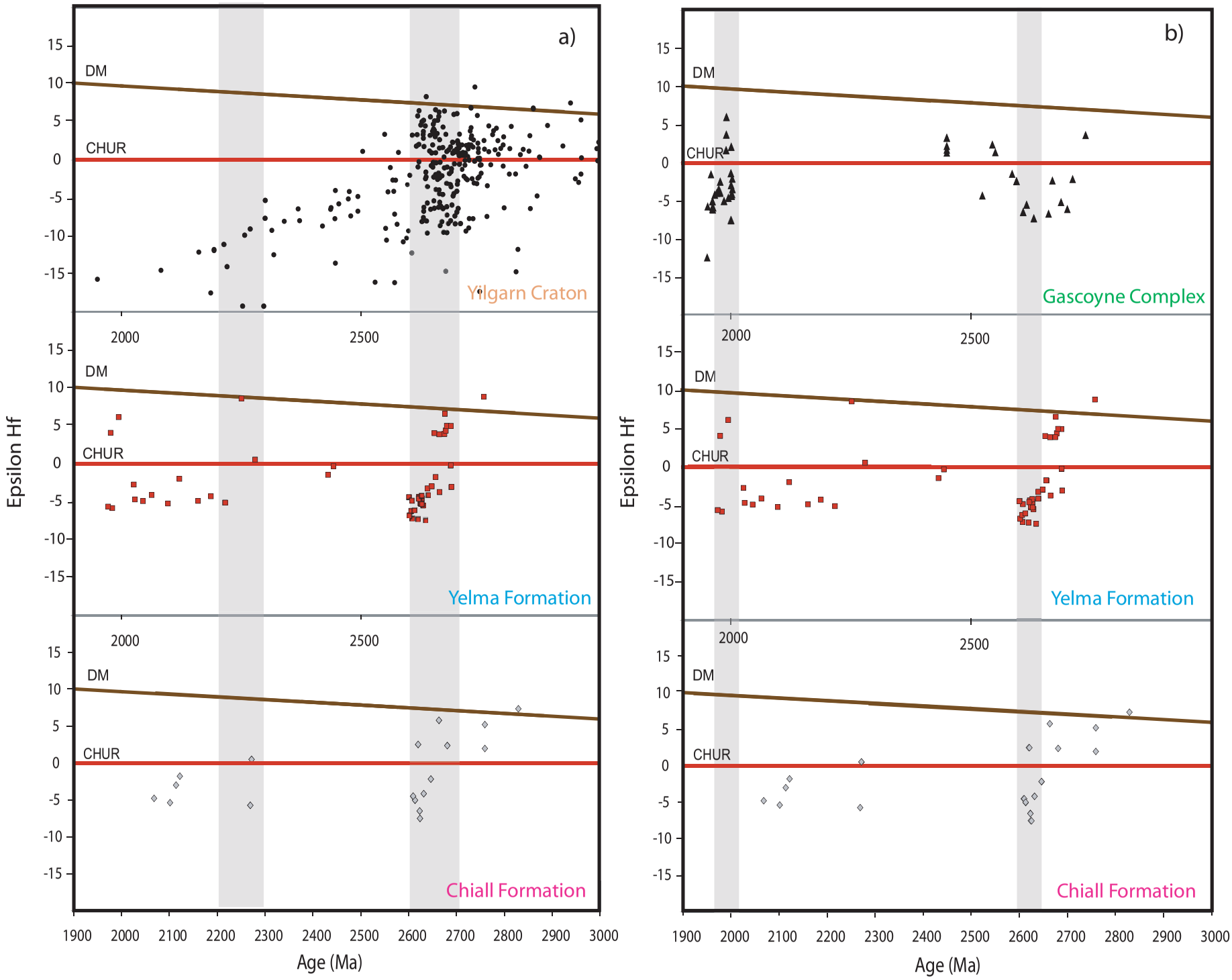
a)
b)
DM
CHUR
Yilgarn Craton
Gascoyne Complex
Yelma Formation
Chiall Formation
Epsilon Hf
Age (Ma)
15
10
5
0
-5
-10
-15
2000
2500
1900
2100
2200
2300
2400
2600
2700
2800
2900
3000

Figure 14

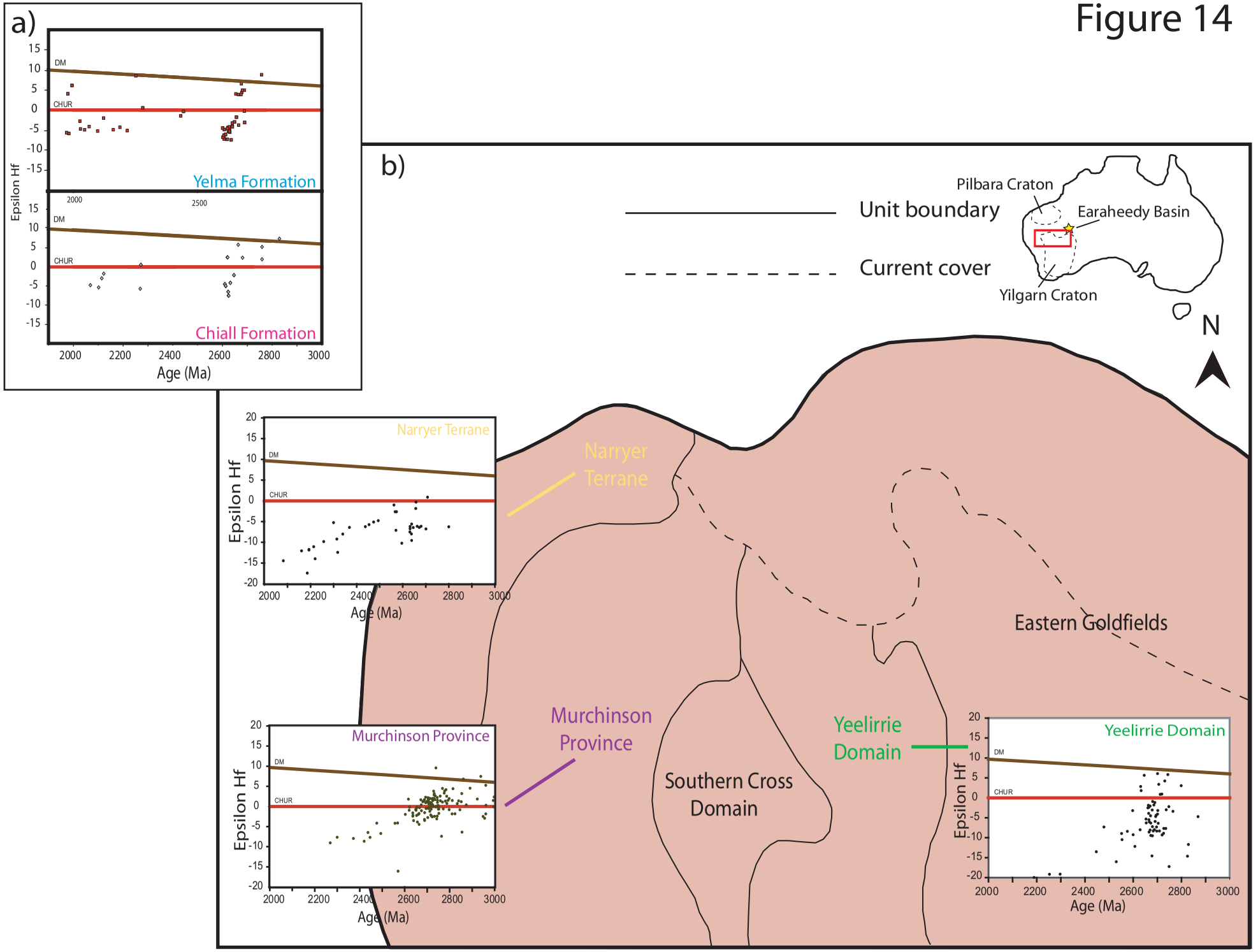
a)
Epsilon Hf
DM
CHUR
Yelma Formation
Chiall Formation
Age (Ma)
b)
Unit boundary
Current cover
Pilbara Craton
Earaheedy Basin
Yilgarn Craton
N
Narryer Terrane
Murchinson Province
Yeelirrie Domain
Southern Cross Domain
Eastern Goldfields

Figure 15

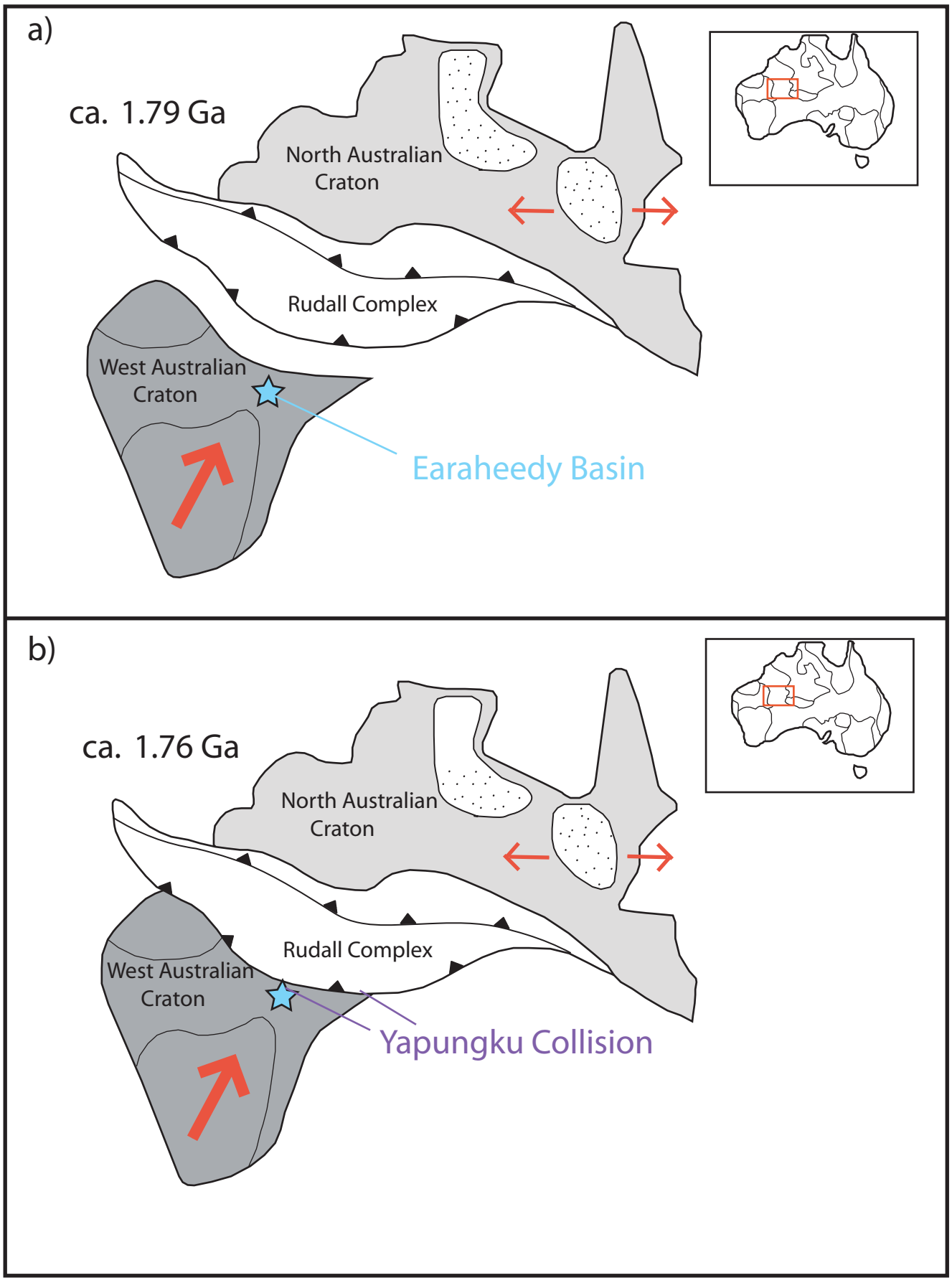
a)
ca. 1.79 Ga
North Australian Craton
Rudall Complex
West Australian Craton
Earaheedy Basin
b)
ca. 1.76 Ga
North Australian Craton
Rudall Complex
West Australian Craton
Yapungku Collision

Table 1. Orogenic events of the Capricorn Orogen

Event	Time (Ma)	Description
Opthalmian	~2000	The ~2200 Ma Opthalmian Orogeny is the oldest orogenic event associated with formation of the Capricorn Orogen and affected the northern and southern regions of the Ashburton and Hamersley Basins, respectively, to form the Opthalmian Fold Belt (Tyler and Thorne, 1990; Rasmussen et al., 2005).
Glenburgh	2005 – 1960	The 2005 – 1960 Ma Glenburgh Orogeny is thought to record the collision of the southwest Gascoyne Complex and the northwest Yilgarn Craton (Occhipinti et al., 2004) causing the closure of the Bryah Basin and formation of the Padbury foreland basin (Pirajno et al., 2004).
Capricorn	1830 – 1780	The 1830 – 1780 Ma Capricorn Orogeny caused widespread deformation across the entire Capricorn Orogen; current work associates the oblique collision of the Yilgarn and Pilbara Cratons to the Capricorn Orogeny (Cawood and Tyler, 2004).
Yapungku	1790 – 1760	The 1790 – 1760 Ma Yapungku Orogeny had a pervasive affect on the Paterson Orogen, northeast of the Capricorn Orogen (Bagas, 2004). Later stages of the Yapungku Orogeny may record the collision of the now amalgamated West and North Australian Cratons; however, felsic intrusives and metamorphism assumed as part of the event have not yet been conclusively related to such a collision (Maidment, 2007).
Mangaroon	1680 – 1620	The 1680 – 1620 Ma Mangaroon Orogeny caused deformation, intracontinental reworking and reactivation of earlier structures within the northern Gascoyne Complex (Sheppard et al., 2005). Recent work has further identified low- to medium- grade metamorphism and tectonic reworking in the central Gascoyne Complex during the 1030 – 950 Ma Edmundian Orogeny (Sheppard et al. 2007).
Edmundian	1030 – 950	Originally thought to affect only the Bangemall Supergroup, the Edmundian Orogeny has been shown to be of higher grade and affect basement rocks in addition to the Bangemall Supergroup (Sheppard et al., 2007).

Table 2. Basins associated with the evolution of the Capricorn Orogen

Basin	Time (Ga)	Description
Yerrida	~2.17 ~ 1.8	The Yerrida Basin is the oldest Palaeoproterozoic basin located along the northern margin of the Yilgarn Craton unconformably overlying the Archaean Yilgarn basement. After a 350 my period of non-deposition, the Yerrida intracratonic sag basin became a foreland basin in response to east verging orogenesis (Pirajno et al., 2004).
Bryah	~2.0	The Bryah Basin formed west of the Yerrida sag basin in an oceanic arm between the northern Yilgarn Craton and southern Gascoyne Complex (Occhipinti et al., 2004). Orogenesis associated with the Glenburgh Orogeny led to basin closure and deformation (Pirajno et al., 2004) and consequent formation of the Padbury foreland basin (Occhipinti et al., 2004).
Padbury	~1.96	Pirajno et al. (2004) considers the Padbury Basin to be directly related to the Glenburgh Orogeny with sediment deposition occurring in a post subduction peripheral foreland basin related to continental collision. The ~1.83 Ga Capricorn Orogeny then thrust the Bryah and Padbury units southeast over the lower Yerrida Group (Pirajno et al., 2004).
Earaheedy	<1810 Ma	The Earaheedy Basin is the youngest Palaeoproterozoic basin associated with both the northern Yilgarn Craton and Capricorn Orogen (Rasmussen and Fletcher, 2002; Halilovic et al., 2004). Consisting of shallow marine chemical and clastic sediments, the Earaheedy Basin developed in a trailing passive margin and was deformed along the northern margin to create the Stanley Fold Belt (Pirajno et al., 2004; Bagas, 2004).

Table 3
Sample evaluation

Sample no.	Location	Formation	Lithology	Rock Type	Point Count	Other mineral
GSWA 189712	325404E	Yelma	Grey to black	Sub-litharenite	91% quartz	Hematite
	7183811N		Medium grained		9% lithics	Garnet
			Quartz rich		0% feldspar	
GSWA 189742	319096E	Yelma	Pale grey to white	Sub-litharenite	92% quartz	Epidote
	7187575N		Medium grained		8% lithics	
			Quartz rich		0% feldspar	
GSWA 189743	344582E	Chiall	Pale grey to white	Quartz-arenite	100% quartz	
	7178849N		Coarse grained		0% lithics	
			Quartz rich		0% feldspar	
GSWA 189735	337053E	Chiall	Pale pink to white	Sub-arkose	96% quartz	Hematite
	7165102N		Medium grained		4% lithics	
			Quartz rich		0% feldspar	

Table 4

U-Pb isotopic ratios and age for all samples

	Ratios								Apparent Ages (Ma)							
Spot	Pb^{207}/Pb^{206}		Pb^{207}/U^{235}		Pb^{206}/U^{238}		Pb^{208}/Th^{232}		Pb^{207}/Pb^{206}		Pb^{207}/U^{235}		Pb^{206}/U^{238}		Pb^{208}/Th^{232}	
Yelma Formation Sample 189712																
Z1	0.15303	0.00169	0.21999	0.00281	4.64162	0.06092	0.01814	0.00022	**2380**	**19**	1282	15	1757	11	363	4
Z2	0.19497	0.00215	0.29063	0.00354	7.81404	0.09659	0.02374	0.00030	**2785**	**18**	1645	18	2210	11	474	6
Z3	0.15344	0.00172	0.16379	0.00196	3.46307	0.04264	0.01184	0.00015	**2385**	**19**	978	11	1519	10	238	3
Z4	0.13465	0.00141	0.39759	0.00519	7.38200	0.09649	0.10595	0.00140	**2159**	**18**	2158	24	2159	12	2036	26
Z5	0.15067	0.00179	0.16480	0.00220	3.42448	0.04802	0.00634	0.00009	**2354**	**20**	983	12	1510	11	128	2
Z6	0.15166	0.00166	0.17889	0.00223	3.74087	0.04785	0.00624	0.00008	**2365**	**19**	1061	12	1580	10	126	2
Z7	0.16011	0.00165	0.20215	0.00250	4.46286	0.05531	0.01577	0.00018	**2457**	**17**	1187	13	1724	10	316	4
Z8	0.17951	0.00206	0.45616	0.00597	11.2907	0.15341	0.08571	0.00113	**2648**	**19**	2423	26	2547	13	1662	21
Z9	0.15341	0.00185	0.14424	0.00194	3.05099	0.04336	0.00878	0.00012	**2384**	**20**	869	11	1421	11	177	2
Z10	0.15454	0.00213	0.22075	0.00290	4.70424	0.07058	0.01165	0.00020	**2397**	**23**	1286	15	1768	13	234	4
Z11	0.12473	0.00138	0.36127	0.00452	6.21257	0.08028	0.08863	0.00114	**2025**	**19**	1988	21	2006	11	1717	21
Z12	0.19042	0.00231	0.25789	0.00350	6.77001	0.09588	0.01759	0.00028	**2746**	**20**	1479	18	2082	13	352	6
Z13	0.15115	0.00242	0.29372	0.00410	6.11647	0.10193	0.01468	0.00045	**2359**	**27**	1660	20	1993	15	295	9
Z14	0.17501	0.00255	0.20745	0.00284	5.00070	0.07734	0.00680	0.00016	**2606**	**24**	1215	15	1819	13	137	3
Z15	0.15814	0.00182	0.18102	0.00240	3.94702	0.05431	0.01279	0.00020	**2436**	**19**	1073	13	1623	11	257	4
Z16	0.19338	0.00274	0.21812	0.00321	5.81049	0.09344	0.01066	0.00022	**2771**	**23**	1272	17	1948	14	214	4
Z17	0.16435	0.00190	0.23670	0.00313	5.36303	0.07340	0.01929	0.00047	**2501**	**19**	1370	16	1879	12	386	9
Z18	0.13498	0.00148	0.28811	0.00383	5.35950	0.07291	0.07614	0.00119	**2164**	**19**	1632	19	1878	12	1483	22
Z19	0.15502	0.00193	0.21838	0.00303	4.65777	0.06910	0.01115	0.00020	**2402**	**21**	1273	16	1760	12	224	4
Z20	0.14398	0.00175	0.19690	0.00260	3.90829	0.05528	0.01228	0.00019	**2276**	**21**	1159	14	1615	11	247	4
Z21	0.14265	0.00172	0.25095	0.00316	4.93816	0.06680	0.02063	0.00064	**2260**	**21**	1443	16	1809	11	413	13
Z22	0.20714	0.00236	0.23903	0.00327	6.82475	0.09618	0.02498	0.00042	**2883**	**18**	1382	17	2089	12	499	8
Z23	0.13673	0.00156	0.36986	0.00470	6.97424	0.09332	0.06918	0.00101	**2186**	**20**	2029	22	2108	12	1352	19
Z24	0.13886	0.00178	0.18050	0.00237	3.45628	0.05004	0.01342	0.00024	**2213**	**22**	1070	13	1517	11	269	5
Z25	0.18772	0.00214	0.43929	0.00572	11.3718	0.15416	0.05992	0.00085	**2722**	**19**	2348	26	2554	13	1176	16
Z26	0.19995	0.00219	0.16167	0.00206	4.45804	0.05860	0.00871	0.00013	**2826**	**18**	966	11	1723	11	175	3
Z27	0.17244	0.00210	0.10561	0.00132	2.51165	0.03374	0.00621	0.00018	**2581**	**20**	647	8	1275	10	125	4
Z28	0.17724	0.00250	0.28181	0.00381	6.88773	0.10546	0.02540	0.00090	**2627**	**23**	1601	19	2097	14	507	18
Z29	0.19759	0.00218	0.11974	0.00147	3.26124	0.04117	0.00657	0.00011	**2806**	**18**	729	8	1472	10	132	2
Z30	0.18642	0.00207	0.45353	0.00551	11.6605	0.14678	0.04862	0.00073	**2711**	**18**	2411	24	2578	12	960	14
Z31	0.14423	0.00150	0.23708	0.00286	4.71166	0.05776	0.02089	0.00032	**2279**	**18**	1372	15	1769	10	418	6
Z32	0.18333	0.00214	0.46698	0.00622	11.7989	0.16523	0.07407	0.00162	**2683**	**19**	2470	27	2589	13	1444	30
Z33	0.14422	0.00154	0.38680	0.00481	7.68500	0.09797	0.04728	0.00090	**2279**	**18**	2108	22	2195	11	934	17

Z34	0.14725	0.00157	0.19433	0.00241	3.94110	0.05017	0.01361	0.00023	**2314**	**18**	1145	13	1622	10	273	5

	Ratios								Apparent Ages (Ma)							
Spot	Pb^{207}/Pb^{206}		Pb^{207}/U^{235}		Pb^{206}/U^{238}		Pb^{208}/Th^{232}		Pb^{207}/Pb^{206}		Pb^{207}/U^{235}		Pb^{206}/U^{238}		Pb^{208}/Th^{232}	
Yelma Formation Sample 189712 (continued)																
Z35	0.14587	0.00154	0.23048	0.00283	4.62836	0.05814	0.03040	0.00058	**2298**	**18**	1337	15	1754	10	605	11
Z36	0.13105	0.00155	0.30041	0.00389	5.42319	0.07489	0.02737	0.00048	**2112**	**21**	1693	19	1889	12	546	9
Z37	0.19689	0.00247	0.13992	0.00189	3.79578	0.05477	0.00669	0.00022	**2801**	**20**	844	11	1592	12	135	4
Z38	0.17923	0.00191	0.38382	0.00471	9.47376	0.11911	0.12869	0.00231	**2646**	**18**	2094	22	2385	12	2447	41
Z39	0.21055	0.00237	0.36523	0.00487	10.5944	0.14530	0.04589	0.00088	**2910**	**18**	2007	23	2488	13	907	17
Z40	0.18396	0.00205	0.51758	0.00668	13.1062	0.17477	0.14467	0.00224	**2689**	**18**	2689	28	2687	13	2731	40
Z41	0.17803	0.00189	0.50302	0.00630	12.3451	0.15781	0.12073	0.00209	**2635**	**18**	2627	27	2631	12	2304	38
Z42	0.17702	0.00188	0.48113	0.00565	11.7433	0.14154	0.09839	0.00158	**2625**	**18**	2532	25	2584	11	1897	29
Z43	0.18151	0.00282	0.52743	0.00719	13.1999	0.20997	0.14479	0.00347	**2667**	**25**	2731	30	2694	15	2733	61
Z44	0.17008	0.00195	0.17979	0.00221	4.21361	0.05441	0.00961	0.00028	**2558**	**19**	1066	12	1677	11	193	6
Z45	0.18117	0.00198	0.52022	0.00674	12.9925	0.17248	0.13523	0.00213	**2664**	**18**	2700	29	2679	13	2564	38
Z46	0.14182	0.00172	0.19727	0.00252	3.85724	0.05317	0.01936	0.00043	**2250**	**21**	1161	14	1605	11	388	9
Z47	0.17508	0.00200	0.50164	0.00644	12.1081	0.16216	0.12853	0.00245	**2607**	**19**	2621	28	2613	13	2444	44
Z48	0.17637	0.00193	0.48452	0.00623	11.7823	0.15548	0.11547	0.00203	**2619**	**18**	2547	27	2587	12	2209	37
Z49	0.19140	0.00217	0.31832	0.00414	8.40186	0.11386	0.02864	0.00071	**2754**	**18**	1782	20	2275	12	571	14
Z50	0.17907	0.00191	0.43270	0.00509	10.6827	0.12850	0.05456	0.00092	**2644**	**18**	2318	23	2496	11	1074	18
Z51	0.18249	0.00202	0.50198	0.00605	12.6313	0.15765	0.12964	0.00229	**2676**	**18**	2622	26	2653	12	2464	41
Z52	0.18270	0.00241	0.50482	0.00681	12.7192	0.18671	0.13952	0.00394	**2678**	**22**	2635	29	2659	14	2640	70
Z53	0.20074	0.00216	0.16002	0.00190	4.42883	0.05388	0.00408	0.00009	**2832**	**17**	957	11	1718	10	82	2
Z54	0.18303	0.00198	0.11846	0.00142	2.98964	0.03665	0.00667	0.00017	**2681**	**18**	722	8	1405	9	134	3
Z55	0.19215	0.00226	0.35093	0.00452	9.29672	0.12582	0.03753	0.00125	**2761**	**19**	1939	22	2368	12	745	24
Z56	0.12162	0.00206	0.35751	0.00503	5.99504	0.10557	0.09541	0.00255	**1980**	**30**	1970	24	1975	15	1842	47
Z57	0.13732	0.00161	0.31542	0.00364	5.96929	0.07485	0.06309	0.00202	**2194**	**20**	1767	18	1971	11	1237	38
Z58	0.14815	0.00154	0.26724	0.00326	5.45882	0.06719	0.15755	0.00530	**2325**	**18**	1527	17	1894	11	2957	93
Z59	0.17467	0.00193	0.29313	0.00370	7.05981	0.09173	0.01206	0.00026	**2603**	**18**	1657	18	2119	12	242	5
Z60	0.16508	0.00200	0.15575	0.00199	3.54511	0.04865	0.00176	0.00006	**2508**	**20**	933	11	1537	11	36	1
Z61	0.14189	0.00173	0.41447	0.00585	8.10349	0.11992	0.07572	0.00306	**2250**	**21**	2235	27	2243	13	1475	57
Z62	0.14357	0.00149	0.13381	0.00165	2.64822	0.03301	0.02874	0.00068	**2271**	**18**	810	9	1314	9	573	13
Z63	0.12989	0.00172	0.34352	0.00451	6.15386	0.09043	0.06927	0.00228	**2097**	**23**	1904	22	1998	13	1354	43
Z64	0.17562	0.00200	0.50619	0.00613	12.2605	0.15487	0.13822	0.00284	**2612**	**19**	2640	26	2625	12	2617	50
Z65	0.19541	0.00284	0.22022	0.00334	5.93149	0.09719	0.00949	0.00056	**2788**	**24**	1283	18	1966	14	191	11
Z66	0.16478	0.00200	0.15074	0.00184	3.42888	0.04469	0.00653	0.00041	**2505**	**20**	905	10	1511	10	132	8
Z67	0.17860	0.00205	0.49516	0.00607	12.2000	0.15645	0.09288	0.00241	**2640**	**19**	2593	26	2620	12	1795	45
Z68	0.19101	0.00257	0.14015	0.00196	3.68918	0.05496	0.01034	0.00072	**2751**	**22**	846	11	1569	12	208	14
Z69	0.19509	0.00205	0.40269	0.00517	10.8335	0.14011	0.07101	0.00167	**2786**	**17**	2181	24	2509	12	1387	31

Z70	0.17233	0.00205	0.27648	0.00342	6.56916	0.08773	0.01285	0.00085	**2580**	**20**	1574	17	2055	12	258	17

	Ratios								Apparent Ages (Ma)							
Spot	Pb^{207}/Pb^{206}		Pb^{207}/U^{235}		Pb^{206}/U^{238}		Pb^{208}/Th^{232}		Pb^{207}/Pb^{206}		Pb^{207}/U^{235}		Pb^{206}/U^{238}		Pb^{208}/Th^{232}	
Yelma Formation Sample 189712 (continued)																
Z71	0.19574	0.00225	0.29931	0.00396	8.07622	0.11099	0.01079	0.00035	**2791**	**19**	1688	20	2240	12	217	7
Z72	0.17731	0.00187	0.50820	0.00600	12.4255	0.14937	0.14248	0.00270	**2628**	**17**	2649	26	2637	11	2692	48
Z73	0.13806	0.00182	0.24783	0.00334	4.71466	0.07052	0.02266	0.00094	**2203**	**23**	1427	17	1770	13	453	19
Z74	0.13908	0.00160	0.41098	0.00568	7.88223	0.11219	0.11611	0.00625	**2216**	**20**	2219	26	2218	13	2220	113
Z75	0.14143	0.00164	0.29051	0.00381	5.66178	0.07872	0.05030	0.00240	**2245**	**20**	1644	19	1926	12	992	46
Z76	0.18821	0.00243	0.05526	0.00076	1.43346	0.02124	0.00273	0.00015	**2727**	**21**	347	5	903	9	55	3
Z77	0.13165	0.00149	0.29367	0.00356	5.33075	0.06820	0.02568	0.00065	**2120**	**20**	1660	18	1874	11	512	13
Z78	0.14956	0.00244	0.25023	0.00345	5.15902	0.08719	0.01322	0.00104	**2341**	**28**	1440	18	1846	14	266	21
Z79	0.17456	0.00231	0.48914	0.00696	11.7711	0.18132	0.12622	0.00581	**2602**	**22**	2567	30	2586	14	2403	104
Z80	0.12739	0.00261	0.34916	0.00555	6.13321	0.12929	0.09417	0.00392	**2062**	**36**	1931	27	1995	18	1819	72
Yelma Formation Sample 189742																
Z1	0.17691	0.00181	0.50379	0.00619	12.2897	0.15027	0.13737	0.00157	**2624**	**17**	2630	27	2627	11	2602	28
Z2	0.16814	0.00175	0.11602	0.00147	2.69004	0.03419	0.01123	0.00013	**2539**	**17**	708	8	1326	9	226	3
Z3	0.15771	0.00168	0.41292	0.00579	8.97627	0.12544	0.04195	0.00080	**2431**	**18**	2228	26	2336	13	831	15
Z4	0.13000	0.00148	0.25021	0.00338	4.48518	0.06264	0.03324	0.00044	**2098**	**20**	1440	17	1728	12	661	9
Z5	0.18382	0.00208	0.51865	0.00695	13.1476	0.18040	0.13283	0.00185	**2688**	**19**	2693	29	2690	13	2521	33
Z6	0.13894	0.00156	0.24827	0.00348	4.75486	0.06791	0.04221	0.00054	**2214**	**19**	1430	18	1777	12	836	11
Z7	0.17219	0.00224	0.39616	0.00588	9.40228	0.14693	0.06658	0.00120	**2579**	**22**	2151	27	2378	14	1303	23
Z8	0.15626	0.00158	0.31265	0.00398	6.73667	0.08541	0.07649	0.00082	**2416**	**17**	1754	20	2077	11	1490	15
Z9	0.17655	0.00183	0.50436	0.00634	12.2779	0.15507	0.13052	0.00147	**2621**	**17**	2633	27	2626	12	2480	26
Z10	0.14020	0.00165	0.16710	0.00218	3.23016	0.04450	0.03043	0.00041	**2230**	**20**	996	12	1464	11	606	8
Z11	0.18388	0.00220	0.44930	0.00661	11.3887	0.17181	0.09558	0.00161	**2688**	**20**	2392	29	2556	14	1845	30
Z12	0.14130	0.00153	0.11060	0.00152	2.15487	0.02985	0.00989	0.00013	**2243**	**19**	676	9	1167	10	199	3
Z13	0.19871	0.00247	0.08755	0.00128	2.39875	0.03628	0.01364	0.00027	**2816**	**20**	541	8	1242	11	274	5
Z14	0.19787	0.00203	0.34304	0.00396	9.35629	0.10903	0.12479	0.00166	**2809**	**17**	1901	19	2374	11	2377	30
Z15	0.11975	0.00125	0.21816	0.00284	3.60150	0.04746	0.04932	0.00066	**1952**	**19**	1272	15	1550	10	973	13
Z16	0.18384	0.00196	0.50671	0.00631	12.8418	0.16332	0.13915	0.00167	**2688**	**18**	2643	27	2668	12	2633	30
Z17	0.16317	0.00166	0.21954	0.00276	4.93818	0.06223	0.01436	0.00018	**2489**	**17**	1280	15	1809	11	288	4
Z18	0.22881	0.00284	0.29848	0.00427	9.41771	0.13914	0.05542	0.00103	**3044**	**20**	1684	21	2380	14	1090	20
Z19	0.14327	0.00171	0.15810	0.00221	3.12232	0.04542	0.01565	0.00025	**2267**	**20**	946	12	1438	11	314	5
Z20	0.18891	0.00203	0.11962	0.00160	3.11310	0.04199	0.00680	0.00014	**2733**	**18**	728	9	1436	10	137	3
Z21	0.12977	0.00181	0.26088	0.00333	4.66509	0.06894	0.01966	0.00044	**2095**	**24**	1494	17	1761	12	394	9
Z22	0.17440	0.00198	0.48578	0.00680	11.6797	0.16792	0.11456	0.00185	**2600**	**19**	2552	29	2579	13	2192	34
Z23	0.18237	0.00194	0.51489	0.00634	12.9439	0.16252	0.14209	0.00171	**2675**	**18**	2678	27	2676	12	2685	30

Z24	0.17715	0.00238	0.46319	0.00696	11.3137	0.18246	0.10815	0.00231	**2626**	**22**	2454	31	2549	15	2076	42

	Ratios								Apparent Ages (Ma)							
Spot	Pb^{207}/Pb^{206}		Pb^{207}/U^{235}		Pb^{206}/U^{238}		Pb^{208}/Th^{232}		Pb^{207}/Pb^{206}		Pb^{207}/U^{235}		Pb^{206}/U^{238}		Pb^{208}/Th^{232}	
Yelma Formation Sample 189742 (continued)																
Z25	0.17536	0.00197	0.09267	0.00119	2.23941	0.03003	0.00645	0.00010	**2610**	**19**	571	7	1194	9	130	2
Z26	0.12671	0.00145	0.27571	0.00347	4.81457	0.06376	0.05619	0.00095	**2053**	**20**	1570	18	1787	11	1105	18
Z27	0.15879	0.00163	0.46235	0.00569	10.1209	0.12527	0.12652	0.00153	**2443**	**17**	2450	25	2446	11	2408	28
Z28	0.13618	0.00163	0.16102	0.00216	3.02261	0.04314	0.03235	0.00051	**2179**	**21**	963	12	1413	11	643	10
Z29	0.12102	0.00177	0.35578	0.00495	5.93614	0.09614	0.10354	0.00187	**1971**	**26**	1962	24	1967	14	1991	34
Z30	0.18037	0.00200	0.50480	0.00607	12.5520	0.15555	0.14416	0.00216	**2656**	**18**	2634	26	2647	12	2722	38
Z31	0.18004	0.00221	0.48658	0.00573	12.0737	0.15242	0.14537	0.00293	**2653**	**20**	2556	25	2610	12	2743	52
Z32	0.12698	0.00135	0.32049	0.00398	5.61006	0.07047	0.06783	0.00140	**2057**	**19**	1792	19	1918	11	1327	26
Z33	0.13590	0.00139	0.30806	0.00366	5.77038	0.06837	0.05202	0.00072	**2176**	**18**	1731	18	1942	10	1025	14
Z34	0.15865	0.00166	0.09929	0.00111	2.17099	0.02442	0.00996	0.00015	**2441**	**18**	610	6	1172	8	200	3
Z35	0.15197	0.00167	0.17735	0.00225	3.71410	0.04826	0.03130	0.00053	**2368**	**19**	1053	12	1574	10	623	10
Z36	0.17719	0.00187	0.49569	0.00611	12.1074	0.15020	0.12609	0.00185	**2627**	**17**	2595	26	2613	12	2400	33
Z37	0.12814	0.00147	0.32034	0.00394	5.65802	0.07306	0.08365	0.00142	**2073**	**20**	1791	19	1925	11	1624	26
Z38	0.13306	0.00134	0.23479	0.00267	4.30583	0.04881	0.06595	0.00086	**2139**	**18**	1360	14	1695	9	1291	16
Z39	0.17920	0.00185	0.06059	0.00071	1.49642	0.01753	0.01023	0.00013	**2646**	**17**	379	4	929	7	206	3
Z40	0.12250	0.00139	0.32102	0.00375	5.42026	0.06708	0.07082	0.00112	**1993**	**20**	1795	18	1888	11	1383	21
Z41	0.18741	0.00197	0.36221	0.00420	9.35919	0.10982	0.05964	0.00105	**2720**	**17**	1993	20	2374	11	1171	20
Z42	0.17969	0.00192	0.37765	0.00437	9.35546	0.11086	0.09731	0.00184	**2650**	**18**	2065	20	2374	11	1877	34
Z43	0.17664	0.00196	0.48083	0.00592	11.7102	0.14836	0.12155	0.00264	**2622**	**18**	2531	26	2582	12	2319	48
Z44	0.17748	0.00199	0.50638	0.00587	12.3922	0.14966	0.14076	0.00240	**2629**	**18**	2641	25	2635	11	2662	43
Z45	0.17421	0.00199	0.09371	0.00110	2.24959	0.02767	0.01615	0.00045	**2599**	**19**	578	6	1197	9	324	9
Z46	0.13367	0.00174	0.30176	0.00404	5.55629	0.08185	0.07402	0.00272	**2147**	**23**	1700	20	1909	13	1443	51
Z47	0.13247	0.00136	0.31951	0.00394	5.83602	0.07234	0.04247	0.00093	**2131**	**18**	1787	19	1952	11	841	18
Z48	0.12903	0.00146	0.26539	0.00291	4.72374	0.05501	0.09096	0.00252	**2085**	**20**	1517	15	1772	10	1760	47
Z49	0.15223	0.00168	0.17683	0.00193	3.71285	0.04243	0.02415	0.00062	**2371**	**19**	1050	11	1574	9	482	12
Z50	0.12935	0.00155	0.32799	0.00367	5.85241	0.07198	0.08178	0.00203	**2089**	**21**	1829	18	1954	11	1589	38
Z51	0.18245	0.00184	0.42228	0.00468	10.6240	0.11791	0.12171	0.00234	**2675**	**17**	2271	21	2491	10	2322	42
Z52	0.13405	0.00170	0.27102	0.00350	5.00796	0.07073	0.05758	0.00166	**2152**	**22**	1546	18	1821	12	1132	32
Z53	0.12136	0.00145	0.35554	0.00470	5.94540	0.08374	0.09375	0.00307	**1976**	**21**	1961	22	1968	12	1811	57
Z54	0.19328	0.00200	0.46384	0.00511	12.3618	0.13754	0.07323	0.00209	**2770**	**17**	2457	23	2632	10	1429	39
Z55	0.26774	0.00277	0.32087	0.00348	11.8439	0.13007	0.06707	0.00249	**3293**	**16**	1794	17	2592	10	1312	47
Z56	0.16649	0.00177	0.37193	0.00410	8.53808	0.09655	0.03001	0.00143	**2523**	**18**	2039	19	2290	10	598	28
Z57	0.17491	0.00194	0.48342	0.00552	11.6572	0.13815	0.13028	0.00305	**2605**	**18**	2542	24	2577	11	2475	55
Z58	0.17688	0.00196	0.44160	0.00502	10.7692	0.12690	0.03766	0.00093	**2624**	**18**	2358	22	2503	11	747	18
Z59	0.13636	0.00168	0.24294	0.00289	4.56704	0.05987	0.05270	0.00138	**2182**	**21**	1402	15	1743	11	1038	26

Z60	0.17512	0.00194	0.50019	0.00568	12.0735	0.14254	0.13919	0.00294	**2607**	**18**	2615	24	2610	11	2634	52

	Ratios								Apparent Ages (Ma)							
Spot	Pb^{207}/Pb^{206}		Pb^{207}/U^{235}		Pb^{206}/U^{238}		Pb^{208}/Th^{232}		Pb^{207}/Pb^{206}		Pb^{207}/U^{235}		Pb^{206}/U^{238}		Pb^{208}/Th^{232}	
Yelma Formation Sample 189742 (continued)																
Z61	0.16694	0.00180	0.09371	0.00109	2.15594	0.02579	0.01585	0.00030	**2527**	**18**	577	6	1167	8	318	6
Z62	0.18128	0.00184	0.50012	0.00624	12.4972	0.15607	0.12676	0.00298	**2665**	**17**	2614	27	2643	12	2412	53
Z63	0.12489	0.00153	0.38043	0.00443	6.54896	0.08428	0.10757	0.00206	**2027**	**22**	2078	21	2053	11	2065	38
Z64	0.12853	0.00148	0.28639	0.00359	5.07334	0.06746	0.03959	0.00097	**2078**	**20**	1624	18	1832	11	785	19
Z65	0.18300	0.00265	0.51716	0.00657	13.0441	0.18965	0.13967	0.00397	**2680**	**24**	2687	28	2683	14	2643	70
Z66	0.11723	0.00123	0.23786	0.00258	3.84343	0.04265	0.05940	0.00171	**1914**	**19**	1376	13	1602	9	1166	33
Z67	0.17720	0.00198	0.50305	0.00581	12.2858	0.14798	0.13686	0.00247	**2627**	**18**	2627	25	2627	11	2593	44
Z68	0.17317	0.00189	0.11760	0.00133	2.80504	0.03269	0.02352	0.00062	**2589**	**18**	717	8	1357	9	470	12
Z69	0.12583	0.00133	0.26024	0.00300	4.51363	0.05336	0.01800	0.00043	**2041**	**19**	1491	15	1734	10	361	9
Z70	0.17854	0.00198	0.45296	0.00556	11.1503	0.14188	0.11367	0.00213	**2639**	**18**	2408	25	2536	12	2176	39
Z71	0.12807	0.00265	0.20038	0.00289	3.53794	0.06626	0.05935	0.01580	**2072**	**36**	1177	16	1536	15	1165	301
Z72	0.12411	0.00147	0.22275	0.00282	3.80857	0.05175	0.03935	0.00207	**2016**	**21**	1296	15	1595	11	780	40
Z73	0.19173	0.00257	0.54925	0.00699	14.5167	0.20380	0.17729	0.00436	**2757**	**22**	2822	29	2784	13	3299	75
Z74	0.12608	0.00136	0.33422	0.00409	5.80802	0.07289	0.06452	0.00265	**2044**	**19**	1859	20	1948	11	1264	50
Z75	0.15137	0.00159	0.10214	0.00120	2.13129	0.02540	0.01407	0.00042	**2362**	**18**	627	7	1159	8	283	8
Z76	0.13630	0.00521	0.28979	0.00632	5.44122	0.18767	0.04481	0.01169	**2181**	**65**	1641	32	1891	30	886	226
Z77	0.17777	0.00259	0.24745	0.00310	6.06621	0.08837	0.06222	0.00414	**2632**	**24**	1425	16	1985	13	1220	79
Z78	0.13167	0.00227	0.37105	0.00538	6.73357	0.12138	0.07010	0.00642	**2120**	**30**	2034	25	2077	16	1370	121
Z79	0.14116	0.00188	0.24246	0.00318	4.71660	0.06947	0.04854	0.00333	**2241**	**23**	1400	16	1770	12	958	64
Z80	0.15687	0.00193	0.13663	0.00178	2.95409	0.04191	0.00717	0.00047	**2422**	**21**	826	10	1396	11	144	9
Chiall Formation Sample 189743																
Z1	0.22398	0.00367	0.23611	0.00357	7.29251	0.13270	0.03880	0.00060	**3010**	**26**	1366	19	2148	16	770	12
Z2	0.13920	0.00295	0.22736	0.00337	4.36213	0.09550	0.02962	0.00045	**2217**	**36**	1321	18	1705	18	590	9
Z3	0.23562	0.00272	0.09111	0.00124	2.95957	0.04205	0.00830	0.00010	**3091**	**18**	562	7	1397	11	167	2
Z4	0.18916	0.00493	0.32190	0.00552	8.38865	0.21971	0.01923	0.00046	**2735**	**42**	1799	27	2274	24	385	9
Z5	0.24697	0.00266	0.10688	0.00134	3.63789	0.04646	0.00558	0.00006	**3166**	**17**	655	8	1558	10	112	1
Z6	0.18749	0.00336	0.11846	0.00168	3.06163	0.05736	0.01245	0.00019	**2720**	**29**	722	10	1423	14	250	4
Z7	0.18252	0.00280	0.16051	0.00224	4.03784	0.06804	0.02022	0.00028	**2676**	**25**	960	12	1642	14	405	6
Z8	0.16633	0.00214	0.16296	0.00214	3.73409	0.05510	0.00834	0.00011	**2521**	**21**	973	12	1579	12	168	2
Z9	0.20157	0.00245	0.17285	0.00233	4.80189	0.06960	0.02132	0.00026	**2839**	**20**	1028	13	1785	12	426	5
Z10	0.12781	0.00155	0.37458	0.00487	6.59939	0.09387	0.10536	0.00119	**2068**	**21**	2051	23	2059	13	2025	22
Z11	0.12136	0.00145	0.35554	0.00470	5.94540	0.08374	0.09375	0.00307	**1976**	**21**	1961	22	1968	12	1811	57
Z12	0.30429	0.00326	0.08425	0.00106	3.53369	0.04517	0.00973	0.00011	**3492**	**16**	521	6	1535	10	196	2
Z13	0.16379	0.00208	0.30791	0.00387	6.94845	0.09824	0.03241	0.00041	**2495**	**21**	1730	19	2105	13	645	8

Z14	0.13644	0.00161	0.28178	0.00367	5.29984	0.07436	0.06160	0.00068	**2183**	**20**	1600	18	1869	12	1208	13

	Ratios								Apparent Ages (Ma)							
Spot	Pb^{207}/Pb^{206}		Pb^{207}/U^{235}		Pb^{206}/U^{238}		Pb^{208}/Th^{232}		Pb^{207}/Pb^{206}		Pb^{207}/U^{235}		Pb^{206}/U^{238}		Pb^{208}/Th^{232}	
Chiall Formation Sample 189743 (continued)																
Z15	0.19198	0.00270	0.51308	0.00670	13.5751	0.20768	0.07655	0.00112	**2759**	**23**	2670	29	2721	14	1491	21
Z16	0.13332	0.00209	0.27773	0.00372	5.10308	0.08665	0.05466	0.00074	**2142**	**27**	1580	19	1837	14	1076	14
Z17	0.14343	0.00161	0.39833	0.00515	7.87569	0.10666	0.09965	0.00116	**2269**	**19**	2161	24	2217	12	1920	21
Z18	0.17530	0.00295	0.49347	0.00693	11.9266	0.21411	0.13738	0.00206	**2609**	**28**	2586	30	2599	17	2602	37
Z19	0.18397	0.00208	0.36454	0.00458	9.24401	0.12248	0.03719	0.00045	**2689**	**19**	2004	22	2363	12	738	9
Z20	0.14859	0.00172	0.35484	0.00443	7.26767	0.09750	0.05044	0.00061	**2330**	**20**	1958	21	2145	12	995	12
Z21	0.17934	0.00219	0.29907	0.00439	7.39480	0.11378	0.04279	0.00073	**2647**	**20**	1687	22	2160	14	847	14
Z22	0.23603	0.00246	0.11000	0.00152	3.57971	0.04953	0.01001	0.00013	**3093**	**17**	673	9	1545	11	201	3
Z23	0.21605	0.00255	0.14011	0.00202	4.17287	0.06229	0.01224	0.00025	**2952**	**19**	845	11	1669	12	246	5
Z24	0.16974	0.00198	0.27717	0.00409	6.48781	0.09901	0.03298	0.00072	**2555**	**19**	1577	21	2044	13	656	14
Z25	0.17643	0.00183	0.49024	0.00672	11.9246	0.16388	0.10508	0.00151	**2620**	**17**	2572	29	2599	13	2020	28
Z26	0.19025	0.00239	0.38587	0.00580	10.1217	0.16027	0.08521	0.00141	**2744**	**20**	2104	27	2446	15	1653	26
Z27	0.17686	0.00191	0.51755	0.00696	12.6215	0.17150	0.14548	0.00219	**2624**	**18**	2689	30	2652	13	2745	39
Z28	0.14634	0.00162	0.35650	0.00485	7.19317	0.10010	0.04159	0.00070	**2304**	**19**	1966	23	2136	12	824	14
Z29	0.14374	0.00155	0.36060	0.00494	7.14620	0.09939	0.03165	0.00051	**2273**	**18**	1985	23	2130	12	630	10
Z30	0.17575	0.00193	0.50270	0.00659	12.1784	0.16272	0.14242	0.00181	**2613**	**18**	2625	28	2618	13	2691	32
Z31	0.21580	0.00332	0.11364	0.00160	3.37931	0.05639	0.02410	0.00078	**2950**	**25**	694	9	1500	13	481	15
Z32	0.19486	0.00345	0.08531	0.00107	2.29171	0.03978	0.01922	0.00084	**2784**	**29**	528	6	1210	12	385	17
Z33	0.24561	0.00310	0.41856	0.00522	14.1749	0.19426	0.04977	0.00122	**3157**	**20**	2254	24	2762	13	982	23
~~Z34~~	~~0.15502~~	~~0.00193~~	~~0.21838~~	~~0.00303~~	~~4.65777~~	~~0.06910~~	~~0.01115~~	~~0.00020~~	~~**2402**~~	~~**21**~~	~~1273~~	~~16~~	~~1760~~	~~12~~	~~224~~	~~4~~
Z35	0.32353	0.00332	0.20149	0.00244	8.98491	0.10884	0.03427	0.00042	**3587**	**16**	1183	13	2337	11	681	8
Z36	0.17854	0.00196	0.16000	0.00204	3.93651	0.05180	0.02816	0.00035	**2639**	**18**	957	11	1621	11	561	7
Z37	0.20931	0.00275	0.16763	0.00228	4.83520	0.07293	0.02071	0.00037	**2900**	**21**	999	13	1791	13	414	7
Z38	0.22979	0.00288	0.15567	0.00186	4.93196	0.06561	0.01809	0.00046	**3051**	**20**	933	10	1808	11	362	9
Z39	0.55903	0.00793	0.18959	0.00235	14.6041	0.20710	0.06638	0.00401	**4405**	**21**	1119	13	2790	13	1299	76
Z40	0.15133	0.00183	0.37216	0.00459	7.76371	0.10522	0.06488	0.00109	**2361**	**20**	2040	22	2204	12	1271	21
Z41	0.14875	0.00209	0.29046	0.00398	5.95774	0.09547	0.05180	0.00109	**2332**	**24**	1644	20	1970	14	1021	21
Z42	0.13120	0.00160	0.40750	0.00508	7.37094	0.10157	0.11486	0.00151	**2114**	**21**	2204	23	2158	12	2198	27
Z43	0.16142	0.00317	0.14008	0.00220	3.11743	0.06439	0.01116	0.00055	**2471**	**33**	845	12	1437	16	224	11
Z44	0.22573	0.00273	0.16832	0.00203	5.23710	0.06898	0.02483	0.00057	**3022**	**19**	1003	11	1859	11	496	11
Z45	0.25066	0.00417	0.09648	0.00130	3.33281	0.05591	0.00663	0.00032	**3189**	**26**	594	8	1489	13	134	6
Z46	0.18545	0.00202	0.42486	0.00523	10.8629	0.13846	0.12597	0.00170	**2702**	**18**	2283	24	2512	12	2398	30
Z47	0.18115	0.00224	0.54797	0.00729	13.6855	0.19869	0.13459	0.00232	**2663**	**20**	2817	30	2728	14	2552	41
Z48	0.21729	0.00230	0.15956	0.00199	4.77997	0.06056	0.02124	0.00030	**2961**	**17**	954	11	1781	11	425	6
Z49	0.20825	0.00246	0.12349	0.00163	3.54576	0.04979	0.01938	0.00033	**2892**	**19**	751	9	1538	11	388	7

Z50	0.19467	0.00296	0.13047	0.00169	3.50030	0.05560	0.01471	0.00046	**2782**	**25**	791	10	1527	13	295	9

	Ratios								Apparent Ages (Ma)							
Spot	Pb^{207}/Pb^{206}		Pb^{207}/U^{235}		Pb^{206}/U^{238}		Pb^{208}/Th^{232}		Pb^{207}/Pb^{206}		Pb^{207}/U^{235}		Pb^{206}/U^{238}		Pb^{208}/Th^{232}	
Chiall Formation Sample 189743 (continued)																
Z51	0.24235	0.00261	0.56496	0.00701	18.8769	0.24131	0.12156	0.00170	**3135**	**17**	2887	29	3036	12	2319	31
Z52	0.15410	0.00237	0.19774	0.00270	4.20126	0.07081	0.03547	0.00082	**2392**	**26**	1163	15	1674	14	705	16
Z53	0.14927	0.00397	0.20126	0.00322	4.14150	0.09375	0.01090	0.00109	**2338**	**45**	1182	17	1663	19	219	22
Z54	0.22874	0.00249	0.04291	0.00052	1.35336	0.01695	0.01506	0.00024	**3043**	**17**	271	3	869	7	302	5
Z55	0.22220	0.00241	0.25764	0.00316	7.89299	0.10022	0.07219	0.00100	**2997**	**17**	1478	16	2219	11	1409	19
Z56	0.17930	0.00251	0.48059	0.00657	11.8803	0.18834	0.11820	0.00296	**2646**	**23**	2530	29	2595	15	2258	53
Z57	0.17657	0.00312	0.16281	0.00212	3.96199	0.06985	0.01869	0.00106	**2621**	**29**	972	12	1626	14	374	21
Z58	0.23306	0.00418	0.06516	0.00095	2.09387	0.03842	0.01524	0.00058	**3073**	**28**	407	6	1147	13	306	12
Z59	0.17770	0.00223	0.44968	0.00547	11.0180	0.15120	0.09620	0.00177	**2632**	**21**	2394	24	2525	13	1856	33
Z60	0.24480	0.00284	0.54397	0.00649	18.3606	0.23565	0.12962	0.00265	**3152**	**18**	2800	27	3009	12	2464	47
Z61	0.25690	0.00278	0.09361	0.00117	3.31557	0.04262	0.02149	0.00030	**3228**	**17**	577	7	1485	10	430	6
Z62	0.13430	0.00177	0.28877	0.00363	5.34628	0.07816	0.06697	0.00117	**2155**	**23**	1635	18	1876	13	1310	22
Z63	0.24235	0.00275	0.08494	0.00101	2.83766	0.03572	0.01464	0.00030	**3136**	**18**	526	6	1366	9	294	6
Z64	0.14601	0.00179	0.35163	0.00446	7.07826	0.09910	0.05353	0.00116	**2300**	**21**	1942	21	2121	12	1054	22
Z65	0.14254	0.00178	0.27569	0.00330	5.41760	0.07370	0.05523	0.00101	**2258**	**21**	1570	17	1888	12	1087	19
Z66	0.14300	0.00219	0.36674	0.00501	7.23060	0.12125	0.08457	0.00263	**2264**	**26**	2014	24	2140	15	1641	49
Z67	0.15345	0.00200	0.34001	0.00456	7.19330	0.10845	0.05335	0.00139	**2385**	**22**	1887	22	2136	13	1051	27
Z68	0.17679	0.00229	0.49298	0.00624	12.0140	0.17310	0.13286	0.00242	**2623**	**21**	2584	27	2606	14	2521	43
Z69	0.30798	0.00396	0.07406	0.00098	3.14472	0.04538	0.01037	0.00030	**3511**	**20**	461	6	1444	11	209	6
Z70	0.17952	0.00277	0.20543	0.00241	5.08432	0.07814	0.02863	0.00156	**2648**	**25**	1204	13	1834	13	571	31
Z71	0.22469	0.00260	0.14257	0.00178	4.41655	0.05905	0.01987	0.00040	**3015**	**18**	859	10	1715	11	398	8
Z72	0.19197	0.00244	0.53023	0.00660	14.0340	0.19759	0.14725	0.00249	**2759**	**21**	2742	28	2752	13	2777	44
Z73	0.21410	0.00254	0.13864	0.00161	4.09290	0.05221	0.01716	0.00045	**2937**	**19**	837	9	1653	10	344	9
Z74	0.20037	0.00301	0.49310	0.00687	13.6217	0.22673	0.11892	0.00362	**2829**	**24**	2584	30	2724	16	2271	65
Z75	0.13027	0.00207	0.37938	0.00490	6.81374	0.11507	0.07971	0.00169	**2102**	**28**	2073	23	2088	15	1550	32
Z76	0.14403	0.00172	0.34957	0.00418	6.94124	0.09217	0.07801	0.00142	**2276**	**20**	1933	20	2104	12	1518	27
Z77	0.15148	0.00244	0.37432	0.00534	7.81675	0.13801	0.05367	0.00205	**2363**	**27**	2050	25	2210	16	1057	39
Z78	0.13180	0.00181	0.36810	0.00448	6.68869	0.09867	0.10248	0.00188	**2122**	**24**	2020	21	2071	13	1972	35
~~Z79~~	~~0.13465~~	~~0.00141~~	~~0.39759~~	~~0.00519~~	~~7.38200~~	~~0.09649~~	~~0.10595~~	~~0.00140~~	~~**2159**~~	~~**18**~~	~~2158~~	~~24~~	~~2159~~	~~12~~	~~2036~~	~~26~~
Z80	0.14366	0.00242	0.37330	0.00475	7.39332	0.12824	0.12250	0.00255	**2272**	**29**	2045	22	2160	16	2336	46
Chiall Formation Sample 189735																
Z1	0.16817	0.00188	0.23278	0.00305	5.39468	0.07212	0.01140	0.00016	**2540**	**19**	1349	16	1884	11	229	3
Z2	0.21425	0.00247	0.14166	0.00197	4.18311	0.05927	0.00722	0.00009	**2938**	**18**	854	11	1671	12	146	2
Z3	0.19081	0.00211	0.13847	0.00201	3.64201	0.05311	0.00645	0.00009	**2749**	**18**	836	11	1559	12	130	2

Z4	0.18306	0.00207	0.46700	0.00638	11.7895	0.16432	0.09554	0.00124	**2681**	**19**	2470	28	2588	13	1844	23

	Ratios								Apparent Ages (Ma)							
Spot	Pb^{207}/Pb^{206}		Pb^{207}/U^{235}		Pb^{206}/U^{238}		Pb^{208}/Th^{232}		Pb^{207}/Pb^{206}		Pb^{207}/U^{235}		Pb^{206}/U^{238}		Pb^{208}/Th^{232}	
Chiall Formation Sample 189735 (continued)																
Z5	0.20843	0.00233	0.30324	0.00414	8.71589	0.12082	0.01183	0.00018	**2893**	**18**	1707	21	2309	13	238	4
Z6	0.21736	0.00226	0.11787	0.00158	3.53270	0.04697	0.00670	0.00008	**2961**	**17**	718	9	1535	11	135	2
Z7	0.13839	0.00177	0.34508	0.00512	6.58386	0.10345	0.05152	0.00079	**2207**	**22**	1911	25	2057	14	1015	15
Z8	0.22145	0.00244	0.15764	0.00210	4.81231	0.06463	0.00872	0.00011	**2991**	**18**	944	12	1787	11	176	2
Z9	0.17877	0.00222	0.30144	0.00410	7.42823	0.10624	0.04804	0.00063	**2642**	**20**	1699	20	2164	13	948	12
Z10	0.17523	0.00278	0.22140	0.00361	5.34819	0.09659	0.00972	0.00017	**2608**	**26**	1289	19	1877	15	196	3

Table 5
Hf isotopic data for all samples

Spot	Hf^{176}/Hf^{177}	1 S.D.	Lu^{176}/Hf^{177}	Yb^{176}/Hf^{177}	U-Pb Age (Ma)	Hf (i)	ε_{Hf}	T_{DM}(Ga)	$T_{DM}^{(Crustal)}$
Yelma Formaiton Sample 189712									
Z4	0.281255	0.000013	0.000796	0.026479	2159.4	0.281221	-4.9	2.68	3.03
Z8	0.280981	0.000100	0.000645	0.019211	2648.3	0.280947	-3.0	3.02	3.29
Z11	0.281392	0.000019	0.000519	0.015734	2025.0	0.281371	-2.8	2.48	2.79
Z23	0.281238	0.000014	0.000407	0.014183	2186.2	0.281220	-4.3	2.67	3.01
Z33	0.281328	0.000110	0.000748	0.025600	2278.5	0.281294	0.5	2.58	2.79
Z40	0.280949	0.000020	0.000608	0.019470	2688.9	0.280917	-3.1	3.06	3.32
Z41	0.280871	0.000016	0.000772	0.024394	2634.6	0.280831	-7.5	3.18	3.55
Z45	0.281167	0.000020	0.000707	0.023741	2663.6	0.281130	3.9	2.79	2.87
Z47	0.280906	0.000100	0.000966	0.031264	2606.8	0.280856	-7.2	3.15	3.51
Z48	0.280867	0.000015	0.000417	0.013617	2619.0	0.280845	-7.3	3.15	3.53
Z51	0.281260	0.000016	0.001186	0.039554	2675.7	0.281197	6.6	2.70	2.72
Z52	0.281180	0.000016	0.000850	0.025412	2677.5	0.281135	4.4	2.78	2.85
Z56	0.281366	0.000018	0.001339	0.043329	1980.1	0.281314	-5.9	2.57	2.95
Z61	0.281610	0.000023	0.001574	0.065821	2250.4	0.281540	8.6	2.26	2.26
Z63	0.281310	0.000013	0.001373	0.048947	2096.5	0.281253	-5.3	2.65	3.00
Z64	0.280912	0.000010	0.000551	0.015913	2611.9	0.280884	-6.1	3.11	3.45
Z67	0.280967	0.000013	0.000894	0.026140	2639.9	0.280920	-4.1	3.06	3.35
Z72	0.280948	0.000016	0.000613	0.019946	2627.8	0.280916	-4.6	3.06	3.37
Z74	0.281212	0.000026	0.000805	0.026774	2215.7	0.281177	-5.1	2.74	3.09
Z79	0.280901	0.000016	0.000583	0.018993	2601.9	0.280871	-6.8	3.12	3.49
Z80	0.281345	0.000026	0.000916	0.029406	2062.2	0.281308	-4.1	2.57	2.91
Yelma Formaiton Sample 189742									
Z1	0.280931	0.000013	0.000536	0.020917	2624.2	0.280903	-5.1	3.08	3.40
Z3	0.281197	0.000011	0.001273	0.056764	2431.2	0.281136	-1.5	2.79	3.03
Z5	0.281062	0.000013	0.001218	0.052305	2687.6	0.280997	-0.3	2.96	3.15
Z9	0.280945	0.000016	0.000488	0.018637	2620.7	0.280920	-4.6	3.06	3.37
Z16	0.281167	0.000018	0.000442	0.017299	2687.8	0.281143	5.0	2.77	2.83
Z22	0.280981	0.000018	0.000831	0.034632	2600.3	0.280938	-4.4	3.04	3.34
Z23	0.281142	0.000014	0.000362	0.013301	2674.5	0.281123	3.9	2.79	2.88

Spot	Hf^{176}/Hf^{177}	1 S.D.	Lu^{176}/Hf^{177}	Yb^{176}/Hf^{177}	U-Pb Age (Ma)	Hf (i)	ε_{Hf}	T_{DM}(Ga)	$T_{DM}^{(Crustal)}$
Yelma Formaiton Sample 189742 (continued)									
Z24	0.280940	0.000015	0.000784	0.031764	2626.4	0.280899	-5.2	3.09	3.41
Z27	0.281215	0.000016	0.001128	0.050651	2442.8	0.281161	-0.3	2.75	2.96
Z28	0.281360	0.000013	0.000892	0.035750	1971.3	0.281325	-5.7	2.55	2.93
Z30	0.281003	0.000016	0.000518	0.018251	2656.2	0.280976	-1.8	2.99	3.22
Z31	0.281193	0.000023	0.000980	0.036498	2653.3	0.281142	4.1	2.77	2.86
Z36	0.280922	0.000013	0.000469	0.016985	2626.7	0.280898	-5.3	3.09	3.41
Z40	0.281669	0.000013	0.000662	0.020841	1993	0.281643	6.1	2.13	2.22
Z43	0.280956	0.000013	0.000586	0.023250	2621.5	0.280926	-4.4	3.05	3.35
Z44	0.280937	0.000016	0.000934	0.039173	2629.4	0.280888	-5.5	3.10	3.43
Z53	0.281668	0.000023	0.001850	0.078253	1976.3	0.281596	4.1	2.20	2.33
Z57	0.280932	0.000018	0.000944	0.038076	2605.2	0.280883	-6.3	3.11	3.46
Z60	0.280949	0.000014	0.000522	0.021832	2607.2	0.280922	-4.9	3.06	3.37
Z62	0.280963	0.000011	0.000921	0.036926	2664.6	0.280914	-3.8	3.07	3.35
Z63	0.281326	0.000013	0.000281	0.010567	2027.3	0.281315	-4.7	2.55	2.91
Z65	0.281229	0.000019	0.001500	0.043576	2680.2	0.281149	5.0	2.76	2.82
Z67	0.280984	0.000012	0.001106	0.048657	2626.8	0.280926	-4.2	3.06	3.35
Z70	0.280989	0.000014	0.000839	0.036734	2639.3	0.280945	-3.3	3.03	3.30
Z73	0.281236	0.000015	0.000559	0.019788	2757.1	0.281205	8.8	2.69	2.64
Z74	0.281332	0.000015	0.000857	0.034232	2044	0.281297	-4.9	2.58	2.94
Z78	0.281394	0.000018	0.001552	0.060560	2120.4	0.281329	-2.0	2.55	2.82
Chiall Formaiton Sample 189743									
Z10	0.281304	0.000015	0.000455	0.016459	2068.1	0.281285	-4.8	2.59	2.95
Z15	0.281032	0.000013	0.000361	0.012211	2759.2	0.281012	2.0	2.94	3.06
Z17	0.281166	0.000012	0.000923	0.038637	2269	0.281125	-5.7	2.80	3.16
Z18	0.280970	0.000014	0.000760	0.027746	2608.9	0.280931	-4.5	3.05	3.35
Z25	0.281158	0.000016	0.000707	0.024453	2619.6	0.281121	2.5	2.80	2.92
Z27	0.280875	0.000015	0.000744	0.023752	2623.7	0.280836	-7.5	3.17	3.55
Z30	0.280945	0.000016	0.000621	0.019227	2613.2	0.280913	-5.0	3.07	3.39
~~Z42~~	~~29252~~	~~0.000009~~	~~0.000547~~	~~0.019119~~	~~2114.1~~	~~0.281305~~	~~-3.0~~	~~2.57~~	~~2.88~~
Z47	0.281203	0.000016	0.000364	0.012143	2663.4	0.281184	5.8	2.72	2.76
Z51	0.280701	0.000015	0.000990	0.035927	3135.4	0.280639	-2.2	3.42	3.61

Spot	Hf^{176}/Hf^{177}	1 S.D.	Lu^{176}/Hf^{177}	Yb^{176}/Hf^{177}	U-Pb Age (Ma)	Hf (i)	ε_{Hf}	T_{DM}(Ga)	$T_{DM}^{(Crustal)}$
Chiall Formaiton Sample 189743 (continued)									
Z56	0.281011	0.000012	0.000754	0.026295	2646.4	0.280971	-2.2	2.99	3.23
Z59	0.280996	0.000011	0.001354	0.052573	2631.5	0.280925	-4.2	3.06	3.35
Z68	0.280890	0.000012	0.000477	0.017257	2623	0.280865	-6.5	3.13	3.48
Z72	0.281128	0.000014	0.000450	0.013333	2759.1	0.281103	5.2	2.82	2.86
Z74	0.281193	0.000012	0.001366	0.040365	2829.2	0.281116	7.4	2.80	2.78
Z75	0.281267	0.000011	0.000496	0.017623	2101.6	0.281246	-5.4	2.64	3.01
Z78	0.281362	0.000013	0.000663	0.025135	2122.1	0.281334	-1.8	2.53	2.81
Z80	0.281317	0.000011	0.000411	0.012648	2271.8	0.281299	0.5	2.57	2.78
Chiall Formaiton Sample 189735									
Z4	0.281145	0.000046	0.001283	0.043024	2680.8	0.281077	2.4	2.86	2.98

Blichert-Toft et al., 1997 - 176Lu decay constant ($1.93x10^{11}$) was used.

$Hf_i = Hf^{176}/Hf^{177}$ ratio - (Lu^{176}/Hf^{177} * (EXP($\lambda^{176}Lu$*Pb^{207}/Pb^{206} ratio/1000)-1))

Value with strike through has been eliminated from ε_{Hf} diagram in Figure 10, 13 and 14

RECORD 2009/19

U-PB AND HF ANALYSIS OF DETRITAL ZIRCONS: IMPLICATIONS FOR PROVENANCE OF THE EARAHEEDY BASIN, CAPRICORN OROGEN

MATONIA

This Record is published in digital format (PDF) and is available online at: www.dmp.wa.gov.au/GSWApublications.
Laser-printed copies can be ordered from the Information Centre for the cost of printing and binding.

Further details of geological publications and maps produced by the Geological Survey of Western Australia can be obtained by contacting:

Information Centre
Department of Mines and Petroleum
100 Plain Street
EAST PERTH, WESTERN AUSTRALIA 6004
Phone: (08) 9222 3459 Fax: (08) 9222 3444
www.dmp.wa.gov.au/GSWApublications